NUMERICAL AND PHYSICAL SIMULATIONS OF THE DISPLACEMENT OF SYNTHETIC OIL MIXTURES

A Thesis

Submitted to the Faculty of Graduate Studies and Research

in Partial Fulfilment of the Requirements

for the Degree of

Doctor of Philosophy

in

Chemical Engineering

Department of Chemical Engineering

University of Saskatchewan

Saskatoon, Saskatchewan

S7N 0W0

by

Sanjoy Saha

January, 1993

To the memory of my
Late Grandfather,
who wished me to be a medical doctor
but I turn out to be Doctor of Philosophy.

ABSTRACT

Numerical simulation and experiments are often used to study the mixing phenomenon of the fluids during an unstable displacement process. One of the deficiencies of the conventional compositional reservoir simulators for predicting the unstable displacement process is that these simulators all involve the use of the assumption that fluids in each grid block are in a state of thermodynamic equilibrium. In reality, the different fluid phases coexisting in each grid block may not be in equilibrium with each other because of insufficient contact time. The main objective of this study is to develop a non-equilibrium phase behaviour model for compositional simulation of the unstable displacement process and is to verify the simulation results with experimental data.

Physical simulations of the displacement process were carried out in a slim-tube apparatus. Four synthetic oil mixtures were used as displaced fluids and four gases were used as displacing fluids. A total of fifteen experiments were performed at displacement pressures ranging from 2390 psia to 3430 psia and with injection rates varying from 0.048 to 0.127 PV/hr. The results of the experiments are presented.

A model has been developed to calculate the non-equilibrium phase behaviour of the fluids under displacement process conditions. The model is based on the mixing parameter model proposed by Todd and Longstaff (1972) and the

concept of Murphree efficiency commonly used in multicomponent, multistage separation calculations. Phase behaviour calculations are performed for the fluids over the entire grid block under non-equilibrium conditions. The deviation from equilibrium in respect of each component is considered a function of the equilibrium K-value and the effective mobility ratio of the in-situ fluids.

Efficient algorithms for phase behaviour calculations (e.g., flash calculations and saturation pressure calculations) generally used in the numerical simulations are presented. An acceleration scheme based on the dominant eigenvalue method coupled with Newton's method is developed for two-phase flash calculations. Effective switching criteria are suggested for the switch over of the acceleration scheme to Newton's method. The proposed method is robust and fast for flash calculations when the specifications are near the critical state values of the fluid mixtures. The performance of the proposed method is compared with those of other improved methods for flash calculations.

An algorithm is developed to accelerate the convergence of phase-boundary calculations using Newton's method. The algorithm takes advantage of the history of the iterates and uses the derivative of the iterates to further improve the iterates after three Newton steps. The performance of the proposed algorithm shows its superiority over that of Newton's method particularly when the specifications are near the

critical state values of the fluid mixtures. Comparisons of the performance of the proposed algorithm with that of Newton's method and other acceleration algorithms for Newton's method are presented.

Comparisons of the numerical simulation results based on the proposed non-equilibrium phase behaviour model with the experimental data obtained from the slim-tube displacement tests for well-defined hydrocarbon systems and with simulation results based on conventional equilibrium phase behaviour model are presented.

ACKNOWLEDGMENTS

I wish to thank first my supervisor Professor D.-Y. Peng for his guidance and patience throughout my thesis work. I would also like to express my thanks to my supervisory committee members, Professors N.N. Bakhshi, M.N. Esmail, D.G. Macdonald and R. E. Verrall, for their time and suggestions rendered during this project.

I would like to thank especially Professor D.L. Flock of the University of Alberta for providing his laboratory for carrying out the experiments. I also thank Bob Smith of University of Alberta for his help in the experiments.

Thanks are also due to Graduate Studies and Research for awarding me the M.Sc and Ph.D scholarships. I thank the secretaries of the Department , Karen and Debbie, my colleagues and friends, especially Khosrow Nikkhah and Pares Das for their co-operation and encouragement. Special thanks go to my friend, Hemant Sinha, for lending me the laser printer, which made the printing of the thesis easier for me. Last but not least, I would like to thank my fiancee, Godhuli, and also my family members. Without their patience and encouragement, it would not have been possible to achieve this.

TABLE OF CONTENTS

APPENDIX E Raw Experimental Data and Computer Programs (Stored in a 3 1/2" DSDD floppy disk)

Filenames	Description
RAWDAT	Raw Experimental Data (in Word Perfect 5.1 format)
COMFLASH	FORTRAN source code for flash calculations
EIFLASH	FORTRAN source code for iteration matrices eigenvalues for flash calculation
SBUB	FORTRAN source code for calculation of bubble-point pressures using Modified Newton's method
SDEW	FORTRAN source code for calculation of dew-point pressures using Modified Newton's method
SIMU	FORTRAN source code for simulation of a one-dimensional compositional reservoir using non-equilibrium phase behaviour model

LIST OF TABLES

LIST OF FIGURES

NOMENCLATURE

A	Area of cross-section, cm^2
A_{mj}	Iteration matrix
D	Diameter, cm
E_m	Degree of non-equilibrium for component m
E	Error
F	An objective function
f_m	Fugacity of component m
J	Jacobian matrix
K	Permeability, cm^2
K_m	Equilibrium factor for component m
K_{rj}	Relative permeability of phase j
K_{wor}	Permeability to water at residual oil saturation, cm^2
L	Liquid fraction
M	Mobility ratio
M_E	Effective mobility ratio
N_c	Number of components
P	Pressure, kPa or Psia*
P_{cm}	Critical pressure for component m, kPa
P_{sm}	Saturation pressure for component m, kPa
q_m	Injection or production rate for component m, mole/s
R	Gas constant
R_m	Fugacity ratio for component m
r	Relaxation parameter
S_j	Saturation of phase j

* 1 psia = 6.894757 kPa

T	Temperature, K
T_{cm}	Critical temperature for component m, K
T_j	Transmissibility of phase j
t	Time, seconds
u	Vector of iteration variables
V	Vapour fraction
V_b	Volume of one grid block, cm^3
V_j	Velocity of phase j, cm/s
x_m	Mole fraction of component m in liquid phase
y_m	Mole fraction of component m in vapour phase
y_{mj}	Mole fraction of component m in phase j
z_j	Compressibility of phase j
z_m	Overall composition of component m

Greek Symbols

α_1	An empirical parameter
Δ	Difference operator
δ	Error norm
λ	Eigenvalue of iteration matrix
μ_j	Viscosity of phase j, cp
μ_w	Viscosity of water, cp
μ_m^*	Viscosity of pure component m, cp
ρ_j	Density of phase j, $mole/cm^3$
σ	Interfacial tension, dyne/cm
Φ	Porosity
Φ_m	Fugacity coefficient for component m

ω Mixing Parameter

ω_m Acentric factor for component m

Superscript

L Liquid phase

l Iteration index

n Index of time

T Transpose

V Vapour Phase

* Non-equilibrium state

Subscript

g Gas phase

i Grid block

j Phase

k Adjacent grid block

m Component

o Oil phase

x, y, z Directions of axis

Abbreviations

BPR Back pressre regulator

DEM Dominant eigenvalue method

FCM First-contact miscible process

GDEM General dominant eigenvalue method

GOR Gas-oil ratio

IMPES	Implicit pressure explicit saturation
IOIP	Initial oil in-place
MCM	Multiple-contact miscible process
MMP	Minimum miscibility pressure
PV	Pore Volume
RBA	Rising bubble apparatus

CHAPTER 1

INTRODUCTION

In the initial stages of oil production, reservoirs are allowed to produce under natural drive until the production rates have become uneconomic. This method of recovery is known as "primary" recovery. The primary recovery method can only recover 10 to 20 percent of the original oil in place. At the end of primary recovery phase, recovery of oil is achieved by introducing the method of artificial drive (water injection). This method is known as the "secondary" recovery method. This definition of secondary recovery method is only of historic interest, because lately the secondary recovery method is often applied to the field, well before the end of primary production phase (Latil, 1980). The secondary recovery method can only recover an additional 10 to 20 percent of the original oil in place. Thus, "tertiary" recovery methods are used to recover the oil left in the reservoir. Tertiary recovery methods consist of artificial drives such as gas (CO_2, hydrocarbon gases) flooding or injection and chemical (polymers and surfactants) flooding. Flooding and injection are used synonymously in the text.

Gas flooding is one of the most promising tertiary recovery methods. A mixture of hydrocarbon gases or pure CO_2 are generally used to displace the reservoir oil during the tertiary recovery (Latil, 1980). Gas injection in an oil

reservoir takes place either into the zone of the reservoir where a gas phase already exists or into the oil zone. When a gas zone originally exists in a reservoir or when it is created during the pressure depletion at the primary production phase of the reservoir, gas injection helps to keep the reservoir pressure at nearly a constant value and at the same time forces the gas into the oil zone and oil towards the production wells.

The compositions of the injected gas and the displacement pressure determine whether the gas can be fully or partially miscible with the in-situ oil. If the injected gas is completely miscible with the in-situ oil, the gas injection process can recover up to 100 percent of the oil-in-place (Holm et al., 1974). This promising potential of the gas injection process has motivated researchers to investigate the process since 1950's (Blackwell, 1981).

During the primary or secondary production phase of the reservoir, research work is usually started to determine the proper tertiary recovery method for a particular reservoir. The most important factor behind the selection of the proper tertiary recovery method is the economic viability of the recovery process. Usually, chemical flooding is more costly than the gas flooding. This fact makes the gas flooding an obvious choice for the tertiary recovery method in most of reservoirs.

In gas flooding process, selection of the

composition of injected gas and the displacement pressure are the most important factors for efficient recovery of oil. Selection of gas composition and the displacement pressure are made on the basis of results of experimental and numerical simulation studies of the recovery process.

Experimental studies are carried out in a laboratory scale reservoir with a porous medium which represents the characteristics of the porous medium of the actual reservoir. Oil used in the experiments is also a sample of the crude oil of the actual reservoir. A series of experiments are performed with different gas compositions at a particular displacement pressure and similarly, series of experiments are performed with each gas as a displacing fluid at different displacement pressures. Based on the experimental recovery of the oil, the optimum displacement pressure and the composition of the injected gas are determined. However, the experimental results obtained from a laboratory scale reservoir are not the actual representation of the results expected from a field scale reservoir study.

Numerical simulation of the recovery process is required for predictions of results expected from a field scale reservoir. The mathematical equations that describe fluid flow in a reservoir and interactions between the fluids are valid for both the laboratory scale and the field scale reservoirs. This means that numerical simulation of the gas injection process can be verified and even adjusted by use of

experimental results and then can be used to predict the field scale reservoir performance. Thus, maximum understanding of the gas injection process may require the optimized use of both the experimental and numerical simulation results.

The numerical simulation of the gas injection process aids the understanding of the fluid interactions under the dynamic displacement conditions and also provides insight into the effects of various variables on the process. The objectives of this study are to investigate the fluid interactions phenomena under the displacement conditions and to evaluate the effects of different process variables on recovery.

Several researchers (Coats, 1980; Nghiem et al., 1981; and Crump, 1988) have used numerical simulations to study oil recovery processes involving gas injection. In all of their work, fluid interaction phenomena are described by an equilibrium phase behaviour model. The basic assumption made in the equilibrium model is that under the dynamic conditions of the displacement process, fluids are at thermodynamic equilibrium. This assumption may be valid when the complete mixing occurs between the injected gas and the in-situ oil. In reality, various factors such as viscosity and density differences between the oil and gas, reservoir geometry, heterogeneity of the porous medium cause incomplete mixing between the gas and oil during the displacement process.

In this study, a non-equilibrium phase behaviour model is proposed to describe the fluid interaction phenomena at the reservoir conditions. The basic assumption made in the development of the non-equilibrium model is that the injected gas and the in-situ oil are in an incomplete mixing state under the dynamic displacement conditions. The numerical simulation results obtained from the non-equilibrium model are compared with the experimental data. The experimental data are also analyzed to determine the effects of process variables on the oil recovery.

CHAPTER 2

LITERATURE REVIEW

2.1 History and Background

The concept of using solvent or gas injection to recover oil is quite old. The recovery of oil using solvent injection is commonly known as miscible flooding if the injected solvent is miscible with oil. The potential of the miscible flooding process has been recognized by the petroleum industry since the 1920's. Nevertheless, the interest in the miscible flooding technique or other enhanced oil recovery techniques was not extensive before World War II (Blackwell, 1981). The sharp increase in oil price in the post World War II era has dictated the necessity of research in finding and evaluating different enhanced oil recovery techniques.

One of the early research studies among the increased research efforts on miscible flooding was published in 1950 (Everett et al., 1950). These researchers made two sets of experiments. In the first set of experiments sugar solutions of various concentration were displaced by other sugar solutions in a linear system made of cemented silica sand grains. The objective of this set of experiments was to evaluate the effects of viscosities of the displaced fluid and displacing fluid on the sweep efficiency of the displacing fluid. In this case the displaced fluid and the displacing fluid were completely miscible. In the second set of

experiments oils were displaced by water. Here the objective was the same as that of the first set of experiments but the displaced fluid and displacing fluids were immiscible. The other objective of this work was to compare the behaviour of a miscible displacement process with that of an immiscible displacement process.

Laboratory scale experiments on oil recovery by injection of solvent other than water was reported in 1953 (Henderson et al., 1953). In this work refined oils from test cores were displaced by liquefied petroleum gas (LPG). The objectives of this work were to evaluate the effects of oil viscosity and displacement rate on recovery efficiency. Researchers had also studied the effect of methane rich gas as displacing fluid on the recovery efficiency of oil (Whorton et al., 1950; and Slobod et al., 1953). The main objective of these studies was to observe the effects of displacement pressure on oil recovery.

Stone et al. (1956) studied the effects of gas composition on oil recovery. At these early stages of research the experimental investigations were mainly directed towards the selection of proper solvent for improved recovery of oil and the determination of the effect of physical factors, such as viscosity ratio and displacement rate, on recovery efficiency.

Theoretical work on the mechanisms of fluid displacement in porous media was first reported in 1942

(Buckley et al, 1942). In this paper, the advancement of the saturation front of the displacing fluid was correlated with the fractional flow of that fluid by a material balance equation. This fundamental relationship developed by Buckley et al. (1942) is used to calculate the recovery of oil by gas flooding or by water flooding. The limitation of this relationship in the prediction of oil recovery is that the oil and injected fluid have to be incompressible and immiscible. Because of this limitation, the Buckley-Leverett relationship is used only in the calculation of oil recovery resulting from water flooding. However, this relationship may be used to calculate approximate oil recovery resulting from gas flooding. A similar method for computing oil recovery by immiscible fluid flooding (water or gas) was reported (Welge, 1952). During these initial stages of research, theoretical work was confined primarily to the predictions of oil recovery and the advancement of the saturation front of a particular fluid phase.

As a result of the studies made by Leverett (1941), Welge (1949), Rose et al. (1949) and Rosenberg (1956), the theory of fluid flow through porous media had become quite established in the early 1950's. However, applications of this theory to study the oil displacement process using a miscible solvent and to describe the internal mixing phenomena between the oil and the injected miscible fluid were not

developed during the early stages. An attempt was made by Hall et al. (1957) to describe the miscible displacement process with the help of the Buckley-Leverett equation and with an assumption that oil and gas mixtures could be represented by a two-component system (oil and gas). However, this study could not rigorously describe the mechanisms of a miscible displacement process because it did not predict, quantitatively, the composition of fluid phases and how mass transfer occurred between the fluid phases. The reason for this inadequacy in theoretical studies could be attributed to the lack of a suitable thermodynamic equation to calculate the composition of fluid phases and the lack of digital computing facilities.

In the previous paragraphs, a brief background of the research efforts towards understanding the oil displacement process by solvent or gas injection was given. The advancement of research work in the area of oil recovery by the gas displacement process will be discussed in the following sections.

2.2 Mechanisms of Oil Recovery by Gas Injection

The displacement pressure and temperature in the reservoir and the compositions of the in-situ oil and injected gas determine the mechanism of displacement of oil using gas injection. The mechanism can be broadly characterized by three processes, namely first-contact miscible, multiple-

contact miscible and immiscible processes. These displacement processes can be conceptually explained with the help of a triangular phase diagram (Hutchinson, et al., 1961). The triangular phase diagrams are used to represent the phase behaviour relations of reservoir fluids by grouping the components of a reservoir fluid into three pseudocomponents. The commonly used grouping scheme involves a volatile pseudocomponent (light) composed of nitrogen and methane, an intermediate volatility pseudocomponent (intermediate) composed of ethane through hexane and a low volatility pseudocomponent (heavy) composed of hydrocarbons with molecular weights greater than hexane (Stalkup, 1984).

2.2.1 First-contact Miscible Process

First-contact miscibility is achieved when the injected gas or solvent mixes with oil in all proportions to form single-phase fluid mixtures. A triangular diagram may be used to illustrate the principles of first-contact miscible process. Let us consider in the diagram (Figure 2.1) the composition of the displaced oil and that of the injected gas which are represented by the points O and G, respectively. The phase envelope defining the compositions of two-phase mixtures formed by the light, intermediate and heavy components at displacement pressure P_f and at temperature T is represented by the arc BCD (C is the critical point of the mixture). The line OG, is the loci of all probable

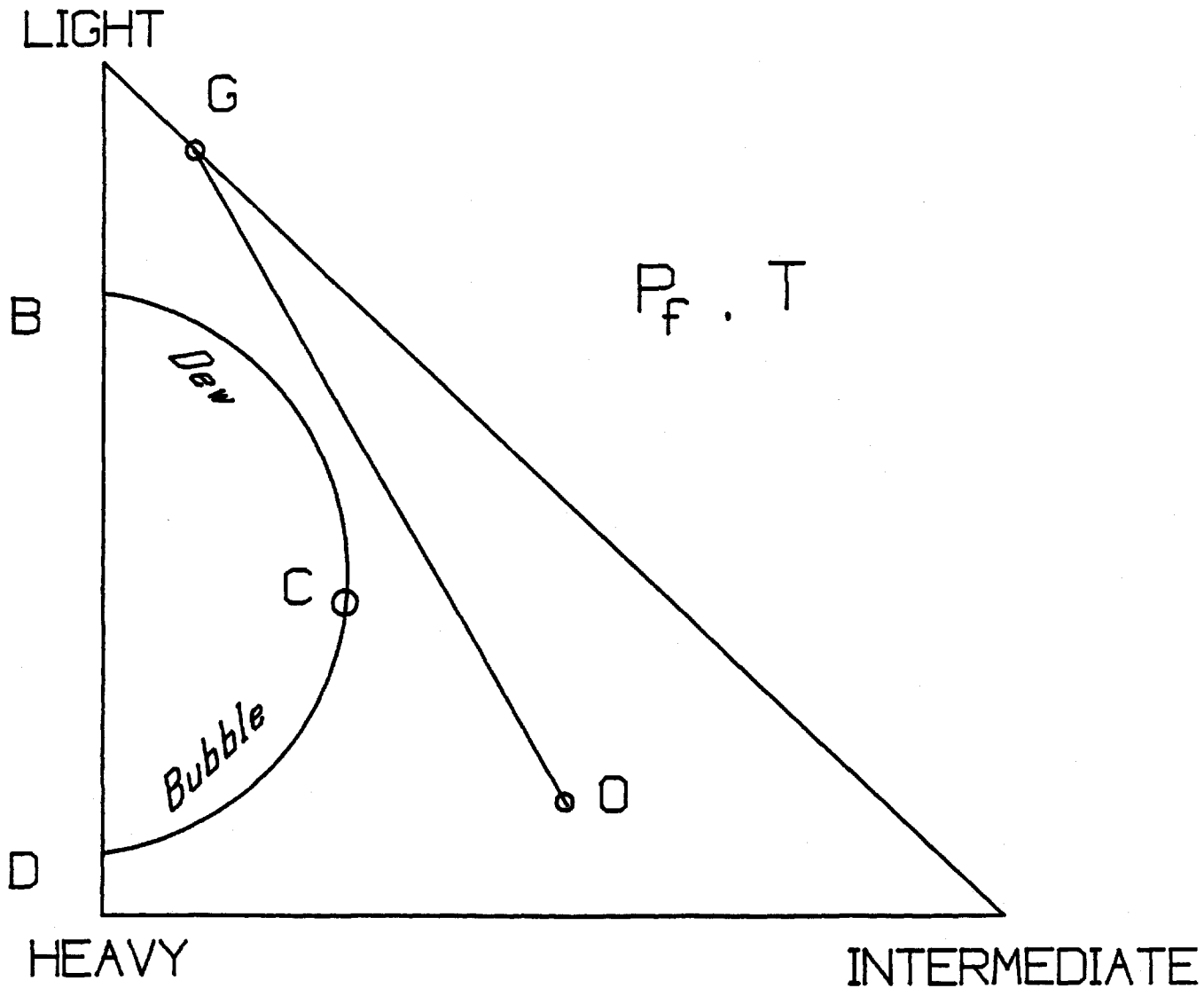

Figure 2.1: Triangular Diagram for a FCM Process

compositions encountered when the two fluids whose compositions are represented by O and G are mixed. The fact that the line OG lies outside the phase envelope (BCD) indicates that the injected gas and the displaced oil form a single-phase fluid mixture in all proportion.

Pressure/ composition (P-X) diagrams can also be used to determine the displacement mechanisms (Stalkup, 1984). Figure 2.2 shows the dependence of saturation pressure of the compositions of the mixture (solvent+in-situ oil) at constant temperature. Up to a certain concentration of the injected solvent in the oil-solvent mixtures, the saturation pressures are bubble-points pressures. When the solvent concentrations are above a certain value, the saturation pressures are dew-points pressues. The critical point of the mixture is the point where the bubble-point curve meets the dew-point curve. Outside the bubble-point and dew-point curves the mixture is at single phase. There is a highest pressure point in the curve where the two-phase mixture can co-exist. This pressure is called the cricondenbar of the solvent-oil mixture. The significance of the cricondenbar is that above the cricondenbar, the injected solvent and the reservoir oil in any proportion will form single phase mixtures. Thus, with the help of a P-X diagram, one can determine the cricondenbar for a particular solvent and oil mixture at a certain temperature and then the first-contact miscibility displacement pressure which will be higher than the

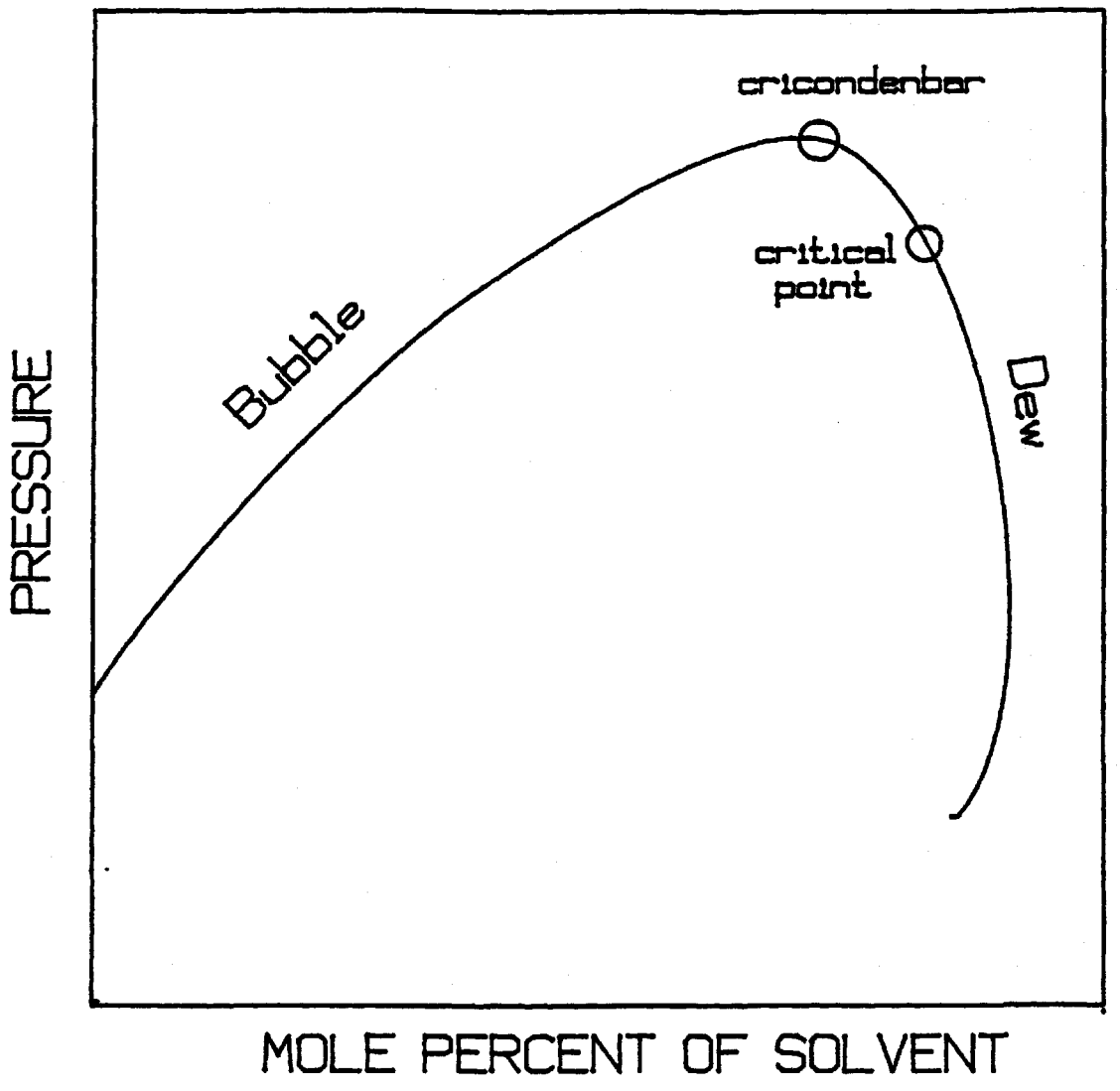

Figure 2.2: Phase Envelope for an Oil/Solvent Mixture

cricondenbar.

Hydrocarbons of intermediate volatility such as propane, butane or mixtures of propane and butane (LPG) are commonly used as injected gas for first-contact miscible flooding (Henderson et al., 1953; Blanton et al., 1970; Connally, Jr., 1972 and Martin, 1982). The reason for using a gas richer in intermediate components for attaining first-contact miscibility is to reduce the cricondenbar of the injected gas and oil mixture so that first-contact miscibility can be achieved at a reasonable pressure. But, the LPG solvents are too expensive to inject continuously. However, for a lighter hydrocarbon gas and an in-situ oil mixture such as natural gas and West Texas oil mixture, the cricondenbar pressure could be as high as 10000 psi (Stalkup, Jr., 1984).

To optimize conditions between the impractical high pressure and the expensive solvent, a process was developed to miscibly displace the oil. In this process, a certain volume of LPG solvent or slug was injected at first so that it could develop first-contact miscibility with the in-situ oil, and the slug was then miscibly displaced by lighter hydrocarbons such as natural gas (Hall et al., 1957; Lacey et al., 1961). This slug process mechanism is more complex than the oil displacement mechanism by a single gas. At the leading edge, the slug is miscible with the oil in place and at the trailing edge, slug is mixed with the driving gas. After a series of

contacts between the slug and driving gas, the slug will be diluted with lighter hydrocarbons to the extent that the diluted slug may not miscibly displace the original oil. So there are many factors, such as the degree of mixing between the driving gas and slug, composition of the diluted slug, temperature and pressure of the process, which determine the first-contact miscibility in the slug process. This slug process is frequently used in the actual field for oil recovery by the first-contact miscible process (Lacey et al., 1961).

2.2.2 Multiple Contact Miscible Process

The multiple contact miscible process (MCM) is operated at a pressure below the operating pressure of the first contact miscible process. The name of the process suggests that the miscibility is achieved between the injected gas and the in-situ oil through repeated contact between the oil and gas. The mechanism of this process can be described in a simple way with the help of a triangular diagram such as that shown in Figure 2.3. Figure 2.3 shows the phase envelope of the same mixture which is used in the FCM process, at the the temperature T and the pressure, P_m which is lower than P_f (operating pressure of FCM process). Due to the lower pressure ($P_m<P_f$), the phase envelope BCD (C is the critical point of the mixture) is more expanded (Figure 2.3) compared to the phase envelope at P_f (Figure 2.1). The line joining

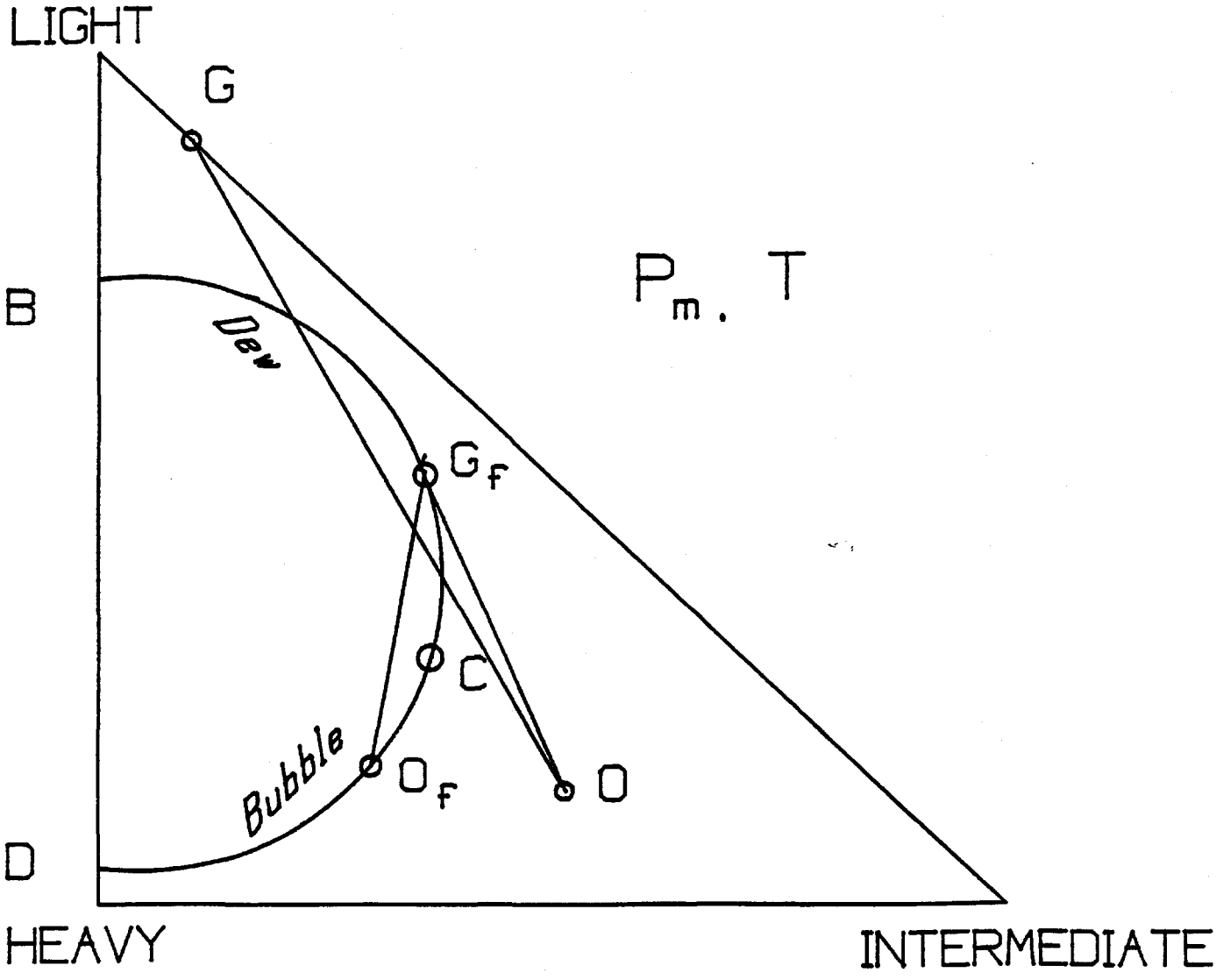

Figure 2.3: Triangular Diagram for a MCM Process

the points of original oil composition, O, and the original injected gas composition, G, crosses the phase envelope which indicates that the initial oil and gas mixture do not form a single-phase mixture. However, the gas mixtures resulting from the repeated contacts between the fresh oil and the invading gas front, will become richer and richer in intermediate components. The composition profile of the enriched gas mixtures will follow the dewpoint line in the direction of richer intermediates until the point G_f is reached. The oil which is getting stipped of the intermediate components follow the bubble-point line until the point O_f is eached. It can be seen from Figure 2.3 that the composition of gas at G_f is rich enough in intermediate hydrocarbons to be miscible with the original oil composition (O). In this illustration, it is found that miscibility is achieved through multiple-contact between the fresh oil and the enriched gas moving towards the front. During the multiple contact process, mass transfer of intermediate components occur from oil to gas phase. This mechanism of MCM processes where miscibility is obtained by the vaporization of intermediate components from the oil to the gas phase is known as the "vaporizing gas drive" mechanism (Hutchinson, 1961). There is another mechanism which is known as the "condensing gas drive" for achieving multiple-contact miscibility in displacement processes. In a condensing gas drive, the mass transfer of intermediate components from the gas phase to the oil phase

develops the miscibility between oil and gas. The mechanism by which multiple-contact miscibility will be obtained depends on the composition of the oil and that of the injected gas. If the concentrations of intermediate components in the oil are low and the injected gas is rich in intermediate components, miscibility will develop between the oil and the gas through condensing gas drive(Stone et al., 1956 and Hutchinson, 1961). On the other hand multiple contact miscibility through vaporizing gas drive is obtained when the concentrations of intermediates in oil are high and the injected gas contains lighter hydrocarbons such as natural gas or flue gas. The condensing gas drive method and the vaporizing gas method are often known as the "rich gas drive" and "high pressure gas drive" method respectively (Hutchinson, 1961).

Because the FCM process involves the use of expensive solvents, the MCM process is commonly used in actual fields for miscible flooding (Reitzel et al., 1977; Desbrisay et al., 1982; Brannan et al., 1977; Griffith et al., 1981; Hardy et al., 1975 and Christian et al., 1981). Prior to the application of the MCM process in the field, the selection of proper solvent and the determination of the displacement pressure should be made. The selection of solvent is made either by laboratory experiments or by theoretical predictive methods such as the construction of the pseudoternary diagrams (Wu et al., 1986; Novosad et al., 1988; Novosad et al., 1989;

and Orr, Jr. et al., 1989). The selection of a proper solvent is made based on the optimum composition of the solvent required to develop multiple-contact miscibility with the in-situ oil. However, the use of pseudoternary diagrams to determine the composition of solvents for MCM processes is an approximate method. This is because the individual components of different volatilities are grouped as a single pseudocomponent. For this reasons, the distribution of the pseudocomponents in the gas and liquid phases will be different from those of the actual individual components in the gas and liquid phases (Hutchinson, 1961).

Another predictive method to determine the solvent composition is based on the procedure where repeated flash calculations are performed (Metcalfe et al., 1973; and Fussel et al., 1979). In this procedure, a flash calculation is performed for the mixture of injected solvent and original oil and then the evolved gas from the previous flash calculation is mixed with the original oil to form a mixture which is again flashed. This procedure is repeated to simulate the composition route of the mixture of solvent and original oil as it moves in the direction of flow. If this procedure predicts the formation of a miscible mixture, the initial solvent composition is found to be adequate for miscible flooding. The deficiency of this procedure is that the prediction of compositions of the mixtures are based on the static contact between the fluids. In field application,

fluids come in contact under dynamic conditions in the porous medium of the reservoir. So this procedure, like the pseudoternary diagrams, is also an approximate method of understanding the mixing phenomena in a MCM process.

Other than the selection of a proper solvent, another important design parameter for miscible flooding is the selection of the operating pressure. The minimum pressure required to develop multiple contact miscibility between the solvent and the oil at the reservoir temperature is defined as the minimum miscibility pressure (MMP) (Yellig et al., 1980; and Mungan, 1980). MMP is an important parameter from the process design point of view because the technical viability of a miscible flood project will depend on whether the reservoir can withstand pressures greater than the MMP for a particular solvent and the reservoir oil. The most frequently used method to determine the MMP is to conduct laboratory scale experiments of the displacement of oil by particular solvent at different pressures (Orr, Jr., 1982; Holm et al., 1982; Harmon et al., 1988 and Bahralolom, 1988). As it is difficult to visualize the mixing phenomena inside the porous medium under dynamic conditions, the determination of MMP from laboratory scale experiments is based on the recovery values of oils. The criteria for determining the MMP based on the recovery values differ from one research paper to another, but in general the criteria are: 1) a minimum of 80-85 percent recovery of the oil in place at breakthrough of the injected

solvent, and 2) ultimate recovery of 90-95 percent of oil at 1.2 pore volume of solvent injection (Holm et al., 1974; and Sigmund et al., 1979).

As alternatives to the time consuming and expensive laboratory experiments, there are a number of theoretical predictive methods reported in the literature (Rhuma, 1992) for the determination of MMP. In these theoretical correlations, reservoir temperature, oil composition and injection gas composition are used as variables to determine the MMP (Benham et al., 1960; and Holm et al., 1974, 1982). These correlations can be used to predict the MMP with an average absolute accuracy of 20 percent, but the maximum error could be as high as 80 percent (Rhuma, 1992). The poor predictions by these correlations can be attributed to the fact that they are empirical in nature and are developed on the basis of experimental MMP values for particular sets of oils and solvents. So, when these correlations are applied to different systems of oils and solvents, good estimations of the MMP values cannot be obtained. However, these correlations can provide a rough estimate of MMP value for a particular set of oil and solvent so that laboratory experiments can be performed in the vicinity of predicted pressure for more accurate determination of MMP. Thus, the number of experiments required to determine the MMP can be reduced.

2.2.3 Immiscible Process

If a solvent is injected to displace an oil at a pressure below the MMP of that oil and solvent, the displacement process will be an immiscible process. The displacement pressure required for an immiscible process is lower than that required for a multiple contact miscible process. Thus, recovery of oil is lower in an immiscible process than that in a MCM process because the gas front and the oil do not form a single-phase mixture. Thus, the sweep efficiency of the invading gas front is low and as a result the amount of oil left in the porous medium is larger than that for the MCM or FCM processes (Nouar et al., 1983).

The mechanism of an immiscible process is described with the help of a triangular diagram shown in Figure 2.4. In Figue 2.4, the injected solvent composition is represented by point G and the in-situ oil composition is represented by point O. The phase envelope for this fluid system at pressure P_i and at temperature T, is represented by BCD where point C is the critical point of the fluid mixture. As the injected gas moves forward, it strips off intermediate components from the oil, and the composition of the gas mixture follows the dew-point line (BC) until the composition reaches the limiting point G_1. The limiting point is determined by the tie-line passing through the original oil and the equilibrium oil composition O_e. In Figure 2.4, it can be seen that the limiting composition (G_1) of the gas phase cannot form a

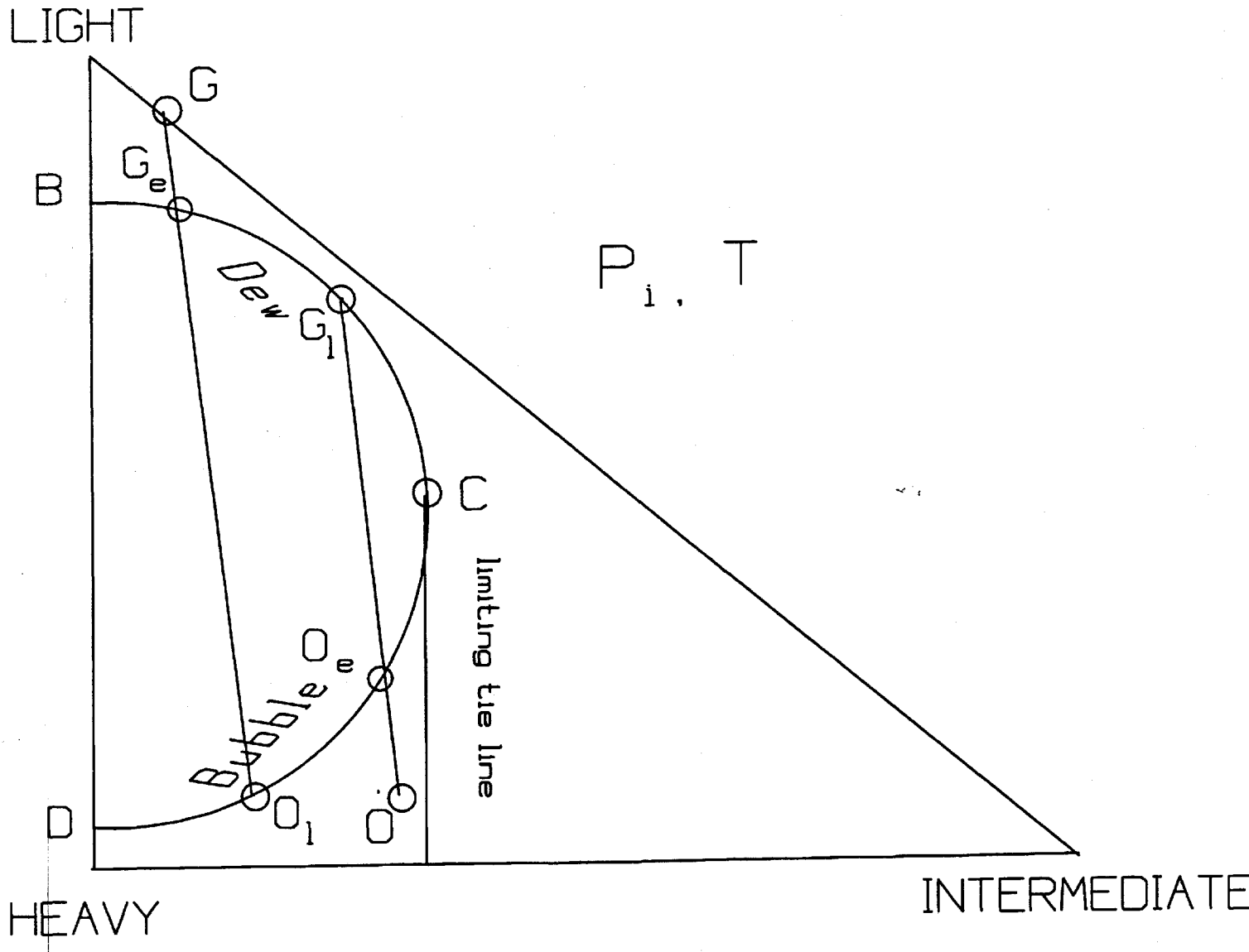

Figure 2.4: Triangular Diagram for an Immiscible Process

single-phase mixture with the in-situ oil (O).

The composition of the oil will follow the bubble point line as the oil is getting stripped of its intermediate components. The limiting composition of the residue oil will be O_1. The limiting composition is determined by the tie-line passing through the point of original gas composition (G) and the point of equilibrium gas composition (G_e).

When a light gas such as pure methane or nitrogen is used to displace an oil depleted of light hydrocarbons, then the displacement process may possibly be an immiscible process at a displacement pressure within the practical range (2000-4000 psia) (Koch et al., 1958 and Stalkup, Jr., 1984). As a rule of thumb, it can be said that if the compositions of the both injected solvent and the reservoir oil lie to the left side of the limiting tie line in a triangular diagram, the displacement process will be an immiscible one (Stalkup, 1984). To use an immiscible process to recover oil is not the desirable choice becaause the recovery of oil will be lower than that obtained from MCM or FCM processes. Sometimes, due to economic constraints such as the high cost of rich solvent, and technical constraint, such as the problem of boosting the low reservoir pressure, the immiscible process is the only choice for gas flooding operations.

2.2.4 Unstable Displacements

In the previous sections, the mechanisms of gas

flooding based on phase interaction phenomena were discussed. The mechanisms of gas flooding operations affected by physical factors, such as viscosity differences and density differences between the in-situ oil and injected solvent, displacement rate, heterogeneity in the porous medium and the dimensions of the reservoir, will be discussed in this section.

Viscosity Difference: Due to the physical factors mentioned above, instability occurs in the displacement process which can be either miscible or immiscible. The most important factor to cause instability in a displacement process is the viscosity difference between the injected solvent and oil. It is quantified by the ratio of viscosity between the oil and the solvent and is commonly known as the "mobility ratio". For mobility ratios smaller than or equal to one, the displacement front followed by solvent and preceded by oil is stable. For mobility ratios greater than one, the displacement front becomes unstable and the solvent penetrates the oil in the form of fingers (Stalkup, 1984). These fingers are called "viscous fingers" because they result from the difference in viscous forces between the oil and the solvent. Viscous fingers cause early breakthrough of solvent and ultimate recovery of the oil is lower than would be the case if viscous fingering does not occur in a displacement process (Blackwell et al., 1959).

There have been several attempts by researchers to

investigate, mathematically, how viscous fingers develop and grow in a displacement process (Perrine, 1961; Peters et al., 1981; Gardner et al., 1984; and Bentsen, 1985). These mathematical approaches to determining the initiation of viscous fingers or the onset of instability are based on the perturbation analysis of the displacement front where a spectrum of wavelengths of perturbations about a smooth line is assumed. Various researchers have proposed a different dimensionless parameter for use in the prediction of the onset of instability or of the initiation of viscous fingering in a displacement process. For example, Peters et al. (1981) proposed a dimensionless parameter which is a function of M, v, μ_w, D, σ and K_{wor}. Once the instability is created, all the fingers generated cannot be damped out by dispersions in the longitudinal and transverse directions (Stalkup, 1984). This postulate is supported by experimental studies (Blackwell et al., 1959; Habermann, 1960; Benham et al., 1963 and Perkins et al., 1965). Longitudinal dispersion is a relatively unimportant factor in the growth of a finger length but very high rates of transverse dispersion can reduce the number of fingers by the suppression of smaller fingers to grow in length (Blackwell et al., 1959 and Perkins et al., 1965). The rate of growth in finger length can be approximately calculated from expression developed in several studies (Perrine, 1963; Perkins et al., 1965 and Koval, 1963).

Several mathematical models are reported in the

literature to predict how viscous fingering in a miscible displacement process can affect the recovery values and how the fingers are generated with the injection of solvent. These mathematical models will be discussed in a later section 2.4.1.2.

Density Difference: When there is a difference between the density of injected solvent and that of the in-situ oil, the displacement in a horizontal reservoir will be unstable (Nouar et al., 1983). This instability will result in the formation of gravity segregation or a gravity tongue. It means that the solvent will tend to override the in-situ oil in the shape of a tongue due to gravity segregation (Poel, 1962). The effect of a gravity tongue is to cause incomplete mixing between the solvent and oil which in turn causes low recovery of oil at the breakthrough of solvent.

Displacement Rate: A high displacement rate has an adverse effect on the immiscible displacement process and on the multiple contact miscible (MCM) process. The degree of the adverse effect is higher for an immiscible process than for a MCM process (Nouar et al., 1983). This is due to the fact that a high injection/displacement rate will propagate viscous fingering and gravity tonguing more in an immiscible displacement process than in a MCM process, where miscibility is achieved dynamically.

The effects of displacement rate on the recovery of oil at the breakthrough of solvent at a constant mobility

ratio of 93 were reported by Blackwell et al. (1959). The results of this study reveal that the higher displacement rate has an adverse effect on recovery values for a narrow laboratory model (length/width =144). But for a wider model (length/width= 3), the displacement rate has no effect on recovery values. These results are explained in the following discussion (Blackwell et al., 1959):

In a narrow model, the solvent fingers, which may grow at the initial stages of flooding, diffuse due to wall impediment as the flooding continues. This phenomenon creates a transition zone with the pure solvent at the rear end and pure oil at the front end. On the other hand, at a higher displacement rate the solvent fingers travel a longer length than that at a lower displacement rate before it diffuses. So, at higher displacement rates the transition zone is longer than that at lower displacement rates. The formation of a longer transition zone in turn renders a lower recovery efficiencies at the higher displacement rates. In the wider models, fingers do not diffuse and the displacement patterns remain unaffected by the rate.

Reservoir Heterogeneity: The term reservoir heterogeneity means that the properties of the porous medium are not uniform in all elements of volume of the reservoir. Let us suppose that in a reservoir, different layers have different permeabilities. Fluids will try to enter the layer of higher permeability and as a result layers of lower

permeability will not be swept by the injected solvent. This phenomenon will cause a low sweep efficiency of the solvent, i.e., inefficient recovery of the oil. The variation of permeability in the vertical direction of flow that accompanies fluids having an adverse mobility ratio will cause additional viscous fingering of the solvent over that in a homogeneous porous medium because the fluid of lower viscosity will tend to channel more through the higher permeable zone. This phenomenon will lead to more instability in displacement than that in a homogeneous porous medium (Blackwell et al., 1959).

2.3 Physical Simulation of Oil Recovery by Gas Injection

The oil recovery by gas or solvent injection is a complex process and involves many parameters that have to be optimized so that the process will be technically and economically successful. The important parameters that have to be optimized are the composition of solvent, displacement pressure, solvent injection rate and production rate of oil. To optimize these parameters, in-depth studies of the oil-solvent displacement characteristics, reservoir geology and oil-solvent phase behaviour are required. These studies are normally performed in laboratory displacement tests. These displacement tests are basically of two-types: slim-tube displacement and core displacement. Each of these laboratory tests provides different information necessary to design a gas

displacement process for field scale applications. Those two laboratory displacement tests will be discussed in detail in the following sections.

The minimum miscibility pressure (MMP) for a gas/solvent-oil pair can also be measured by means of a rising bubble apparatus in a shorter time compared to those required by slim-tube and core-displacement tests. The measurement of MMP by using a rising bubble apparatus will also be discussed.

2.3.1 Slim-Tube Displacement Test

The slim-tube displacement tests are carried out primarily to determine if an oil can be miscibly displaced by a particular solvent at a certain temperature and pressure. A series of experiments in a slim-tube packed with an unconsolidated porous medium are performed either for the determination of minimum miscibility pressure for a oil/solvent pair or for the screening of solvents which can miscibly displace the oil (Sayegh et al., 1981; Henry et al., 1983; and Sayegh et al., 1987).

A summary of the dimensions of the slim-tubes used by several investigators was presented by Orr et al. (1982). The inside diameters and the lengths of the slim-tubes used by different investigators vary from 0.46 cm to nearly 2 cm and from 1.5 m to nearly 26 m respectively. The porous medium generally consists of uniformly packed sand or glass beads. The packed slim-tube is first saturated with oil and then gas

is injected from one end to displace the oil at a certain temperature and pressure. The oil produced from the slim-tube passes through a sight-glass, which is for visual observation, a back-pressure regulator (BPR), and then a separator maintained at atmospheric conditions. The BPR is used to maintain constant displacement pressure at the production end. The volumes of the produced oil and gas are measured separately by means of a graduated cylinder and a gas meter, respectively. The produced gas is also analyzed. The measurements made for the slim-tube experiments include oil recovery, gas produced, pressure drop across the slim-tube, and the appearance of two phases as a function of pore volume of gas injected.

The amount of oil and gas produced and the sight glass observation data are used to determine if a displacement process is miscible or not. The criteria for determining the miscible-type displacement process based on the oil recovery values were discussed in section 2.2.2. The displacement data obtained from experiments for a particular oil-solvent pair depend on the length of the slim-tube (Gardner et al., 1981 and Nouar et al., 1983), the injection rate (Gardner et al., 1981) and the particle diameter of the packing material (Perkins et al., 1963). Thus, the determination of miscibility in a displacement process for a particular oil-solvent pair may not agree from one laboratory to another because of the variations in the dimensions of the slim-tube

apparatus, properties of the porous medium and the injection rate. Thus, the results of slim-tube experiments should include, in addition to the amount of oil and gas produced, specifications of the slim-tubes dimensions, the porous medium and the injection rates.

A systematic study of the effect of the length of the slim-tube and the effect of injection rate on the oil recovery was made by Nouar et al. (1983). One of the major conclusions by these authors is that the recovery of oil at a particular pressure increases with an increase in the length of the slim-tube. Another major conclusion is that the effect of the injection rate on the recovery of oil for a miscible process is of lesser significance than that of the length of the tube. One of the important recommendations for miscible displacement was that the length of the tube should be at least 12 m long. The injection rate would not have a significant effect on the results as long as the length of the tube is greater than the minimum length. Their conclusions and recommendation are similar to that made by other researchers (Gardner et al., 1981 and Sayegh et al., 1981).

The displacement characteristic in a slim-tube is assumed to be closest to the ideal displacement, i.e., piston-like because the tube length is very high compared to the diameter of the tube and because the porous medium is homogeneous. A homogeneous porous medium is one in which the porosity and permeability of the porous medium are uniform .

However, the displacement in a slim-tube may not always be piston-like. Displacements can be unstable depending on the dimensions of the slim-tubes and process conditions (Orr et al., 1982 and Nouar et al., 1983).

In summary, slim-tube displacement tests are effective means for investigating the miscibility between a oil-solvent pair under dynamic conditions. But, the displacement characteristic displayed in a slim-tube is not a true representation of the actual reservoir behaviour because the displacement characteristics (mixing) of fluids will be different in a reservoir due to complex heterogeneities in the rock properties of the reservoir.

2.3.2 Core Displacement Tests

Core displacement tests are used for more realistic simulation of the actual reservoir displacement phenomena than those in the slim-tube displacement tests. Core displacement tests are performed to investigate the following important factors: recovery mechanisms, diffusion and dispersion coefficients of the fluids, relative permeabilities of the fluids, rock interactions with solvent and oil and dynamic oil-solvent phase behaviour (Sayegh et al., 1981).

In a core displacement test, pieces of cores are placed inside a core holder under an overburden pressure. An important aspect of the core displacement test is the selection of cores. The cores should be sampled from the pay

zone of the reservoir such that the chosen core samples properly represent the actual rock type present in the reservoir (Sayegh et al., 1981). If the cores selected show large heterogeneities which are not the actual properties of the reservoir pay zone, then the displacement efficiency will exaggerate the effects of heterogeneities such as viscous fingering, gravity segregation and channelling (Orr et al., 1982). The types and the dimensions of the cores usually used in the laboratory for understanding the displacement mechanism were summarised by Orr et al. (1982). The most commonly used cores in laboratory experiments are sandstone types. Little work has been done with the carbonate type cores because the interactions of the carbonates with oil and solvent make the interpretations of the experimental results difficult. The length and the diameter of the core assembly may vary from 0.15 m to about 15 m and 2.5 cm to about 5 cm respectively. Each short piece of core which is placed inside the core holder, is usually 8-10 cm long (Sayegh et al., 1981).

The core assembly is flooded with brine, water and oil in proper sequence at the displacement pressure to achieve the actual saturation conditions of water, brine and oil of the particular reservoir of interest. The saturated core assembly is then flooded with solvent for the recovery of oil. As in the slim-tube displacement tests, the displaced oil passes through a sight glass to a BPR and is then flashed under atmospheric conditions. The amount of oil and gas

produced, the pressure drop across the core assembly and the visual observation through the sight glass are recorded. The oil recovery data serves as an indication of the potential of the solvent to recover oil at conditions that are closer to field displacement conditions than those in slim-tube displacements. The pressure drop data can give an indication of the changes in core permeability (Orr et al., 1982). An increase in the pressure drop means that the core permeability has decreased and vice versa. However, the mechanisms by which core permeabilities have been changed are not well known (Orr et al., 1982). A possible mechanism of the changes of permeability may be the interactions between the solvent, oil and the minerals present in cores, which in turn causes the dissolution of the cementing materials of the cores. These cementing materials may create blockage to the flow of fluids.

Core displacement tests may also be used to estimate the residual oil saturation (unrecovered oil) in the cores after the flooding by solvent (Watkins, 1978). The estimated residual oil saturation is made by measuring the oil left in each short piece of the core assembly. The other use of the core displacement results is the testing of numerical simulation results (Leach et al., 1981 and Renner et al, 1989).

2.3.3 Rising Bubble Apparatus

Experiments using a rising bubble apparatus (RBA)

provides a fast, alternative way to a slim-tube displacement test for measuring the minimum miscibility pressure (MMP) for an oil-solvent pair. RBA consists of a rectangular cross section glass tube which is mounted vertically in a high-pressure sight gauge in a temperature controlled bath (Christiansen et al., 1987). The internal dimensions of the cross section of glass tube are 1 X 5 mm, and the visible portion of the glass tube is 20 cm long. A hollow needle for injecting gas bubbles into the glass tube is placed at the bottom end of the sight gauge. A light source at the back of the sight gauge is used to enable visual observation of the bubbles in the glass tube.

The sight gauge and the glass tube are filled with distilled water and then oil is injected into the glass tube to replace all but a short column of water at the bottom end of the tube. Then, at a certain pressure a gas bubble of desired composition is injected into the tube and the shape and motion of the gas bubble are observed and photographed as the bubble rises upwards through the tube. For an oil-gas pair this experiment is repeated over a range of pressures. The characteristics of the rising gas bubbles are pressure dependent. The MMP is inferred from the pressure dependence behaviour of the rising gas bubbles. The shape and motion of gas bubbles differ significantly over the range of pressures and can be categorized into three distinct patterns (Christiansen et al., 1987):

1. At pressures far below the MMP, the bubble retains its spherical shape as the bubble rises but shrinks in size due to mass transfer from the gas phase to the oil phase. As the pressure approaches the MMP, the bubble remains spherical at the top, but the bottom of the bubble becomes flat.

2. At pressures slightly above or at the MMP, a tail consisting of tiny bubbles forms at the bottom of the bubble but at the top, the bubble remains spherical. After some time the interface between the gas/oil vanishes and the bubble disperses into the oil. This behaviour is an indication of the multiple-contact miscible process because the bubble becomes miscible with oil after repeated contact with fresh oil.

3. At pressures well above the MMP, the bubble disperses more rapidly into the oil than it does at pressures close to the MMP.

The differences in behaviour of the gas bubbles over a range of pressures are quite evident at temperatures above 120^{o} F. But at temperatures below 120^{o} F, the behaviour of the gas bubbles for CO_2/oil systems are different from those discussed earlier (Christiansen et al., 1987). As a result it becomes difficult to interpret the observations of the rising gas bubbles for the determination of the MMP. Though the determination of the MMP can be made rapidly in a RBA compared to the slim-tube displacement test, the use of this apparatus

is not widespread in the literature (Huang et al., 1991). The reasons for limited use of the RBA are: i) difficulties often arise in interpreting the visual observations of rising gas bubbles which do not follow any particular pattern discussed earlier. and ii) the mixing phenomena of gas/oil in RBA do not mimic the actual mixing that occurs in a porous medium and so the MMP measured in this apparatus may not agree with the MMP determined from slim-tube displacement tests (Huang et al., 1991).

2.4 Numerical Simulation of The Gas Displacement Process

The numerical simulation of the gas displacement process is a useful means for understanding the complex displacement phenomena. It is generally used to predict the ultimate recovery of oil and to measure the sensitivity of the predictions to various parameters of the displacement process. Numerical simulation of a process consists of three steps: i) development of mathematical models in the form of equations describing the physical process, ii) application of numerical methods to solve these equations, and iii) coding of the computer program to obtain results.

2.4.1 Models

The mathematical models for a gas displacement process consist of a set of mass conservation equations for each fluid phase (oil, gas and water) and a set of constraint

equations (example: summation of the saturation of the phases is equal to unity) for a control volume or segment of the reservoir (Aziz et al., 1979). The reservoir is treated as if it is composed of a number of segments, which are generally known as grid blocks. The models used to describe the fluid flow may involve one, two or three spatial variables.

In the mass conservation equations, the velocity of a fluid phase in a porous media is represented by Darcy's law. The basic structure of all types of mathematical models developed for a gas displacement process is based on the same principle of law of mass conservation. The model-types differ from one to another on the aspect of the mixing between the oil and the gas under the displacement conditions. The models used in numerical simulations of the gas displacement process can be categorized into three types: i) Black Oil Model, ii) Mixing Parameter Model and iii) Compositional Model.

2.4.1.1 Black Oil Model

In a black oil model, the reservoir fluid is assumed to be a binary system (Coats et al., 1967 and Lantz et al., 1970). This means that the oil and the gas each is considered individually as a single component. This assumption obviously is an over simplification because reservoir oil actually consists of a large number of components and the injected gas may also be a mixture of several components. Thus, the simulation results obtained

from the black oil model do not provide information about the actual mixing process which occurs between the in-situ oil and the injected gas (Stalkup, 1984). However, black oil simulators can provide reasonable estimates of the effects of the operating conditions, such as pressures and injection rates, on the recovery of oil and breakthrough time (Christian et al., 1981).

In a black oil model, the description of mixing is generally accomplished by considertion of a simple mass transfer between gas and oil phases. The amount of mass transfer of gas to oil depends on the bubble-point pressure of the in-situ oil or on the solution gas-oil ratio. Similarly, the amount of mass transfer of oil into the gas phase depends on the dew-point pressure of the gas phase or on the vapour oil-gas ratio (Cook et al., 1974). However, this manner of considering mass transfer between both the phases is not comprehensive (Banks et al., 1981). This is because the interphase mass transfer in a process depends on the number of parameters such as the relative volatility of each component in each phase and thermodynamic equilibrium criteria of individual components, which are not considered to determine the interphase mass transfer in a black oil model. As a result, the black oil model cannot be used to predict accurately whether a certain oil-gas pair will develop miscibility by interphase mass transfer. In conclusion, black oil models cannot be used to represent rigorously the

multicomponent mass transfer mechanisms.

2.4.1.2 Mixing Parameter Model

The mathematical models for describing the unstable displacement processes usually include parameters that serve to account for the effects of mobility ratio, heterogeneity and other causes of unstable displacement (Dougherty, 1963; Koval, 1963; Todd et al, 1972 and Fayers, 1988). The numerical values of the parameters are determined from matching the results calculated from the models with experimental results. The models are commonly known as mixing parameter models.

Koval (1963) developed a mathematical model for describing the viscous fingering in an unstable displacement process. In this model, a parameter "K" is used to account for the viscous fingering, which occurs due to a high mobility ratio between the oil and solvent, and heterogeneity in the porous medium. The fractional flow of solvent through porous media is derived from the Buckley-Leverett equation where K is a variable. This model is used to predict the recovery of oil as a function of pore volume of solvent injected. The predictions obtained from Koval's model were found to be in good agreement with the experimental data obtained by other researchers (Blackwell et al., 1959; Kyle et al., 1965 and Handy et al., 1959). The results obtained from Koval's method, however, do not always agree with the experimental

data (Perkins et al., 1965).

Dougherty (1963) proposed a mathematical model for describing the incomplete mixing in unstable displacement processes. Conceptually, the model is similar to that of Koval's model. However, Dougherty's model takes into account the effects of mixing between the oil and the injected fluid. In this model, a mixing parameter similar to that used in Koval's model is used to charcterize the viscous fingering phenomena. In addition to this, the degree of mixing between the injected solvent and oil is characterized by three more mixing parameters. Altogether, four parameters are calculated by matching the model predictions with experimental data. Because of the wide variations in the values of the parameters that are required to match experimental data at different mobility ratios of the same physical system, this method is not widely applied.

Todd and Longstaff (1972) developed a mathematical model for the simulation of oil recovery in a viscous fingering dominated displacement process by assuming that partial mixing occurs between oil and solvent. In this model, fractional flow of solvent is calculated from the Buckley-Leverett equation. The fractional flow equation includes a mixing parameter which is used to characterize the degree of mixing between the oil and the gas phases. The mixing parameter is determined by comparing the results obtained from the model with those obtined from experiments. The numerical

values for the mixing parameter for laboratory and field scale experiments were suggested by Todd and Longstaff (1972).

Recently, Fayers (1988a) proposed a model for simulating the unstable displacement process. In this model, the initiation of viscous fingers and the growth of fingers during the displacement process are correlated with two mixing parameters and the fractional flow of solvent is a function of these two parameters. One of the parameter has been assigned a constant value and the other is correlated against the mobility ratio between oil and solvent. The results obtained from the model are in good agreement with the experimental data (Fayers et al., 1988b).

The four models described above are based on the common concept that the fractional flow of solvent is altered to account for the effects of viscous fingering and heterogeneities. Comparisons of the results obtained from the three models (Koval, Todd and Longstaff and Fayers) are reported by Fayers et al. (1992). These authors suggested that Todd and Longstaff's model is most widely used in conventional field scale simulators. The principal attraction of this model is that the use of the model requires the determination of only one parameter that accounts for the effects of viscous fingering on displacement efficiency of the oil. However, all the models for unstable displacement processes are semi-empirically developed and they do not rigorously describe the thermodynamic and transport phenomena

that determine the details of the local fluid composition and flow characteristics. In all the models, it is assumed that the solvent and oil are first-contact miscible. Thus, the mixing parameter models cannot simulate satisfactorily the process where miscibility is generated upon multiple-contact.

2.4.1.3 Compositional Model

In compositional models, the oil and gas are represented by multicomponent system rather than a binary system, as in black oil models. The equations required to constitute the compositional model include the calculations of the fluid flow between the grid blocks, fluid saturations and pressures of each grid block. The equations are derived from: (1) the mass balance equation for each component , (2) Darcy's equation for flow through porous media, and (3) the thermodynamic correlations (Staggs et al., 1971). It is assumed in all the compositional models to date that the fluid phases in each grid block of the reservoir are at thermodynamic equilibrium. Based on this assumption, the equilibrium compositions of the phases coexisting in each grid block of the reservoir are calculated by equilibrium flash calculations. When cubic equations of state such as the Redlich-Kwong (Redlich et al., 1949) and Peng-Robinson (Peng et al., 1976) were not used for the calculation of the fluid compositions and the fluid properties, the flash calculations were performed by using the K (equilibrium constant)-factor

correlations which were expressed as a function of pressure (Price et al., 1967; Culham et al., 1969; Roebuck et al., 1969; Huang, 1972; Van Quy et al., 1972; Nolen, 1973 and Kazemi et al., 1978). In the compositional model, flash calculations and fluid properties have been calculated from an equation of state since the early 1980's (Coats, 1980; Nghiem et al., 1981 and Young et al., 1983). Thus, the effects of phase behaviour on the displacement characteristics of the fluids are better represented in a compositional model than those in a black oil model. The use of the compositional model aids the rigorous understanding of the mechanisms of the displacement process where multiple contact miscibility is obtained through composition dependent mechanisms such as vaporization or condensation of the hydrocarbons (Leach et al., 1981; Nghiem et al., 1986 and Williams, 1989).

The research efforts in compositional simulation are mainly directed towards the development of an efficient solution method for the equations of the compositional model and to search for efficient algorithms for phase equilibrium calculations. Generally, two numerical methods for the solution of equations in a compositional model are used. The two methods are: (1) Newton's method and (2) a quasi-Newton's method (Young et al., 1983). Coats (1980) and Fussell et al. (1979)used Newton's method for the solution of equations in the compositional model formulation. Kazemi et al. (1978) and Nghiem et al. (1981) used quasi-Newton's method for the

solution of equations in the compositional model formulation. A comparison of the three formulations of compositional simulations (Coats, Nghiem et al. and Young et al.) based on an equation of state was reported by Thele et al. (1983). These authors reported that the largest computer memory is required for the formulation of Coats (1980) and the least memory is required for the formulation of Nghiem et al. (1981). They also reported that the solution for the formulation of Young et al. (1983) requires the least computer time among these three formulations.

Calculations of oil/solvent phase behaviour using an equation of state are very difficult near the critical point of the phase envelope of the oil/solvent. Failure to perform flash calculations for the oil/solvent mixture near the critical point will lead to wrong interpretations of the simultion results (Stalkup, Jr., 1984). Constant research is being carried out for the development of efficient and robust algorithms for phase calculations (Fussell, 1979; Michelsen, 1982; Nghiem et al., 1983; Nghiem et al., 1984 and Baker et al., 1980). These studies differ with regard to their application of numerical techniques to develop a fast and robust convergence schemes for the phase calculation. Detailed discussion of these numerical techniques used for phase calculations will be presented in Chapter 4.

If the phase behaviour of the oil/solvent can be predicted with sufficient accuracy under displacement

conditions, then it is possible to simulate adequately the characteristics of the gas displacement process with a compositional model. However, the limitations of the current compositional models are as follows: (1) a large number of hydrocarbon components may be required for accurate predictions of phase behaviour of oil/solvent and (2) an inability to describe the instability in a displacement process resulting from viscous fingering, density differences between the oil and the solvent, and heterogeneities in the reservoir. The requirement of a large number of hydrocarbons to represent an oil-solvent system can be solved by grouping the heavier hydrocarbons (heavier than C_7) into a few number of pseudocomponents based on the experimental data of molecular weight, density values of heavier hydrocarbons, bubble point pressure and the solution gas-oil ratio of the oil (Young et al., 1983 and Nghiem et al., 1981).

Complete mixing of the fluids within a grid block necessarily follows for a compositional model when it is assumed that fluids are at equilibrium state. Thus, the use of the compositional model suffers from an inability to account for the incomplete mixing phenomena which results from the viscous fingering, density differences between oil and solvent and heterogeneities in the porous medium. Recently, several attempts have been made to describe incomplete mixing by the use of compositional model (Crump, 1988 and Nghiem et al., 1989).

Crump (1988) proposed a compositional model which was coupled with a mixing parameter model similar to Todd and Longstaff's (1972) model. However, the results obtained from Crump's model for the recovery of oil, especially after the breakthrough of solvent, are not in good agreement with the experimental data. The results obtained from the model are unsatisfactory because of the fact that there is an anomaly in the physical concept of coupling a mixing parameter model with a compositional model. The anomaly arises because the mixing parameter model determines the degree of mixing between the fluids in a grid block, whereas in a compositional model, equilibrium flash calculations are performed for fluids in a grid block as if fluids are completely mixed. Crump (1988) overcame this problem by creating an artificial phase envelope of the fluid mixture. However, he concluded that this approach was not theoretically sound. He suggested a different approach for describing the unstable displacement process with the use of the compositional model. This approach is based on the concept that there are two different regions of fluids in each grid block. One region is occupied by the viscous fingers and the other region is occupied by well mixed fluids and flash calculations have to be performed separately in the two regions.

Nghiem et al. (1989) reported a "fingeing model" which is used to describe the unstable displacement process. The method is conceptually similar to the approach suggested

by Crump (1988), which is to account for the fluids present in the two regions (well mixed and fingered regions) in a grid block of the reservoir. It is assumed in the model that mass transfer occurs between the two regions. The mass transfer rate of an individual component of the fluid system is calculated from a mixing parameter model which has two parameters. One of the parameters is assigned to a fixed value and the other parameter is correlated with the mobility ratios of oil and solvent. The results calculated from the model are in good agreement with the experimental data of Koval (1963), Blackwell et al. (1959), and Lacey et al. (1961). The total recovery of oil calculated from the model is less than that calculated from the equilibrium model simulation. However, comparisons of results calculated from the model with experimental data for gas displacement processes were not reported. Hence, the numerical values of mixing parameters obtained by Nghiem et al.(1989) were not tested for gas displacement processes.

2.4.2 Model Formulations

The equations used in a compositional model for mass conservations of components of a fluid system are unsteady state convection equations. The finite difference forms of the equations can be formulated in several ways based on the method of solution. The formulation where the unknown variables (pressure, saturation of the fluid phases, and composition of individual phases) are evaluated at the current

time step is called the implicit formulation and the formulation where the pressure is calculated at the current time step and the remaining unknowns are calculated at the old time step is called the implicit pressure-explicit saturation (IMPES) formulation.

2.4.2.1 Implicit Formulation

One of the advantages of the implicit formulation is that it guarantees stability in the solution of finite difference equations when one or more of the computed variables (pressure, saturation and composition) undergo large changes over a time step. The other advantage of the implicit formulation is that a large time step can be used for the solution of the finite difference equations. The implicit formulation of a reservoir simulator was first developed by Blair et al. (1969) and subsequently Weinstein et al., (1970); Coats et al. (1980) and Trimble et al. (1981) developed implicit simulators. The advantages of implicit formulations are often offset by time-truncation errors, long computation time and computer storage requirements.

Appleyard et al. (1981) reported a method to reduce the time-truncation errors by taking a new form of the time averaged relative permeability values at the current time step. However, because of considerable computation time and storage requirements, most implicit reservoir simulators do not use the fully implicit formulation (Thomas et al., 1983).

Generally, implicit formulation is used in the grid blocks where large changes in saturations and pressures occur and for the rest of the grid blocks, IMPES formulations are used (Thomas et al., 1983; Fung et al., 1989 and Collins et al., 1992). This type of formulation is called 'adaptive implicit formulation'. It is more practical for reservoir simulator because, normally, only a small fraction of the total grid blocks in a reservoir model undergo large changes in the computed variables over a time step (Thomas et al., 1983).

2.4.2.2 Implicit Pressure-Explicit Saturation Formulation (IMPES)

The IMPES formulation was first reported in studies by Sheldon et al. (1959) and Stone et al. (1961). The advantages of this formulation are smaller computing time and storage requirements than those required for the implicit formulation. Nevertheless, the risk of truncation errors resulting from this formulation is greater than that in the implicit formulation. The remedy of reducing the truncation error is to properly select the time step and grid block sizes (Aziz et al., 1979). This can be accomplished by a stability analysis of the IMPES formulation (Aziz et al., 1979). If there is no water phase present in the reservoir, the stability analysis dictates that the grid block size and time step size should be such that the volumetric flow of reservoir fluid in a time step through a single grid block should not exceed the pore volume of the grid block (Coats, 1982). Based

et al. (1979), an automatic time step selection procedure is generally adopted in an IMPES formulation. IMPES formulation with automatic time selection procedure has been applied to reservoir simulators by many researchers (Gottfried et al., 1966; Nghiem et al., 1981; Chase et al., 1984 and Nghiem et al., 1986).

2.5 Summary

The compositional model cannot be used to describe the incomplete mixing phenomenon in the displacement process because of the assumption made in the model that oil and gas are at equilibrium, i.e., at complete mixing state. The mixing parameter model is commonly used to describe the incomplete mixing phenomenon in an unstable displacement process. However, the use of the mixing parameter model is unable to account for the compositional effects of the oil and the gas on the mechanisms of displacement process.

In this study, a compositional model with the assumption that fluids are at non-equilibrium during the displacement process, is developed. A non-equilibium phase behaviour calculation procedure is used where the degree of incomplete mixing between the oil and gas phases, is determined by the use of a mixing parameter model. The results obtained from the numerical simulation using the non-equilibrium calculations are compared with that obtained from euilibrium calculations and experimental data.

CHAPTER 3

SLIM-TUBE EXPERIMENTS

3.1 Scope

Usually slim-tube experiments are performed to determine the minimum miscibility pressure for a particular oil and solvent pair and to evaluate the potential of the solvent to recover the oil. The slim-tube experiments are also performed to investigate the effects of injection rate and compositions of the solvents and oils on the displacement mechanisms and recovery efficiencies of the displacement processes. The effects of solvent composition on oil recovery for miscible displacement processes were studied by other researchers, but the effects of solvent composition on oil recovery for near miscible and immiscible displacement processes have not been studied extensively.

The effects of injection rate on oil recovery for miscible displacement processes are reported in the literature, but the effects of injection rate on oil recovery for immiscible displacement processes were not studied by other researchers. The objectives of the experiments are summarised as follows:

(1) To investigate the effects of solvent composition on oil recovery for miscible, near miscible and immiscible displacement processes.

(2) To investigate the effects of the heavier

components in oil on the recovery efficiency and the displacement mechanisms.

(3) To investigate the effects of injection rate of solvents on the recovery of oils for miscible and immiscible displacement processes.

Data obtained from slim-tube experiments are useful for the validation of the results obtained from numerical simulation of displacement processes. In this study, data obtained from slim-tube experiments are used to validate the results obtained from a one dimensional compositional reservoir simulator, in which a non-equilibrium phase behaviour model was used.

3.2 Equipment

The slim-tube apparatus used in this study (see Figure 3.1) consisted of:

a. An injection system which was used to displace fluid at constant injection rate.

b. An unconsolidated porous medium (slim-tube).

c. A sight glass (observation of the fluid at the outlet end).

d. A back pressure regulator for continuous downstream pressure control.

e. A separator at atmospheric conditions, a condenser and metering devices for the liquid and gaseous phases.

f. A gas-chromatograph (GC) for the analysis of gaseous phases.

g. Two high-pressure floating piston cylinders (500 ml each) to store oil and injection gas.

h. Two Heise digital pressure gauges (Model 710 A), one of which was connected to the upstream end of the slim-tube and the other to the downstream end of the slim-tube.

A Ruska double cylinder type positive displacement pump was used as the injection system. The discharge rate of the pump could vary from 2.5 to 560 ml/hr per cylinder.

The slim-tube utilized was 24.4 m long. It consisted of four interconnected 316 S.S. tubes (O.D of 0.635 cm), each of which was 6.1 m long. The tube was packed with 100 mesh Ottawa sand which is a specially graded natural silica sand. A 250 mesh steel filter was securely placed at each end of tube.

A Ruska high-pressure sight glass (Model No. 2328-702) was connected to the downstream end of the slim-tube. It allowed observation of the effluents at the operating conditions of the displacement processes.

A back-pressure regulator (BPR) was connected to the downstrem end of the sight glass to control the displacement pressure. The outlet of the BPR was at atmospheric conditions. The device, which was designed by Fausto Nicola (Calgary, Alberta), allowed the downstream pressure to be accurately controlled (±0.02 MPa of the desired value).

The oil was flashed at the outlet of the BPR under atmospheric conditions. The produced liquid was collected in

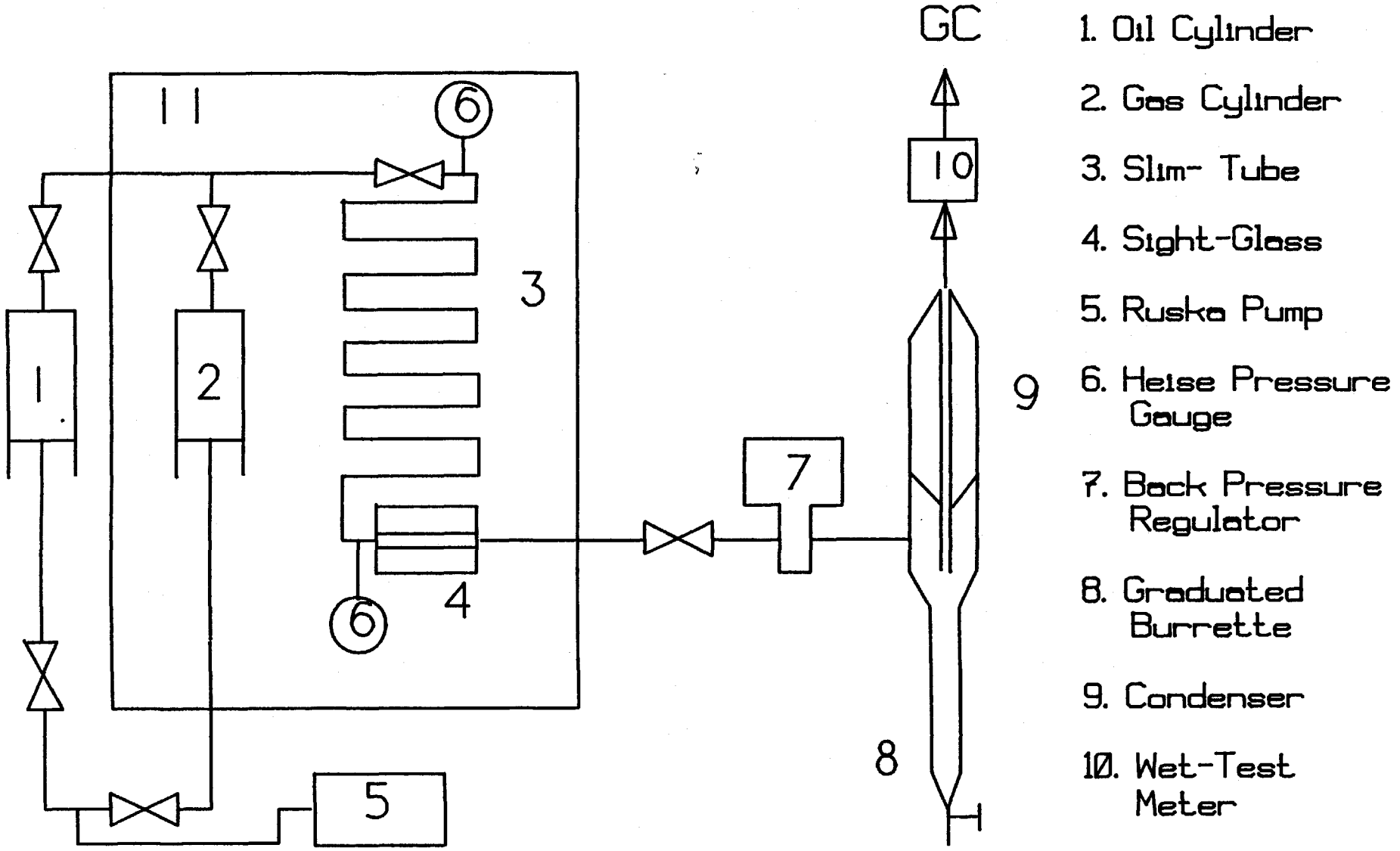

Figure 3.1: Schematic Diagram of the Slim-Tube Apparatus

a 250 ml graduated burette. The produced gas passed through a condenser prior to entering a wet-test meter which was used to measure the cumulative volume of the produced gas. The produced gas was analyzed in a Hewlett-Packard GC (Model 5830 A).

The floating piston gas cylinder, the slim-tube and the sight glass were placed inside a constant temperature air-bath. A light source was placed inside the temperture bath to enable clear observation through the sight glass.

3.3 Materials

The compositions of oil mixtures used in the experiments are shown in Table 3.1 and those of the gases are shown in Table 3.2. The compositions of the oil mixtures and the gas mixtures are chosen based on the objectives mentioned earlier and particularly C_1-nC_4-nC_{10} system is selected because the experimental data for this ternary system is readily available in the literature.

Table 3.1: Composition of Oil Mixtures

Oil #	Mole Fraction		
	C_1	nC_4	nC_{10}
A	0.000	0.498	0.502
B	0.252	0.191	0.557
C	0.000	0.060	0.940
D	0.000	0.020	0.980

Table 3.2: Composition of Gas Mixtures

Gas #	Mole Fraction C_1	C_3	nC_4
A	1.000	0.000	0.000
B	0.844	0.000	0.156
C	0.701	0.299	0.000
D	0.799	0.100	0.101

The n-decane of 99% minimum purity, the n-butane of 99.5% minimum purity and the methane of 99.5% minimum purity were used to prepare the oil mixtures. The oil mixtures were prepared by Matheson Gas Products Canada (Edmonton) within ±0.2% of the analyzed compositions. Each oil mixture was supplied in a 1 gallon cylinder at a pressure below the bubble-point pressure of the particular oil mixture.

Pure methane and other gases of ultra high purity grade were used in the experiments. All the gas mixtures were supplied at 100-200 psia pressure. Methane was supplied at 2000 psia pressure. All the hydrocarbons except n-decane were supplied by Matheson Gas Products Canada (Edmonton), and n-decane was supplied by Fisher Scientific Company (Edmonton).

3.4 Preparation for Experiments

The preparation for the experiments consisted of four steps. The first step was to bring the prepared oil mixture to a single phase state. This process was defined as the handling of oils. The second step was to transfer the gas or gas mixture from the supplier's cylinder to the high pressure floating piston cylinder placed inside the bath at

the desired displacement pressure. This process was defined as gas fill-up technique. The third step was the cleaning of the slim-tube. The fourth step was the start up procedure of the experiments which was defined as the start up technique.

3.4.1 Handling of Oils

The oil mixture, at a pressure well below its bubble-point pressure, was supplied in 1 gallon storing cylinder. To bring the oil mixture to a single liquid phase state, water was injected stepwise at the bottom of the storing cylinder. At each step, pressure was raised by 300 psia, and the storing cylinder was shaken for about 30 minutes to allow the components of the oil to be well mixed. This process was repeated until the storing cylinder pressure was well above the bubble-point pressure of the particular oil mixture. The storing cylinder pressure was raised to 1200 psia and the storing cylinder pressure was maintained at 1200 psia throughout the use of that particular cylinder.

The volume of oil in the storing cylinder was calculated by taking the difference between the volume of the cylinder and the volume of water injected to raise the pressure. For a particular experiment, a sufficient amount of oil was transferred from the storing cylinder at a constant pressure of 1200 psia to the floating piston cylinder so that approximately 325 ml of oil was present in the floating piston cylinder at the displacement pressure. Oil from a storing cylinder was used until 100 ml of oil was left in that

cylinder. The last 100 ml of oil was not used in the experiments to avoid possible contamination of oil by water at the interface.

3.4.2 Gas Fill-up Technique

It was mentioned earlier that except for pure methane, all other gas mixtures were supplied at low pressures (100-200 psia). At low pressure, it was not possible to transfer a sufficient amount of gas from the supply cylinder to the floating piston cylinder at the displacement pressure which was about 15-20 times higher than the pressure of the supply cylinder. This problem was circumvented by the following process:

The gas mixture was transferred to a 1000 ml floating piston cylinder from the supply cylinder, then gas in the floating piston cylinder (booster cylinder) was boosted to an intermediate pressure which was approximately half of the displacement pressure. The gas was transferred at this constant intermediate pressure from the booster cylinder to the floating piston cylinder which was placed inside the constant temperature air bath. This process was repeated until the floating piston cylinder was full. Gas in the floating piston cylinder was again boosted to the specified displacement pressure. Approximately, 5-6 hours were allowed for raising the temperature of the gas to the temperature of the air bath, which was maintained at the displacement temperature.

3.4.3 Tube Cleaning Procedure

If the slim-tube was at a high pressure, it was depressurized by opening its production end to atmospheric conditions. Toluene was then injected in the slim-tube at a constant rate of 10 ml/hr to clean the porous medium and, simultaneously, a vacuum was drawn at the production end for 5 hours. Toluene saturation was continued until 1 PV of toluene was injected. Then, the slim-tube pressure was raised to the specified displacement pressure and an additional 1.5 PV of toluene was cycled through the slim-tube at a rate of 20 ml/hr. At this stage, the slim-tube was considered to be clean. The cleaning procedure was selected after consultation with D.B. Robinson & Associates Ltd. (Edmonton).

3.4.4 Start-up Technique

The slim-tube was saturated with the oil under the displacement pressure and temperature at an injection rate of 7.5 ml/hr. The total volume of oil injected in the slim-tube was approximately 2 PV. It was found in practice that the gas-oil ratio of the oil was established after an injection of 1.2-1.3 PV of the oil. At least 7-8 hours were required to bring the oil temperature to the temperature level of the air-bath.

The back pressure regulator (BPR) was fine tuned by a hand screw pump to the required displacement pressure. The outlet end of the slim-tube was connected to the BPR and 15 minutes were allowed to make the BPR pressure steady.

Pressure at the inlet end of the slim-tube was raised by 20-30 KPa above the displacement pressure. The inlet valve to the slim-tube was opened and the Ruska pump was set at the constant volumetric discharge rate to inject the gas into the slim-tube.

3.5 Design of Experiments

A set of fifteen experiments was chosen. The description of each experimental condition are shown in Table 3.3. The selection of groups of experiments for the analysis of data are described in the following.

To investigate the effect of solvent composition on oil recovery, data for three pairs of experiments (experiments 2 and 13; experiments 3 and 4; and experiments 10 and 9) were analyzed.

To investigate the effect of oil composition on oil recovery, data for two pairs of experiments (experiments 1 and 14; and experiments 7 and 8) were analyzed.

To investigate the effect of injection rate on recovery, data for three pairs of experiments (experiments 1 and 15; experiments 11 and 12; and experiments 5 and 6) were analyzed.

To investigate the effect of displacement pressure on the recovery, data for three pairs of experiments (experiments 1 and 10; experiments 3 and 13; and experiments 2 and 9) were analyzed.

The operating temperature of 160 ^{o}F (71 ^{o}C) was

selected for all experiments, which is a common characteristic temperature of actual reservoirs. The operating pressures of the experiments were chosen in such way that the displacement mechanisms for most of the experiments would be immiscible. This was done because the results obtained from numerical simulations with a new phase behaviour model, which was primarily developed to describe the incomplete mixing phenomena, could be compared with the experimental results.

Table 3.3: Descriptions of Experimental Conditions

Experiment #	Oil #	Gas #	Pressure (psia)	Injection Rate (PV/hr)
1	A	A	3430	0.096
2	A	B	2390	0.096
3	A	C	2700	0.096
4	A	D	2700	0.096
5	B	D	2700	0.096
6	B	D	2700	0.048
7	B	C	2700	0.096
8	D	C	2940	0.096
9	A	B	2700	0.096
10	A	A	2700	0.096
11	A	A	3100	0.096
12	A	A	3100	0.127
13	A	C	2390	0.096
14	C	A	3430	0.096
15	A	A	3430	0.048

3.6 Results

The physical characteristics of the slim-tube, pore

volume and total permeability of the slim-tube were measured. The measurement procedure is described in Appendix A. Pore volume of the slim-tube was 156.9 cc and the liquid permeability was 22.0 E-12 m^2.

Experimental data were collected as a function of time. Time was converted to PV of gas injected by multiplying the time by the injection rate in terms of PV/hr. The recovery of oil, the pressure drop across the slim-tube and the cumulative gas-oil ratio (GOR) were obtained with respect to the PV of the gas injected. Cumulative GOR is the ratio of cumulative volume of the gas produced and the cumulative volume of the oil produced. A sample calculation for converting the raw data to processed data for experiment 1 is shown in Appendix A. The raw experimental data are presented in Appendix A. Breakthrough time (appearance of gas at the production end) and the total volume of gas produced were also obtained. Experiments are arbitrarily repeated to determine the reproducibility of the results. It is found that the recovery data could be reproduced within 2%.

The experimental results are summarised in Table 3.4. It can be seen from Table 3.4 that recoveries of oil for experiments 3 and 15 are above 90%. According to the criterion of identifying a multiple contact miscible (MCM) process ,i.e, more than 90% recovery at 1.2 PV of gas injection, these experiments can be identified as MCM displacement processes. The displacement mechanism in

Table 3.4 : Summary of Experimental Results

Experiment #	Total PV of gas Inj.	Total % Recovery of Oil	Total Gas produced in litre	B.T* time in PV of gas inj.
1	1.270	89.55	1.37	1.120
2	1.075	49.40	3.91	0.880
3	1.220	94.32	1.05	1.140
4	1.195	69.15	4.65	0.780
5	1.174	52.62	11.36	0.780
6	1.171	61.78	9.86	0.785
7	1.220	71.40	12.79	0.910
8	1.270	54.81	-	N.O**
9	1.176	58.00	3.81	0.990
10	1.290	56.41	2.15	1.160
11	1.380	73.93	2.78	1.220
12	1.240	67.24	7.75	0.980
13	1.170	59.60	-	N.O
14	1.220	47.48	1.25	1.090
15	1.220	91.20	1.59	1.150

*** Breakthrough**
**** Not obtained**

Experiment 1 may be identified as a near MCM process because almost 90% recovery of oil is obtained after 1.2 PV of gas injection. All other experiments are immiscible displacement processes which are evident from the corresponding oil recovery values.

To illustrate the characteristics of recovery, pressure drop and GOR profiles with respect to PV of gas injected, each of those profiles for experiment 1 are shown in Figures 3.2, 3.3 and 3.4, respectively. Figure 3.2 shows that at the initial stages of gas injection (approximately

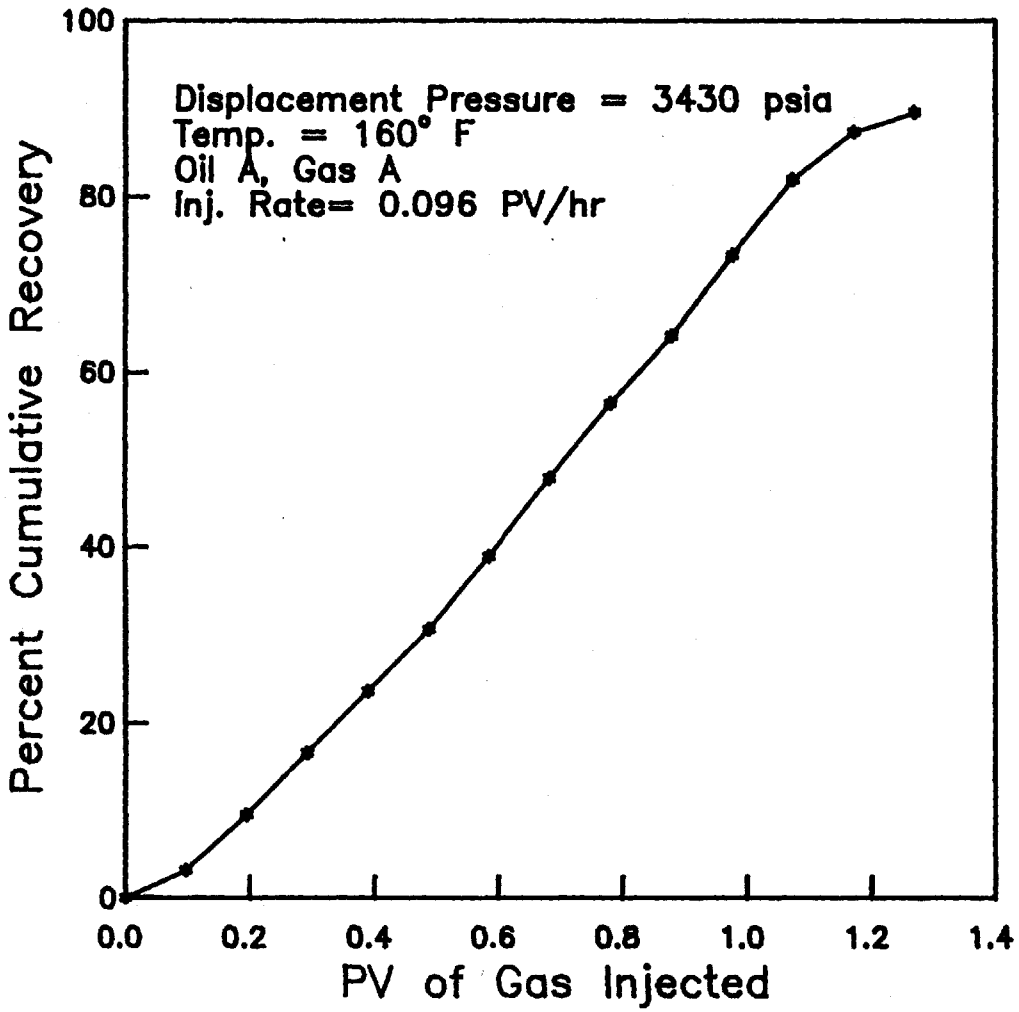

Figure 3.2 :Recovery Profile for Experiment 1

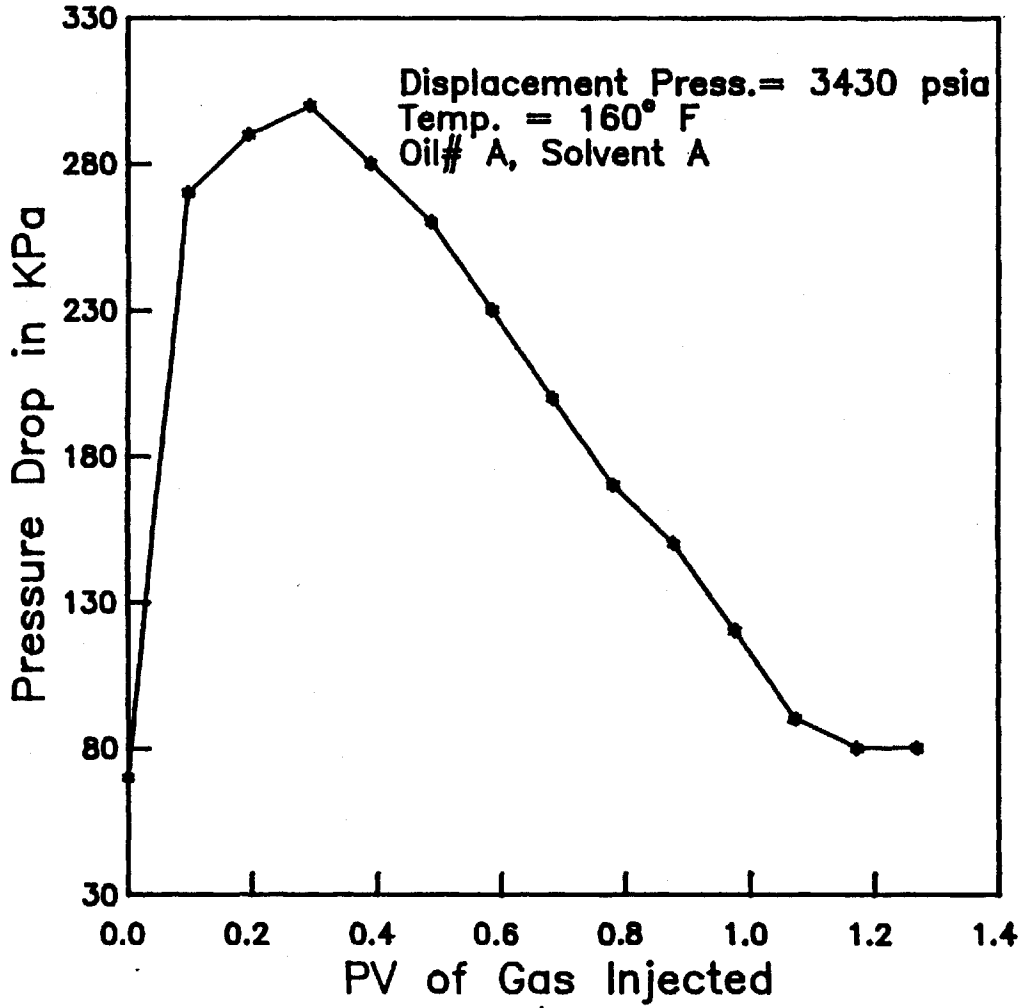

Figure 3.3 Pressure Drop Profile Across Slim Tube For Experiment 1

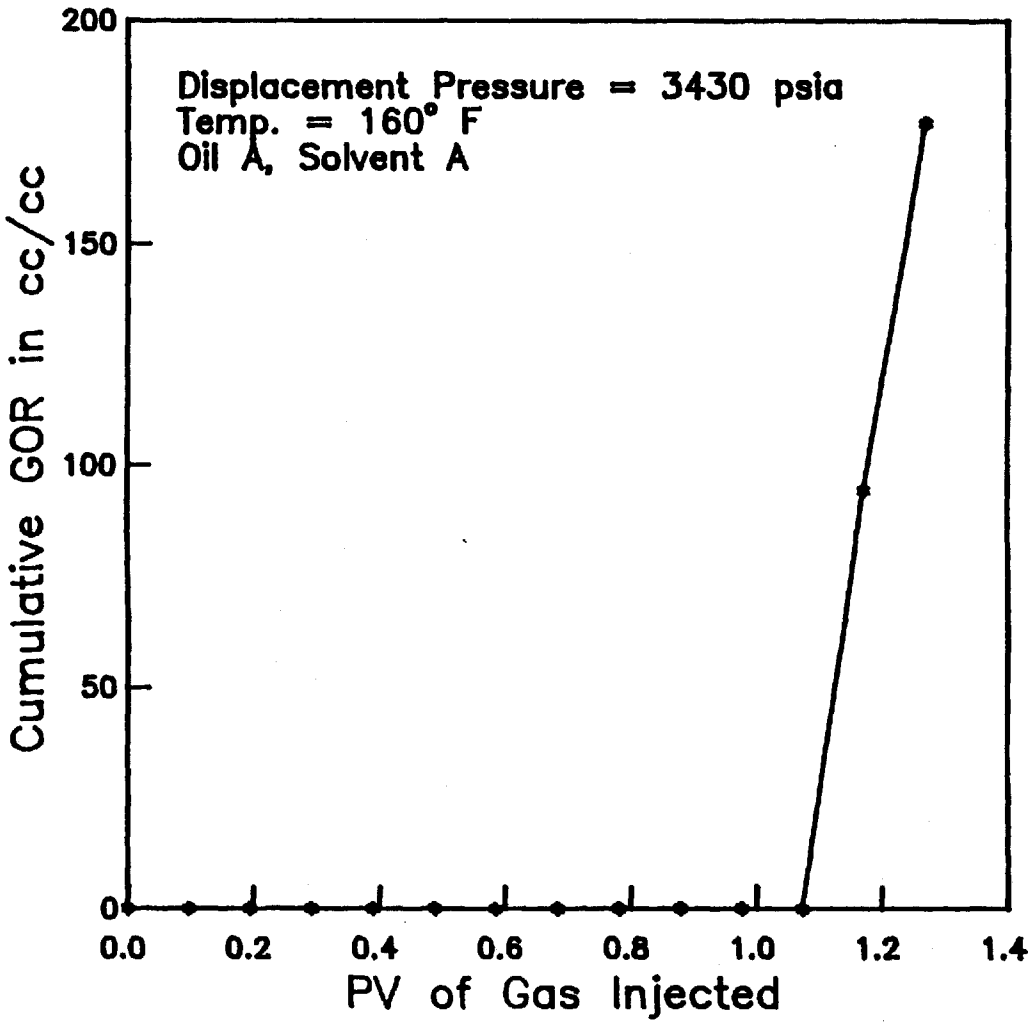

Figure 3.4: Gas–Oil Ratio Profile for Experiment 1

until 0.1 PV), the recovery rate is lower than that of the rest of the period of gas injection until breakthrough is obtained at approximately 1.1 PV of gas injection. The rate of recovery is almost identical during 0.1 PV to 1.1 PV of gas injection. After the breakthrough, gas production starts and the rate of gas production increases rapidly during this period. This observation can be verified from Figure 3.4. Figure 3.4 shows that the gas-oil ratio increases sharply after the breakthrough because of the increased production of gas. This behaviour of the recovery curve can be observed from Figure 3.2. If gas injection is continued for a longer period after breakthrough the recovery profile will be flat. Similar characteristics of recovery and GOR profiles are observed for other experiments.

The pressure drop profile (Figure 3.3) for experiment 1 is of a parabolic nature. The pressure drop reaches a maximum after certain time and then gradually falls. After the breakthrough, the pressure drop becomes constant, which can be observed in Figure 3.3. Pressure drop profiles for other experiments are similar to the profile shown in Figure 3.3.

3.7 Discussion

The discussion of the experimental results is presented in the following four sections. The analysis of the results are made based on the summary of experimental results shown in Table 3.4.

3.7.1 Effects of Solvent Composition on Results

To investigate the effect of solvent or gas compositions on the results obtained from the experiments, four experiments (Experiments 10, 9, 3 and 4) which were performed with oil A and four different gases at fixed pressure 2700 psia, are chosen. If the richness of the gases are categorized based on their capability to recover oil; the richness of gases in ascending order is: gas A, gas B, gas D and gas C.

Experiment 3 is identified as a MCM process and all other experiments are identified as immiscible processes. The earliest breakthrough time (0.78 PV) is observed in experiment 4. It is to be observed that with increasing recovery values the breakthrough time does not necessarily follow the same pattern (i.e., delayed). In experiment 4, C_3 is not present in the gas phase after the breakthrough, although injected gas D contains 10 mole percent of C_3. The reason behind this phenomenon may be explained by the fact that C_1 in the gas overrides C_3 to reach the mixed zone (contact zone of oil and gas) and when gas production starts C_1 comes out with nC_4 which is present in oil A. However, in experiment 3, after the breakthrough, (1.14 PV) the produced gas contains C_3. This phenomenon indicates that in experiment 3, C_3 present in gas C moves along with C_1 into the mixed zone. However, this is not the case in experiment 4 where gas D is used. This contrasting behaviour between experiment 3 and experiment 4

suggests that in a MCM process (experiment 3) mixing between the injected gas and oil is better than that in an immiscible process (experiment 4). Comparing the recovery values between experiment 3 and 4, it may be inferred that increasing the intermediate hydrocarbon in the injected gas by 10 mole percent (comparing compositions of gases C and D) may cause a significant increase in the oil recovery and change the mechanism of the displacement process.

As expected, among the four experiments, the lowest recovery is obtained in experiment 10 as gas A is the least rich gas. However, in experiment 10 breakthrough occurred later than that observed in experiments 9 and 4. This observation is contrary to the usual concept that for a lean injected gas, breakthrough occurs early because of the channelling phenomenon.

Experiments 2 and 13 were performed with the same oil A and with gas B and gas C, respectively at 2390 psia. Higher recovery is obtained in experiment 13 than that in experiment 2 because gas C is richer in intermediate components than gas B. At lower displacement pressure (2390 psia) the difference in recovery values is not as high as those observed between experiments 3 and 4. This observation may be explained by the fact that in experiments 3 and 4, the difference in gas composition changes the displacement mechanism from MCM to immiscible, but, in experiments 2 and 13, the difference in gas composition does not change the

displacement mechanism.

3.7.2 Effects of Oil Compositions on Results

To investigate how the heavy hydrocarbon component of oil affects the displacement process, results of two pairs of experiments were analysed (experiments 1, and 14; experiments 7 and 8). Experiments 1 and 14 were performed with the same gas A at the same pressure (3430 psia) with different oils A and C, respectively. It is evident from the corresponding recovery values that experiment 14 is an immiscible process but experiment 1 is a close MCM process. However, the breakthrough time and the total amount of gas produced are almost the same in both of the experiments. The mole fractions of C_1 in the produced gas after 1.17 PV of gas injection are 0.92 in experiment 14 and 0.62 in experiment 1. This observation may be explained by the argument that since there is a higher density gradient between oil and gas in experiment 14 than that in experiment 1, channelling of the gas phase due to a density gradient has occurred more in experiment 14 than that in experiment 1. The channelling phenomenon is also observed through the sight-glass. Similar arguments can be drawn by comparing the results of experiment 7 with those of experiment 8, although those experiments were performed at two different pressures, 2700 psia and 2940 psia, respectively.

3.7.3 Effects of Injection Rate on Results

To investigate the effects of injection rate on miscible displacement and immiscible displacement processes, results of the three pairs of experiments (experiments 1 and 15; experiments 11 and 12; and experiments 5 and 6) are compared. The injection rate of gas in experiment 1 was 0.096 PV/hr and that in experiment 15 was 0.048 PV/hr. It was mentioned earlier that experiment 1 is considered to be a near MCM process. Nouar et al. (1983) reported that in MCM process there is no significant increase in oil recovery at the lower injection rate of gas. Comparing the recovery value of experiment 1 with that of experiment 15, it is observed that 1.8% increase in recovery is achieved at the lower injection rate in experiment 15. The breakthrough time and the total amount of gas produced are almost the same in both of those experiments (15 and 1). This phenomenon may be explained by the fact that the frontal advancement of the three zones usually present in miscible displacement processes are of similar nature in the above two experiments. The three zones are oil front followed by miscible or mixed front and gas front. The cause for the higher recovery at a lower injection rate may be attributed to the fact that the formation of a longer miscible front at the lower injection rate improves the sweep efficiency of the injected gas.

The injection rates for experiments 11 and 12 are 0.096 PV/hr and 0.127 PV/hr, respectively. Oil and gas

compositions for both these experiments are the same and have the same displacement pressure of 3100 psia. These two experiments are identified as immiscible displacement processes. Breakthrough occurred earlier in experiment 12 (0.980 PV) than that in experiment 11 (1.22 PV). Recovery of oil is 6.67% higher in experiment 11 than that in experiment 12 and the amount of total gas produced is higher in experiment 12 than that in experiment 11. The differences in results between these two experiments are similar to that observed between experiments 1 and 15. However, the magnitude of the differences between experiments 11 and 12 are greater than those between experiments 1 and 15.

In immiscible displacement processes, higher recovery and late breakthrough are obtained at a lower injection rate because of the better formation of a mixed zone than that obtained at a higher injection rate. A mixed or miscible zone cannot form fully in an immiscible displacement process, because two phases are formed after a series of contact between the fresh oil and gas.

Comparing the results of experiment 5 with those of experiment 6, it is observed that approximately a 7.5% increase in recovery is obtained at the lower injection rate (0.048 PV/hr) in experiment 6 than that obtained at the higher injection rate (0.096 PV/hr) in experiment 5. This is similar to the differences observed between experiments 11 and 12. However, unlike the differences in results between experiment

11 and 12, in this pair of experiments (5 and 6) there are no significant differences in the amount of total gas produced and breakthrough time. These observations in experiments 5 and 6 may be explained by the fact that channelling of the gas, because of density segregation between oil and gas, is less than that in experiments 11 and 12. In experiments 11 and 12, the density difference between oil A and gas A is higher than that between oil B and gas D, which are used in experiments 5 and 6. It may be concluded that at a lower density ratio between oil and gas, the effect of low injection rate results in only increased oil recovery, whereas at a higher density ratio between oil and gas, the effect of injection rate manifests itself in affecting not only the recovery, but also the breakthrough time and the amount of gas produced.

3.7.4 Effects of Pressure on Results

Experiments 1, 10 and 11 were performed with oil A and gas A, and with the same injection rate at different pressures. The pressure studies show an increased total oil recovery at higher pressures and a higher amount of gas production at lower pressures. It is observed from these experiments that decreasing the displacement pressure by approximately 350 psia decreases the recovery values by approximately 15%.

Experiment 2 and experiment 9 were performed with

oil A and gas B at 2390 psia and 2700 psia, respectively. The recovery value decreases by 9% with a decrease in displacement pressure of approximately 300 psia. The only difference between the operating conditions of experiments (1, 10 and 11) and those of experiments (2 and 9), other than operating pressures, is that the former set of experiments were performed with gas A, which is less rich, compared with gas B, which was used in the latter set of experiments. Hence, it may be concluded that for rich gas the effect of pressure on recovery is less pronounced.

A significant difference in total oil recovery is observed between experiments 3 and 13. These experiments were performed with oil A and gas C at 2700 psia and 2390 psia, respectively. It is evident from the corresponding total oil recovery values that experiment 3 is a MCM process whereas experiment 13 is an immiscible process. Thus, it may be inferred that, if a pressure difference causes the change of displacement mechanism, then a significant difference in recovery is obtained.

CHAPTER 4

NUMERICAL SIMULATION

4.1 Reservoir Model

The reservoir model describes the flow of oil and gas through a porous media by the use of Darcy's law. Capillary and gravitational forces are neglected in the formulation. Capillary force arises due to the pressure difference existing across the interface of two immiscible flluids in a capillary or porous system. The capillary force is neglected because it is assumed that there is no water present in the reservoir. The gravitational force is not taken into account because it is assumed in the formultion that the reservoir is horizontal.

The model takes into account the thermodynamic behaviour of the hydrocarbon components of oil and gas by the use of an equation of state. The primary objective of developing the model is that it can be used to simulate the oil recovery process which can be immiscible or multiple-contact miscible.

4.1.1 Mathematical Model Description

The material balance equation for a component m in each grid block of the reservoir (shown in Figure 4.1) is

$$A_x\left(\sum v_{jx}\rho_j y_{mj}\Big|_x - \sum v_{jx}y_{mj}\Big|_{x+\Delta x}\right) + A_y\left(\sum v_{jy}\rho_j y_{mj}\Big|_y - \sum v_{jy}\rho_j y_{mj}\Big|_{y+\Delta y}\right) +$$

$$A_z\left(\sum v_{jz}\rho_j y_{mj}\Big|_z - \sum v_{jz}\rho_j y_{mj}\Big|_{z+\Delta z}\right) + Q_m = V_b\phi\frac{\partial}{\partial t}\left(\sum \rho_j S_j\right) z_m \qquad (4.1)$$

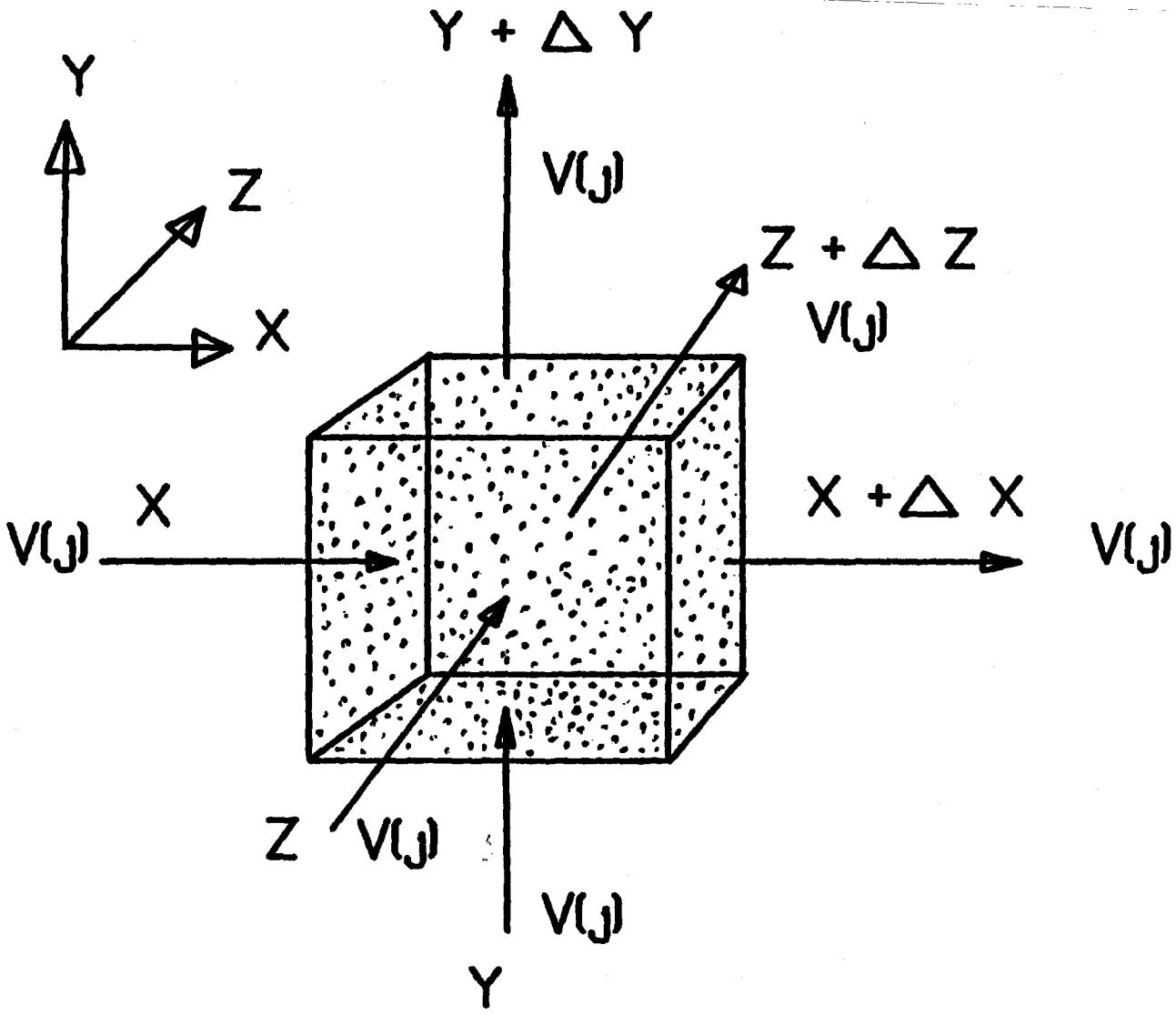

Figure 4.1: A Three Dimensional Grid Block of the Reservoir

where j=o,g ; m=1,...N_c ; N_c = number of components;

v_j = velocity of fluid phase j in porous medium.

According to Darcy's law,

$$v_{jx}=-\frac{KK_{rj}}{\mu_j}\frac{\partial P_j}{\partial x} \tag{4.2}$$

Equation (4.1) may be written in the differential form,

$$A_x\Delta x\frac{\partial}{\partial x}\left(\sum v_{jx}\rho_j y_{mj}\right)+A_y\Delta y\frac{\partial}{\partial y}\left(\sum v_{jy}\rho_j y_{mj}\right)+A_z\Delta z\frac{\partial}{\partial z}\left(\sum v_{jz}\rho_j y_{mj}\right)$$

$$+q_m=V_b\phi\frac{\partial}{\partial t}\sum\left(\rho_j S_j\right) z_m \tag{4.3}$$

If fluid flow is considered only in the x-direction, equation (4.3) reduces to the following form:

$$A_x\Delta x\frac{\partial}{\partial x}\left(\sum v_{jx}\rho_j y_{mj}\right)+q_m=V_b\phi\frac{\partial}{\partial t}\left(\sum\rho_j S_j\right) z_m \tag{4.4}$$

where j=o,g and m=1,..N_c

Darcy's equation can be substituted into equation (4.4) to give the following equation:

$$A_x\Delta x\frac{\partial}{\partial x}\left(\frac{KK_{ro}}{\mu_o}\rho_o y_{mo}\frac{\partial P}{\partial x}+\frac{KK_{rg}}{\mu_g}\rho_g y_{mg}\frac{\partial P}{\partial x}\right)$$

$$+q_m=\frac{V_b\Phi}{\Delta t}\Delta_t\left(\rho_o S_o+\rho_g S_g\right) z_m \tag{4.5}$$

The finite difference form of equation (4.5) is as follows:

$$\frac{A_x\Delta x}{\Delta x}\Delta_x\left(\frac{KK_{ro}}{\mu_o}\rho_o y_{mo}\frac{\Delta P}{\Delta x}+\frac{KK_{rg}}{\mu_g}\rho_g y_{mg}\frac{\Delta P}{\Delta x}\right)$$

$$+q_m=\frac{V_b\phi}{\Delta t}\Delta_t\left(\rho_o S_o+\rho_g S_g\right) z_m \tag{4.6}$$

Let T_j, the transmissibility of phase j, be defined as;

$$T_j=\frac{A_x K K_{rj}}{\mu_j \Delta x}\rho_j \qquad (4.7)$$

where j= o, g

By introducing T_j into equation (4.6), a simple equation is obtained

$$\Delta_x(T_o y_{mo}\Delta P+T_g y_{mg}\Delta P)+q_m=\frac{V_b\phi}{\Delta t}\Delta_t(\rho_o S_o+\rho_g S_g)\, z_m \qquad (4.8)$$

where m=1,...,N_c

The expansion of the differential form on the left hand side of equation (4.8) is shown in Appendix B.

Using the above equation and summing over all N_c components the flow equation for each grid block is obtained. The flow equation is

$$\Delta_x(T_o\Delta P+\Delta T_g\Delta P)+q_h=\frac{V_b}{\Delta t}\Delta_t(\rho_o S_o+\rho_g S_g) \qquad (4.9)$$

where $q_h = \Sigma\ q_m$ (4.10a)

and

$$q_m=T_o y_{mo}\Delta P+T_g y_{mg}\Delta P \qquad (4.10b)$$

q_h will be zero for all grid blocks except for the injection and production grid blocks. A constant injection rate is assumed in the formulation. q_h is positive for an injection grid block and is negative for a production grid block.

It is assumed in the compositional reservoir model that oil and gas phases are in thermodynamic equilibrium in each grid block of the reservoir. The thermodynamic constraint equation will be the equality of fugacity criterion;

$$f^{L}_{m} = f^{V}_{m} \qquad (4.11)$$

where $m=1,\ldots N_c$

The other constraint equations are the sum of the mole fractions of all the components in each phase must equal unity and the sum of the saturation of the phases must also equal unity.

$$\sum x_m = 1.0 \qquad (4.12)$$

$$\sum y_m = 1.0 \qquad (4.13)$$

where $m=1,\ldots,N_c$

$$S_o + S_g = 1.0 \qquad (4.14)$$

Equations (4.8), (4.11), (4.12), (4.13) and (4.14) add up to a total of $2N_c+3$ equations which are to be solved for each grid block of the reservoir for the $2N_c+3$ unknowns which are x_m's, y_m's, P, S_o and S_g with the following boundary conditions.

The boundary conditions are defined as follows;

i) q_h= constant for all t, i.e., constant rate of injection.

ii) P_{outlet}= constant for all t, i.e., constant pressure at the outlet end of the reservoir.

4.1.2 Solution Method

The semi-implicit formulations of the flow equation (4.9) and composition equation (4.8) are used. In the semi-implicit formulation, the compositions and saturations of the phases are calculated at the previous time step and the pressure is calculated at the current time step. This formulation is called Implicit Pressure Explicit Saturation(IMPES). A Quasi-Newton iteration scheme is used to solve the flow equation (4.9).

4.1.2.1 Quasi-Newton Scheme

The flow equation (4.9) can be rewritten in the following form:

$$\Delta_x T_o^{\,n} \Delta P^{n+1} + \Delta_x T_g^{\,n} \Delta P^{n+1} + q_b - \frac{V_b}{\Delta t}(\alpha^{n+1} - \alpha^n) = 0.0 \qquad (4.15)$$

where $\alpha = \rho_o S_o + \rho_g S_g$ and n is the index of time.
If f_i be left hand side of equation (4.15) for the i th grid block of the reservoir and P^l be the l th iterate of P^{n+1}, then the (l+1)th iterate of P^{n+1} can be obtained from the following Newton-like iteration;

$$\sum_k J_{ik}^{(l)} [P_k^{(l+1)} - P_k^{(l)}] = -f_i^{(l)} \qquad (4.16)$$

where i=1,...,n_b , n_b= number of grid blocks, k=index of adjacent grid blocks which are the (i-1)th and the (i+1)th grid blocks.

J_{ik} is the approximate Jacobian and the sum in equation (4.16)

is over the ith grid block and its adjacent grid blocks. J_{ik} is computed as follows;

$$J_{ik}^{(1)} = \left(\frac{\partial f_i}{\partial P_k}\right)^{(1)} = (T_o + T_g)^n_{(i+k)/2} \qquad (4.17)$$

and

$$J_{ii}^{(1)} = \left(\frac{\partial f_i}{\partial P_i}\right)^{(1)} = -\sum_{k \neq i} (T_o + T_g)^n_{(i+k)/2} + \left(\frac{\partial q_b}{\partial P}\right)_{(i)}^{i} - \frac{V_b}{\Delta t}\phi \left(\frac{\partial \alpha}{\partial P}\right)_i \qquad (4.18)$$

where the subscript (i+k)/2 denotes the interface between grid blocks i and k.

In equation (4.18), the actual partial derivative of α involves the partial derivatives of the saturation of the phases and partial derivatives of the density of the phases. The density of a phase at a constant temperature is a function of the composition, pressure and compressibility of the phase. It was mentioned earlier that the composition and saturation of the phases are calculated explicitly. If the dependencies of the phase composition and saturation on pressure are neglected, the partial derivative of α with respect to pressure may be approximately calculated from the following equations;

$$\left(\frac{\partial \alpha}{\partial P}\right)_i^{(1)} = \left(S_o \frac{\partial \rho_o}{\partial P} + S_g \frac{\partial \rho_g}{\partial P}\right)_i^{(1)} \qquad (4.19)$$

$$\rho_j = \frac{P}{Z_j RT} \qquad (4.20)$$

$$\frac{\partial \rho_j}{\partial P} = \frac{1}{RTZ_j}\left(1 - \frac{P}{Z_j}\frac{\partial Z_j}{\partial P}\right) \qquad (4.21)$$

where j= o, g, and the analytical expression for the partial derivative of Z_j with respect to pressure is shown in Appendix B.

The partial derivative of q_h with respect to pressure is;

$$\frac{\partial q_h}{\partial P} = -(T_o + T_g)^n \qquad (4.22a)$$

for the production grid block and

$$\frac{\partial q_h}{\partial P} = 0 \qquad (4.22b)$$

for the injection grid block

Since in this formulation, a constant injection rate is assumed, the derivative in equation (4.22b) is zero for the injection block.

To solve a system of non-linear equations does not always require an exact Jacobian. An approximate Jacobian is calculated in this solution scheme. The compositions and saturations are updated explicitly after each iteration. This solution method is intermediate between the successive substitution method and Newton's method.

If equations (4.17) and (4.18) are evaluated, the Jacobian matrix defined in equation (4.16) will be symmetric and strictly diagonally dominant. Equation (4.16) is solved for P^{l+1} by the direct matrix elimination method.

Once $P^{(l+1)}$ is determined, the composition of each component in each grid block of the reservoir is obtained by rearrangement of equation (4.8):

$$z_m^{(l+1)} = \frac{\Delta [(T_o y_{mo} + T_g y_{mg})^n \Delta P^{(l+1)}] + q_m + \frac{V_b}{\Delta t}\phi(\rho_o S_o + \rho_g S_g)^n z_m^n}{\frac{V_b}{\Delta t}\phi(\rho_o S_o + \rho_g S_g)^{(l+1)}} \qquad (4.23)$$

The denominator of equation (4.23) is obtained from the rearrangement of equation (4.9):

$$\frac{V_b}{\Delta t}\phi(\rho_o S_o + \rho_g S_g)^{(l+1)} = \Delta [(T_o + T_g)^n \Delta P^{(l+1)}] + q_h + \frac{V_b}{\Delta t}\phi(\rho_o S_o + \rho_g S_g)^n \qquad (4.24)$$

Two-phase flash calculations are performed on $z_m^{(l+1)}$, $m=1,\ldots,N_c$ at $P^{(l+1)}$ to obtain (l+1)th iterate of the compositions and densities of the phases at each grid block of the reservoir. Based on the results of the flash calculations, the saturations of the phases are calculated from the following equations;

$$S_o^{(l+1)} = \left(\frac{L\rho_g}{L\rho_g + V\rho_o}\right)^{(l+1)} \qquad (4.25)$$

and

$$S_g^{(l+1)} = 1 - S_o^{(l+1)} \qquad (4.26)$$

A new method for flash calculations is developed in this study and is described in section 4.2.1.

Algorithm

The steps involved in the solution method are shown in the following flow chart (Figure 4.2):

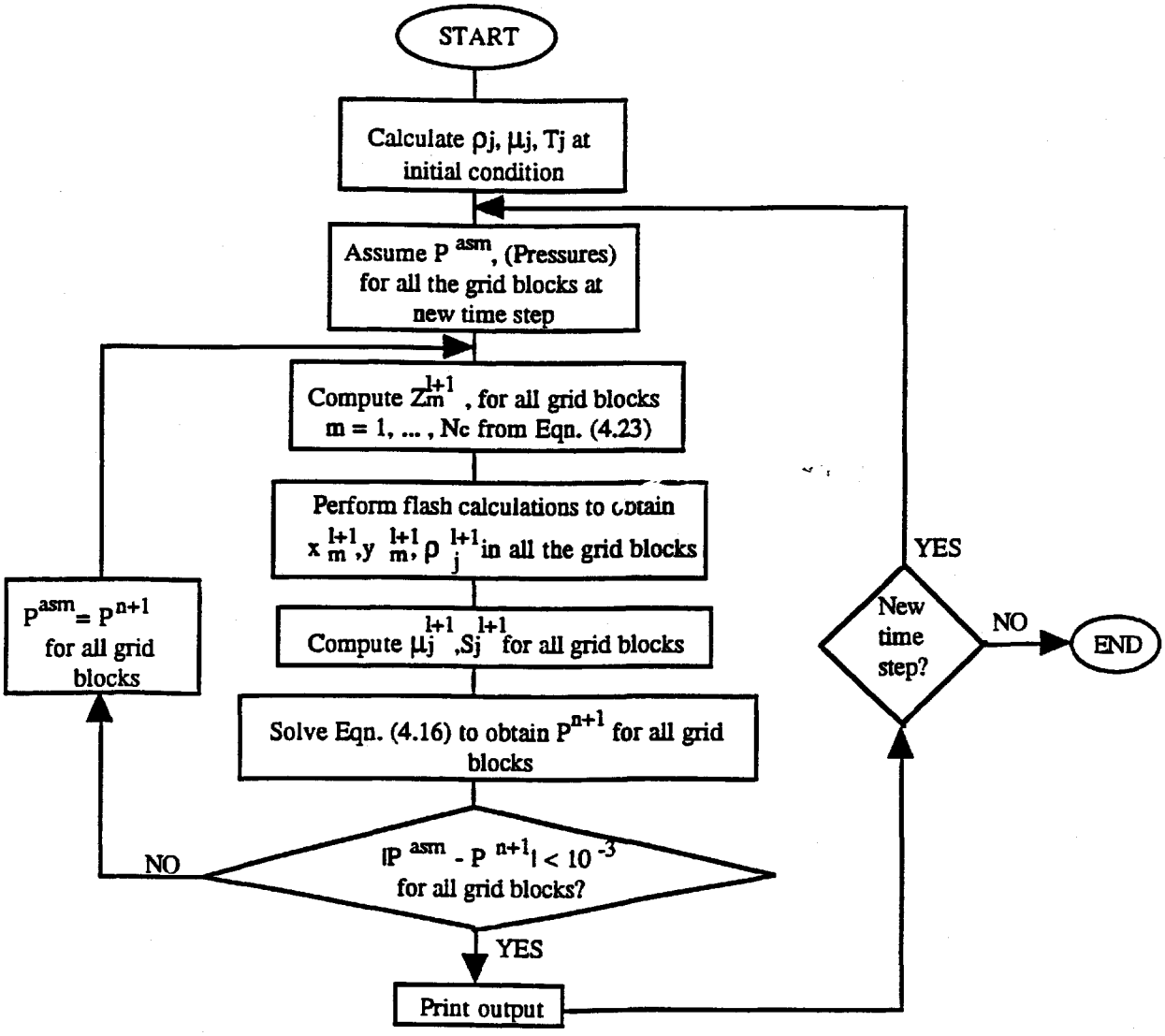

Figure 4.2: Flow Chart for Reservoir Simulator

4.1.2.2 Numerical Dispersion Control

To eliminate the effects of numerical dispersion in the simulation results, the following steps were used:

1) The size of grid blocks and the time steps are selected such that the Courant number of each grid block should always be less than unity. The Courant number for a grid block is defined by $u \Delta t/\Delta x$, where u is the velocity of a fluid phase, Δt is the time step and Δx is the length of the grid block. A predetermined value for the size of the grid block is chosen, and to satisfy that condition only a time step has to be selected. The time step selection procedure is as follows:

The Courant number of each grid block is calculated at each time step with the fluid phase (oil or gas) having the greater velocity. The velocities of fluid phases in a grid block are calculated from Darcy's equation. If the Courant number in a grid block is not less than unity, the time step value is adjusted to satisfy this condition. Once the time step is calculated by this method for each grid block of the reservoir, the smallest value of the time step is chosen.

2) A two-point upstream weighting for compositions and single point upstream weighting for the transmissibilities of the phases were used. The detailed formula for the two-point upstream weighting and the single point upstream weighting is described in Appendix B.

4.2 Phase Behaviour Calculations

Phase behaviour calculations include two-phase flash calculations and saturation pressure calculations.

4.2.1 Two-Phase Flash Calculations

4.2.1.1 Background

Two-phase flash calculations at isothermal and isobaric conditions are commonly used in the chemical industry and in reservoir simulations. In this study, flash calculations are used in the reservoir simulation.

The set of equations required to formulate the isothermal-isobaric two-phase flash calculations are as follows:

Material Balance Equations:

$$L + V = 1.0 \tag{4.27}$$

$$Lx_m + Vy_m = z_m \tag{4.28}$$

$$m = 1, \ldots\ldots, N_c$$

L and V are liquid and vapour fractions respectively. x_m, y_m and z_m are liquid, vapour and feed mole fractions, respectively, of an individual component m.

Constraint Equations:

$$\sum_m (y_m - x_m) = 0 \tag{4.29}$$

$$f_m^L = f_m^V \qquad (4.30)$$

$m=1,\ldots,N_C$

f_m's are the fugacities of component m in the phases and are calculated from an equation of state. Equations (4.27) to (4.30) constitute a set of $(2N_C+2)$ equations which are to be solved for liquid and vapour mole fractions (x_m, y_m), liquid fraction (L) and vapour fraction (V).

Solution Method for Flash Calculations

y_m and x_m can be correlated by the following equation which is an alternative form of equation (4.30):

$$y_m = K_m x_m \qquad (4.31)$$

$m=1,\ldots,N_C$

K_m is the equilibrium constant for component m. Combining equations (4.31), (4.27) and (4.28), x_m and y_m can be expressed in the following forms:

$$x_m = \frac{z_m}{1+(K_m-1)V} \qquad (4.32)$$

$$y_m = \frac{K_m z_m}{1+(K_m-1)V} \qquad (4.33)$$

$m=1,\ldots,N_C$

The following equation is obtained by incorporating x_m and y_m

from equations (4.32) and (4.33), respectively, into the constraint equation (4.29):

$$\sum_m \frac{(K_m-1)\,z_m}{1+(K_m-1)\,V}=0 \qquad (4.34)$$

If a set of K_m's are assumed from the Wilson equation (Wilson, 1969), equation (4.34) becomes a function of V. Then equation (4.34) can be expressed as follows:

$$g(V) = 0 \qquad (4.35)$$

Equation (4.35) is a monotonically decreasing function of V and the root of V between zero and one is possible only if the following two conditions are satisfied:

$$\sum_m K_m z_m > 1 \qquad (4.36)$$

$$\sum_m \frac{z_m}{K_m} > 1 \qquad (4.37)$$

Once equations (4.36) and (4.37) are satisfied by the set of assumed value of K_m's, equation (4.35) can be solved for V by Newton's method. Using the value of V and the assumed set of K_m's, x_m's and y_m's are calculated from equations (4.32) and (4.33), respectively. Subsequently, fugacities of the phases are calculated by using the Peng-Robinson equation of state which is described in Appendix C. If the equilibrium condition defined by equation (4.30) is not satisfied, K_m's are updated for the next iteration. The updating procedure of K_m depends on the numerical technique employed for the

iteration. Basically, there are two types of numerical methods, successive substitution (SS) and Newton's method, which are used for the iterative procedure involved in flash calculations.

Successive Substitution (SS)

K_m's are updated according to the following equation:

$$K_m^{l+1}=K_m^l\times\left(\frac{f_m^L}{f_m^V}\right)^l \qquad (4.38)$$

$m=1,\ldots,N_c$

The advantages of SS method are that it is computationally faster (approximately 6.5 times using the VAX 8650) than Newton's method and is more tolerant to wild initial guesses of the iteration variables (K_m) than Newton's method. For flash calculations near the critical region of the phase envelope, where fugacity coefficients are strongly dependent on phase compositions, the convergence speed of the SS method is slow. The large number of iterations required in these situations outweigh the advantages of the SS method.

Newton's Method

In this study, the logarithm of K_m is used as an iteration variable for the implementation of Newton's method in two-phase flash calculations. The objective function to be solved by Newton's method is the modified form of the constraint equation (4.30).

$$F_m = \ln f_m^L - \ln f_m^V = 0 \qquad (4.39)$$

$m=1,\ldots,N_c$

The iteration variables are updated according to the following equation:

$$J\Delta \ln K = -F \qquad (4.40)$$

$\Delta \ln K$ is the correction vector and F is the objective function vector. J is the Jacobian matrix which is calculated from the following equation:

$$J_{mj} = \frac{\partial F_m}{\partial \ln K_j} \qquad (4.41)$$

whee $j=1,..,N_c$

Calculation of the Jacobian matrix and solving equation (4.40) at every iteration step requires extra computation time compared with that of the SS method. The other disadvantage of the Newton's method is that iterations may diverge because of bad initial guesses of the iteration variables. This problem prohibits the use of Newton's method to start the iteration process. However, the advantage of Newton's method over the SS method is that the convergence speed of Newton's method is superlinear in comparison with the linear convergence speed of the SS method.

4.2.1.2 Existing Algorithms

The SS method slowly converges near the critical point of the fluid mixture because of its inherent linear

convergence speed. Several algorithms have been proposed to accelerate the convergence speed of the SS method .

Risnes (1980) proposed an acceleration scheme for the SS method to be used in flash calculations. According to this proposed scheme, the acceleration step was taken as the following step:

$$K_m^{l+1}=K_m^{l}R_m^{l(\frac{1}{1-k})} \qquad (4.42)$$

where R_m is the fugacity ratio and k is calculated from the following equation:

$$k=\frac{R_m^{l}-1}{R_m^{l-1}-1} \qquad (4.43)$$

The limitation of this method is that the acceleration step has to be rejected if it does not bring the fugacity ratios closer to unity.

Michelsen (1982) proposed an acceleration scheme for flash calculations based on the general dominant eigenvalue method (GDEM) of Crowe et al. (1975). Michelsen suggested a method where each acceleration step was taken after five iteration steps of the SS method. If the iteration process did not converge after two acceleration steps, iteration was completed by Newton's method.

Mehra et al. (1983) proposed three algorithms for the acceleration of the SS method for flash calculations. These acceleration schemes were based on the concept that SS method might be regarded as a method of steepest descent for

free energy minimization. Acceleration of the iteration process was obtained by multiplying equation (4.38) with a factor for updating the iteration variables. This factor was calculated at each iteration step and there was a set upper limit for the value of the factor. Similar to the schemes proposed by Mehra et al. (1983), Nghiem et al. (1982) suggested an acceleration scheme which is known as the quasi-Newton scheme.

Gupta et al. (1988) proposed two acceleration schemes for SS method based on the dominant eigenvalue method of Orbach et al. (1971) and the general dominant eigenvalue method of Crowe et al. (1975), respectively. Liquid and vapour mole fractions were used as iteration variables in these schemes instead of the equilibrium factors (K_m) which were used in all the acceleration schemes discussed earlier. Each acceleration step was taken after three iteration steps by the SS method.

Several researchers have employed Newton's method in different ways for flash calculations and other equilibrium calculations. Fussel et al. (1978) developed a minimum variable Newton-Raphson (MVNR) algorithm for two-phase flash calculations. Fussel (1979) later extended that algorithm to be used for three-phase flash calculations. The other algorithms for flash calculations using Newton's method were reported by Hirose et al. (1978), Asselineau et al. (1979), Michelsen (1980) and Kinoshita et al. (1986). All the

algorithms differ from each other on the basis of formulations of equations and selection of iteration variables.

The alternative forms of Newton's method were used for flash calculations by Nghiem et al. (1983) and Boston et al. (1978). Nghiem et al. (1983) used Powell's hybrid method and Boston et al. (1978) used an approximate Newton's method where Jacobian matrices were calculated by numerical extrapolation.

4.2.1.3 Development of a Coupled Algorithm

The dominant eigenvalue method (DEM) of Orbach et al. (1971) is used as an acceleration means and ln K_m's are chosen as iteration variables. According to the DEM, the linearly convergent iteration scheme such as the SS method can be approximated by the linear difference equation of the following form:

$$\Delta \ln K^{l+1} = A \Delta \ln K^{l} \qquad (4.44)$$

where ln K is the vector of iteration variables, A is the iteration matrix and l is the iteration index. The iteration matrix is denoted by,

$$A_{mj} = \frac{\partial \ln K_m^{l+1}}{\partial \ln K_j^{l}} \qquad (4.45)$$

where $j=1,\ldots,N_c$

and $K_m^{(l+1)}$ is defined by,

$$K_m^{l+1}=\frac{\Phi_m^{L(l)}}{\Phi_m^{V(l)}} \qquad (4.46)$$

where Φ_m^L is the fugacity coefficient of component m in the liquid phase and Φ_m^V is the fugacity coefficient of component m in the vapour phase.

Equation (4.44) may be expanded according to the following equation:

$$A_{mj}=\sum_{i=1}^{N_c}\left(\frac{\partial \ln\Phi_m^L}{\partial x_i}\frac{\partial x_i}{\partial \ln K_j}-\frac{\partial \ln\Phi_m^V}{\partial y_i}\frac{\partial y_i}{\partial \ln K_j}\right) \qquad (4.47)$$

where N_c is the number of iteration variables, x_i is the mole fraction of component i in the liquid phase and y_i is the mole fraction of component i in the vapour phase.

It is assumed in the DEM that there is only one dominant eigenvalue (λ_1) of the iteration matrix A. In that case, the solution of equation (4.44) is only possible if λ_1 is less than unity. λ_1 is calculated according to the following equation:

$$|\lambda_1|=\frac{\|\Delta \ln K^l\|}{\|\Delta \ln K^{l-1}\|} \qquad (4.48)$$

where

$$\|X\|=\sqrt{\langle x, x\rangle} \qquad (4.49)$$

The sign of λ_1 is determined from the ratio of components of

$\Delta \ln K^{l}$ and $\Delta \ln K^{l-1}$. If the successive values of λ_1 are close, then equation (4.44) holds well. Thus, the acceleration step will be;

$$\ln K^{l+1}=\ln K^{l-1}+\frac{(\ln K^{l}-\ln K^{l-1})}{1-\lambda_1} \qquad (4.50)$$

The first acceleration step is taken after 3 iteration steps by the SS method and the subsequent acceleration steps are taken when the successive values of $|\lambda_1|$ are within 10%. However, in the vicinity of the critical region of fluid mixtures, at least two eigenvalues of the iteration matrix, A, are of equal magnitude and close to unity which is shown in section 5.1.1. Hence, the basic assumption of the DEM does not hold, i.e., only one dominant eigenvalue exists for the iteration matrix. Thus, acceleration step by DEM will not be effective. The remedy of this problem is to switch to another iteration method. It is proposed that the iteration method may be switched to Newton's method.

The key point is to select the switching criteria. The following switching criteria are proposed based on the extensive testing of the flash calculations:

i) $R_c^{-1} > 10$ and ii) Number of Acceleration Steps > 2

R_c is the rate of convergence and the value of R_c is equal to the logarithm of the largest eigenvalue of the iteration matrix.

$$R_c=-\log_{10}|\lambda_1| \qquad (4.51)$$

The reason behind choosing the rate of convergence as a switching criterion is that rate of convergence is an indicator of the number of iterations required to obtain the solution. When the value of R_c is greater than 10, two eigenvalues of the iteration matrix, A, will be of comparable magnitude. This finding will be discussed in section 5.1.1. The second switching criterion is incorporated to overcome the disadvantage of undertaking too few acceleration steps.

Once, the iteration method is switched to Newton's method there are two options to perform the calculations; i) iteration is completed by Newton's method after the switch over and ii) iteration is performed by Newton's method until the successive eigenvalues of the iteration matrix become close, and then bring back the iteration method to the acceleration method of DEM.

In short, the two-phase flash calculation is started with the acceleration method by DEM using ln K_m's as iteration variables and after changing to the iteration by Newton's method, iteration is completed by either of the two options mentioned above. The first option will be referred as Scheme 1 and the second option as Scheme 2. Two Newton's steps are taken in scheme 2 before the iteration method is brought back to the acceleration method by DEM. The computer program for flash calculations using the algorithm developed in this study, is provided in the Appendix E.

4.2.2 Saturation Pressure Calculations

4.2.2.1 Background

Saturation pressures calculation of mixtures at a particular temperature are an important part of computational phase equilibria. Saturation pressure calculations are used in this study to check the results of flash calculations. If a single phase is obtained by flash calculation for a mixture at a particular temperature and pressure, the saturation pressure is calculated for that mixture to check whether or not the pressure at which the flash calculation is performed, is more than the saturation pressure.

The algorithms frequently used for saturation pressure calculations are similar to the algorithms used for flash calculations, i.e., SS method and Newton's method. The iteration variables are the saturation pressure (bubble-point or dew-point) and the compositions for N_c-1 components of the incipient phase (vapour or liquid). The initial value of the saturation pressure is assumed from the following equations (Peng, 1991):

$$P^{o}-\sum x_m p_m=0 \qquad (4.52a)$$

for bubble-point prediction

$$P^{o}\sum y_m/p_m-\prod p_m^{y_m}=0 \qquad (4.52b)$$

for dew-point prediction

where P^{o} is the inital value of the saturation pressure and

$$p_m = P_{Sm} \quad \text{when } T \le T_{cm} \tag{4.52c}$$

$$= (P_{Sm}\, P_{cm})^{0.5} \quad \text{when } T > T_{cm} \tag{4.52d}$$

P_{sm} and the values of K_m are calculated from the Wilson's equation (Wilson, 1969);

$$K_m^{(0)} = P_{Sm}/P^0 \tag{4.52e}$$

where

$$P_{Sm} = P_{cm} \exp\,[5.373\ (1+\omega_m)(1 - T_{cm}/T)] \tag{4.52f}$$

Successive Substitution Method (SS)

The iteration variables for saturation pressure calculations are updated in the SS method according to the following procedure:

$$y_m^{l+1} = K_m^{l+1} z_m \tag{4.53}$$

m=1,....,N_c-1; for bubble-point pressure

$$x_m^{l+1} = \frac{z_m}{K_m^{l+1}} \tag{4.54}$$

m=1,...,N_c-1; for dew-point pressure

$$p^{l+1} = p^l \left[2 - \frac{1}{\sum K_m^{l+1} z_m}\right] \tag{4.55}$$

for bubble-point pressure

$$p^{l+1} = p^l / \sum \frac{z_m}{K_m^{l+1}} \tag{4.56}$$

for dew-point pressure

K_m is updated from equation (4.38). The updating procedure of pressure in the SS method is empirical. It is assumed in the updating procedure that at constant temperature K-factors are inversely proportional to the pressure.

Newton's Method

The objective function to be solved in Newton's method for saturation pressure calculations is an alternative form of equation (4.39):

$$F_m=\frac{f_m^L}{f_m^V}-1=0 \qquad (4.57)$$

$m=1,\ldots,N_c$

Equation (4.57) is a function of the set of N_c variables (P and compositions of the N_c-1 components).

The iteration procedure of Newton's method may be written in the following form:

$$X^{l+1}-X^l=-J^{-1}f(X^l) \qquad (4.58)$$

where X is the vector of iteration variables, J is the Jacobian matrix and F is the vector of the objective function (equation 4.57). The Jacobian matrix is calculated by the following equation:

$$J_{mj}=\frac{\partial F_m}{\partial X_j} \qquad (4.59)$$

$m=1,\ldots,N_c$ and $j=1,\ldots,N_c$

4.2.2.2 Algorithms for Saturation Pressure Calculation

It was mentioned earlier that the SS method shows poor performance near the critical region of the mixture because of its linear convergence speed . On the other hand, the evaluation of the Jacobian matrix and its inverse in Newton's method, particularly for systems involving a large number of components, demands considerable computational effort at every iteration. More recently, a number of researchers have proposed alternative solution methods.

The newer methods include the different kinds of accelerated SS schemes which are described in section 4.2.1.2 (see for example, Risnes et al. (1981), Michelsen (1982) and Mehra (1983)) and hybrid methods such as the one developed by Powell (1970) and adapted by Nghiem et al (1983). These methods are usually applied to flash calculations to show their superiority over the conventional solution methods. An exception is a paper by Nghiem et al. (1985). These authors applied an accelerated SS algorithm (in particular, Algorithm 3) proposed by Mehra et al. (1983) in their quasi-Newton scheme for saturation-point calculations to correct the K-factors and showed that the quasi-Newton scheme is generally more reliable than the three multivariate Newton methods they developed.

More recently, Peng (1991) has shown that the Algorithm 1 proposed by Mehra et al. (1983) for flash calculations can also be applied to saturation-point

calculations.

There are several multivariate Newton formulations for saturation-point calculations. Among the more notable ones that involve the application of an equation of state in the calculations are those proposed by Fussel et al. (1979, 1978), Asselineau et al. (1979), Baker et al. (1980), Michelsen (1980) and Nghiem et al. (1985). Peng et al. (1976, 1977) have also presented an algorithm for bubble-point and dew-point calculations using Newton's method. The various Newton methods differ in the number and type of iteration variables used in the formulations. Depending on the choice of independent variables, the size of the Jacobian matrix for N_c-component system can be either $N_c x N_c$ or $(N_c+1) \times (N_c+1)$. It may be inferred that a formulation based on the use of a $N_c \times N_c$ Jacobian should be computationally more economical than a formulation which is based on a larger Jacobian. The algorithm proposed by Peng et al. (1976, 1977) is based on the use of a $N_c \times N_c$ Jacobian. The procedure can be described by use of equations (4.57), (4.58) and (4.59).

Unfortunately, because of less-than-quadratic convergence rates of the accelerated SS schemes, the number of iterations required in an accelerated SS method is generally greater than that required using Newton's method. This is particularly true for calculations near critical regions, where Newton's method is still the preferred choice. Newton's method shows a quadratic convergence rate under certain

conditions when the iterates are close to the solution (Ortega et al., 1970). However, quadratic convergence rate and the numerical stability of Newton's method may not be achieved if the Jacobian matrices are singular or near to singularities (Griewank, 1985). This situation may arise when Newton's method is applied to calculations near the critical region of the fluid mixtures. However, despite its instability problem Newton's method is able to achieve a solution with desired accuracy which is acceptable at the singularities. (Griewank, 1985). This property of the Newton's method encourages researchers to develop acceleration schemes for Newton's method by keeping the iteration scheme unchanged at the singularities or near singularities of the Jacobian matrices.

The acceleration schemes for Newton's method are the following (Griewank, 1985); i) Richardson extrapolation, ii) Overrelaxation, iii) Bordering by a singularity condition, and iv) Appending a linear model by a quadratic term. The last two acceleration schemes require the determinations of the derivatives of the Jacobian matrices which are cumbersome and difficult procedures for the saturation pressure calculations. The first two methods are described in Appendix D.

4.2.2.3 Development of an Acceleration Algorithm

The Newton's algorithm based on Peng et al. (1976, 1977) is applied in the calculation of saturation pressures

for selected mixtures and its convergence behaviour is studied. It is observed that in all cases the convergence of the iterates becomes monotone without oscillation after only a few iterations. This benign characteristic of Newton's algorithm suggests that the convergence promotion may be realized by taking into consideration the behaviour of the iterates.

From a study of the performance of the above-mentioned Newton's method for a number of hydrocarbon mixtures typically encountered in the hydrocarbon processing and petroleum industry, the following acceleration algorithm is developed for calculating the saturation pressures:

For each component m, m=1,...,N_c

Step 1. Calculate the rate of change of mole fraction according to

$$d_{mj}=\frac{(X_m^{1}-X_m^{(1-j)})}{j} \qquad (4.60)$$

where j= 1, 2 and 3.

X_m is the mole fraction of m in the incipient phase.

Step 2. Select the d_{mj} which corresponds to the steepest slope

$$s_m=Max(d_{m1}, d_{m2}, d_{m3}) \qquad (4.61)$$

Step 3. Choose the appropriate sign for the correction term

$$\epsilon_m = Sign(s_m, d_{m1}) \tag{4.62}$$

Step 4. Revise the mole fraction according to

$$X_m^1 = X_m^1 + r\epsilon_m \tag{4.63}$$

where the relaxation parameter r is chosen to be 0.7 for the bubble-point calculations and 1.2 for the dew-point calculations. The relaxation parameters are selected based on the extensive testing of the saturation pressure calculations. The variation of each of the relaxation parameter in the vicinity (±0.2)of its selected value will only increase the the number of iterations.

Step 5. Normalize the mole fractions.

The first acceleration step is taken after three iterations using Newton's method and the subsequent acceleration steps are taken thereafter at an interval of every three iterations, when necessary. However, an acceleration step is not taken if the error norm is already less than 10^{-5}. The error norm is defined as

$$\text{Error norm} = F^T F \tag{4.64}$$

The computer programs for saturation pressure calculations are provided in the Appendix E.

4.3 A Non-Equilibrium Phase Behaviour Model

4.3.1 Introduction

The compositional reservoir model was discussed in section 4.1. The assumption made in that model is that the fluids in the reservoir are at equilibrium. Thus, to describe the phase behaviour of the fluids, the equilibrium criterion is used, i.e., there is an equality of fugacity of each component in both liquid and vapour phases. However, under dynamic conditions the fluids may not be at equilibrium in the reservoir. In other words under dynamic condition fluids may not be completely mixed.

There has been continuing efforts by researchers (see for example Blackwell et al., 1959; Haberman, 1960; Koval, 1963; Dougherty, 1963; Todd et al., 1972; Crump, 1988; and Nghiem et al., 1989) to describe the incomplete mixing phenomena under the displacement conditions. Except for the work of Crump (1988) and Nghiem et al. (1989), in all other work, the major assumptions made in developing the model are that the fluid mixture involved in the displacement process consists of two components, oil and gas, and fluids are incompressible. These models may be categorised generally as 'mixing parameter ' models which were described in section 2.4.1.2. However, for displacement processes which are not first contact miscible, mixing parameter models do not perform well because they are unable to account for the thermodynamic exchanges of the components between the oil and gas phases.

Crump (1988) and Nghiem et al. (1989) incorporated the mixing parameter models into the compositional model to describe the unstable displacement processes. They used different mixing parameter models to simulate the incomplete mixing in a displacement process. The major assumption made in those two compositional models is that fluids are at thermodynamic equilibrium in each grid block of the reservoir.

In reality, fluid phases are arbitrarily distributed over the grid block and may not get sufficient contact time under dynamic conditions to attain a thermodynamic equilibrium state. Thus, it is reasonable to anticipate that incomplete mixing in a displacement process may be described more rigorously by incorporating a mixing parameter model into the compositional model where non-equilibrium flash calculations are performed at each grid block of the reservoir. Based on this anticipation, an attempt is made to develop a phase behaviour model which can be used to calculate the phase compositions of fluids at non-equilibrium states. The assumption made in developing the model is that the two phases (oil and gas) are heterogeneously distributed in the grid block of the reservoir. The vapour phase and the liquid phase do not represent thermodynamic equilibrium states because of the heterogeneous distribution of the phases and the availability of less dynamic contact time to reach an equilibrium state.

4.3.2 Model Description

The equality of fugacity criterion at equilibrium is

$$f^{L}_{m} = f^{V}_{m} \qquad (4.65)$$

where m= component index, L,V= liquid and vapour phases, respectively.

The fugacity of each component in a phase is a function of its composition in that particular phase. This can be represented as :

$$f^{V}_{m} = F(y_{m}) \qquad (4.66)$$

where y_{m} is the equilibrium composition of component m in the vapour phase and F is a functional relationship.

Let the non-equilibrium composition of component m in the vapour phase be defined as y^{*}_{m}, then it follows:

$$y_{m} = G(y^{*}_{m}, E_{m}) \qquad (4.67)$$

where E_{m} is the degree of non-equilibrium for component m and G is a functional relationship.

E_{m} may be considered as a parameter which is a function of the Murphree efficiency parameter (Murphree, 1925) and the degree of mixing between the fluid phases. Hence, it may be expressed as:

$$E_{m} = H(N,W) \qquad (4.68)$$

where N is the Murphree efficiency parameter, W is the degree of mixing and H is a functional relationship.

Combining equations (4.66), (4.67) and (4.68) vapour phase fugacity may be expressed as follows:

$$f^{V}_{m} = U(y^{*}_{m},N,W) \qquad (4.69)$$

where U is a functional relationship.

Equation (4.67) may be redefined in an algebraic form

$$\frac{y_m - y_m^*}{y_m} = E_m \qquad (4.70)$$

or,

$$y^*_m = y_m(1-E_m) \qquad (4.71)$$

According to Murphree (1925) the parameter N is an exponential function of the product of the mass-transfer coefficient and contact time, assuming that all other variables considered in the original derivation by Murphree (1925) are constant. Though the definition of E_m is not exactly similar to the definition of Murphree efficiency, it may be logical to assume that E_m may also be considered as an exponential function of the mass-transfer coefficient and the contact time between the fluid phases. From a thermodynamic point of view, the degree of mass transfer for a component from one phase to another depends on the equilibrium factor, i.e., 'K' value of the component. Contact time between the phases is inversely proportional to the effective mobility ratio of the two phases. In an empirical way, equation (4.68) may be redefined as:

$$E_m = \alpha_1 [Exp(\frac{1-\sqrt{K_m}}{M_E}) - 1] \qquad (4.72)$$

where α_1 is a variable which may be correlated with the effective mobility ratio of the phases and M_E is the effective

mobility ratio of the phases.

The mixing parameter model proposed by Todd et al. (1972) is used to calculate the effective mobility ratio. According to the model, M_E is defined as:

$$M_E=\frac{\mu_{oe}}{\mu_{ge}} \tag{4.73}$$

where μ_{oe} is the effective viscosity of the oil phase and μ_{ge} is the effective viscosity of the gas phase.

μ_{oe} and μ_{ge} are calculated from the following equations;

$$\mu_{oe}=\mu_o^{1-\omega}\mu_{mx}^{\omega} \tag{4.74}$$

$$\mu_{ge}=\mu_g^{1-\omega}\mu_{mx}^{\omega} \tag{4.75}$$

where μ_{mx} is the viscosity of the mixed region of oil and gas, and ω is the mixing parameter which is equal to 2/3 for laboratory scale experiments and 1/2 for field scale experiments (Todd et al. 1972). The suggested ω value for laboratory scale experiments was used.

μ_{mx} is calculated from the 1/4-power fluidity mixing rule:

$$\mu_{mx}=[S_o\mu_o^{-\frac{1}{4}}+S_g\mu_g^{-\frac{1}{4}}]^{-4} \tag{4.76}$$

Equations (4.72) to (4.76) are used to calculate the degree of non-equilibrium (E_m) for each component m.

4.3.3 Calculation Procedures

At non-equilibrium state, compositions of the phases and vapour fraction will be different from the equilibrium state. Equilibrium flash calculations are performed and the values of equilibrium K_m's are obtained. Then equation (4.72) is used to obtain the values of E_m. The value of M_E at the previous time step is used to calculate the value of E_m. If the fluids at a particular grid block are in a single phase at the previous time step, one should take the value of the initial mobility ratio which is the ratio of the viscosity of initial oil and viscosity of solvent. The value of α_1 is set equal to $1.2M_E$.

Once, the values of E_m are calculated, the non-equilibrium K_m^*'s can be calculated from the following equation:

$$K^*_m = K_m\ (1-E_m) \qquad (4.77)$$

$m=1,\ldots,N_c$

A new set of equations are defined to perform the non-equilibrium flash calculations. The equations are:

$$L^* + V^* = 1.0 \qquad (4.78)$$

where L^* is the non-equilibrium liquid fraction and V^* is the non-equilibrium vapour fraction.

$$L^* x_m^* + V^* y_m^* = z_m \qquad (4.79)$$

$m=1,\ldots,N_c$

where x_m^* is the non-equilibrium liquid mole fraction for component m and y_m^* is the non-equilibrium vapour mole fraction for component m.

$$y_m^* = K_m^* x_m^* \qquad (4.80)$$

$m=1,\ldots,N_c$

$$\sum x_m^* - \sum y_m^* = 0 \qquad (4.81)$$

Equations (4.78) to (4.81) constitute a set of $2N_c+2$ equations which are to be solved for $2N_c+2$ unknowns (x^*_m, y^*_m, L^*, V^*). These equations are solved by a procedure which is similar to that used for equilibrium flash calculations.

The computer program of the numerical reservoir simulator using the non-equilibrium phase calculations, is provided in the Appendix E.

CHAPTER 5

RESULTS and DISCUSSION of NUMERICAL SIMULATION

In this chapter, the performance of the proposed algorithms for two-phase flash and saturation pressure calculations and the comparisons of the non-equilibrium model simulation results with that of the equilibrium model simulation and experimental data, are presented.

5.1 Results of Two-Phase Flash Calculations

5.1.1 Evaluation of the Dominant Eigenvalue Method

The numerically largest eigenvalue of the iteration matrix (A_{mj}) is calculated by the dominant eigenvalue method (DEM). The calculated dominant eigenvalue is compared with the rigorously calculated eigenvalues of the same iteration matrix (A_{mj}). This comparison is made to investigate the validity of the assumptions of the DEM when it is applied in flash calculations. The assumptions of the DEM are; i) there is only one dominant eigenvalue of the iteration matrix, and ii) eigenvalues of the iteration matrix in successive iterations are close.

The iteration matrix (A_{mj}) defined for two-phase flash calculations is calculated from equation (4.45) and its eigenvalues are determined rigorously. This method of calculating eigenvalues is referred to as the rigorous method. According to the DEM, the dominant eigenvalue of the A_{mj} matrix is calculated from equation (4.48). This method of

calculation of eigenvalue is referred as DEM.

Eigenvalues of the iteration matrix (A_{mj}) were calculated by both of the methods for two-phase flash calculations of a seven component gas condensate mixture (composition in mole percent :CO_2 = 10.0, C_1 = 86.08, C_2 = 2.47, C_3 = 0.67, nC_4 = 0.45, nC_5 = 0.24 and nC_6 = 0.09) at eight different temperatures and pressures. Gupta et al. (1988) used this mixture first to test their flash calculation algorithm. The temperatures and pressures are chosen in such a way that some were close to the critical point of the mixture and some are removed from the critical point. The critical pressure and the critical temperature of the mixture are 6408.31 KPa and 213.62 K, respectively.

The three numerically largest eigenvalues of the iteration matrix calculated by the rigorous method and the dominant eigenvalue of the iteration matrix calculated by the DEM are presented in Table 5.1 for flash calculations at eight different points. These eigenvalues are calculated from the iteration matrix which is obtained at the convergence of the iteration scheme. Table 5.1 shows that for flash calculations at points (1, 2, 7 and 8) removed from the critical point of the mixture, the three numerically largest eigenvalues calculated by the rigorous method differ significantly in magnitude. In other words, for flash calculations away from the critical point of the mixture, only one dominant eigenvalue of the iteration matrix is obtained from

Table 5.1: Eigenvalues of iteration matrix A_{mj} calculated by both rigorous method and DEM for flash calculations of a mixture at series of points

Points	T (K)	P (MPa)	Eigenvalues Calculated by Rigorous Method			Eigenvalue by DEM
			λ_1	λ_2	λ_3	
1	184.0	3.00	0.4503	0.0084	0.11E-19	0.4503
2	200.0	4.80	0.6016	0.1794	0.22E-01	0.6016
3	212.0	6.20	0.9112	0.9464	0.73E-01	0.9465
4	213.0	6.31	0.9342	0.9627	0.81E-01	0.9626
5	214.0	6.41	0.9324	0.9645	0.92E-01	0.9646
6	214.5	6.45	0.9035	0.9567	0.98E-01	0.9567
7	231.0	7.50	0.7132	0.1796	0.16E-03	0.7132
8	250.0	6.41	0.3476	0.0547	0.37E-16	0.3473

calculation by rigorous method. Thus, the assumption of the DEM that the iteration matrix has only one dominant eigenvalue is valid for flash calculations far from the critical point.

For flash calculations at points (3, 4, 5 and 6), close to the critical point of the mixture, at least two eigenvalues calculated by the rigorous method are of similar magnitude and close to unity. This observation indicates that for flash calculations close to the critical point of the mixture, the iteration matrix has at least two dominant eigenvalues. Thus, the assumption of the DEM that the iteration matrix has only one dominant eigenvalue is not valid for flash calculations near the critical point. However, Table 5.1 shows that for flash calculations at all of the eight points the eigenvalues calculated by the DEM are almost

equal to the numerically largest eigenvalues calculated by the rigorous method. This observation is proof that the DEM can be used to calculate the numerically largest eigenvalue of the iteration matrix.

To investigate how the eigenvalues of the iteration matrix change with successive iterations, the absolute values of the eigenvalues of similar magnitude, which are calculated by the rigorous method and the dominant eigenvalue calculated by the DEM are plotted against the number of iterations in Figure 5.1 and Figure 5.2 for points 3 and 1, respectively. Figure 5.1 shows that the two eigenvalues (λ_1 and λ_2) of similar magnitude calculated by the rigorous method are equal until approximately 20th iterations because these eigenvalues are complex conjugate. The eigenvalues calculated by DEM are smaller than those calculated by the rigorous method at the initial stages of iteration. However, as the iterations progress, the eigenvalue calculated by the DEM approaches the numerically largest eigenvalue calculated by the rigorous method. Figure 5.1 also shows that the average change of eigenvalues in the successive iterations are approximately 0.5%. This observation substantiates the assumption of DEM that eigenvalues of the iteration matrix in successive iterations are close. It may also be observed from Figure 5.1 that the eigenvalues calculated by both methods are increasing with the number iterations. This implies that the applied iteration scheme (Successive Substitution Method) will take a

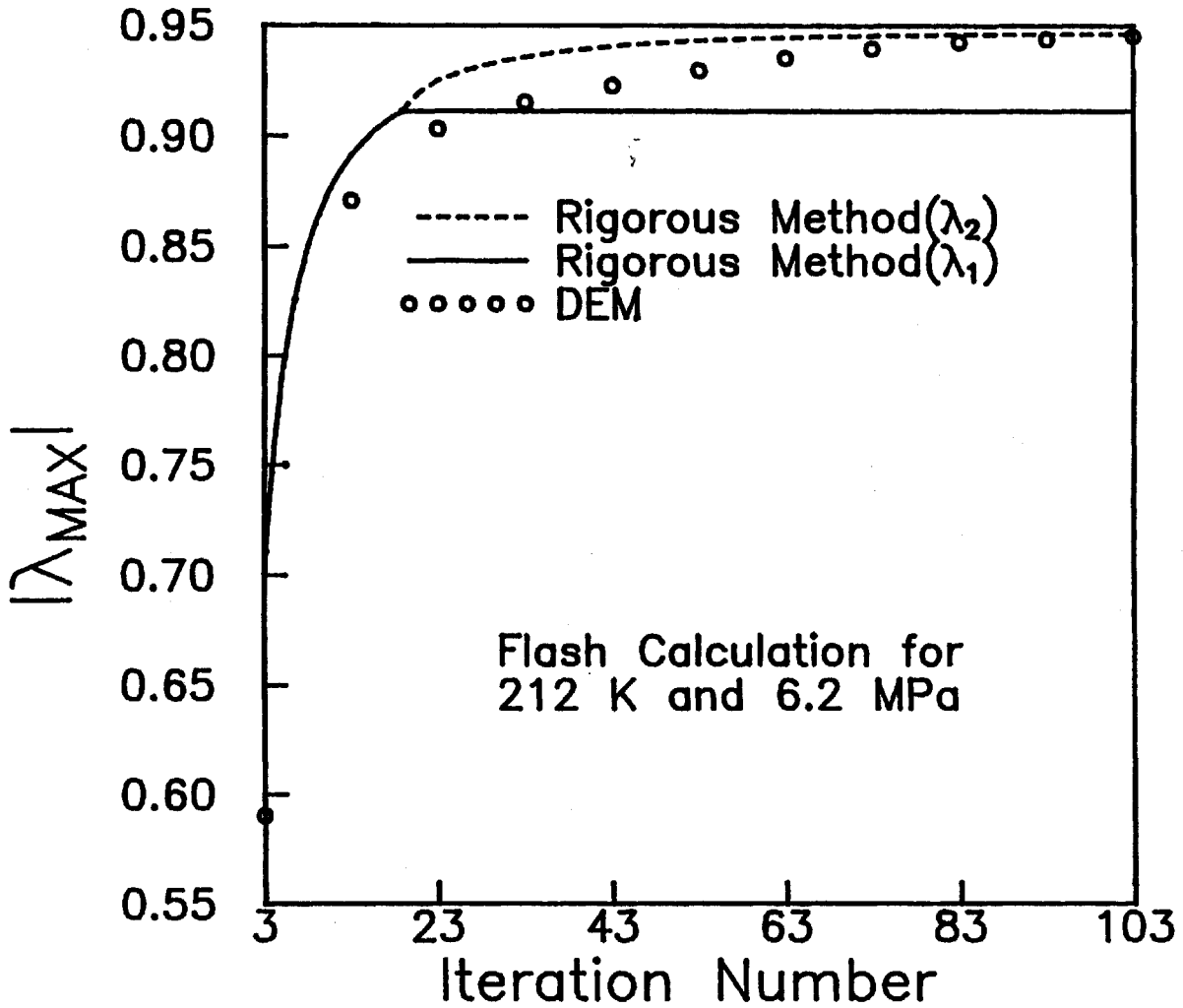

Figure 5.1 Changes of Dominant Eigenvalues of A_{ij} with Iterations for Flash Calculations for a Mixture close to its Critical Point

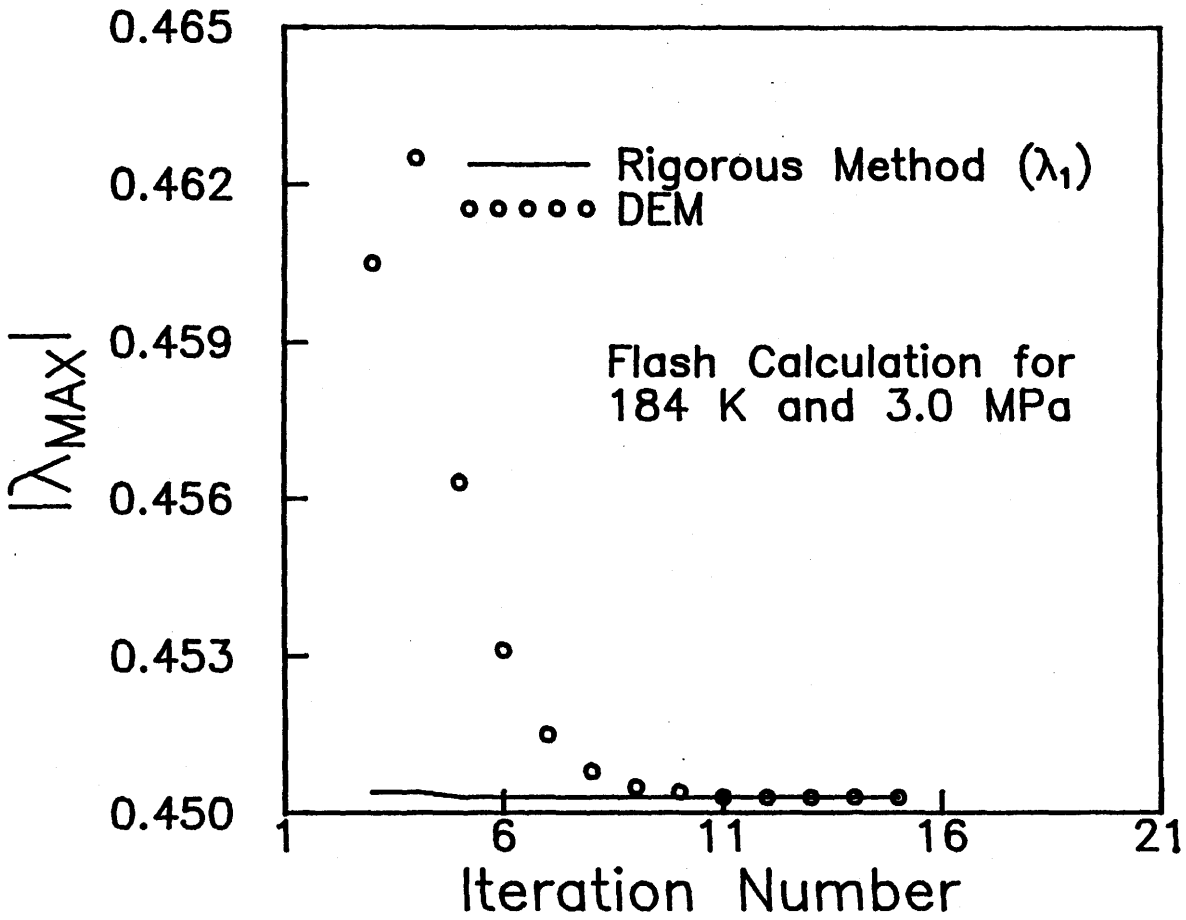

Figure 5.2 Changes of Dominant Eigenvalue of A_{ij} with Iterations for Flash Calculations for a Mixture removed from its Critical Point

large number of iterations to attain a solution for flash calculations at point 3 which is close to the critical point of the mixture.

For flash calculations at point 1 which is removed from the critical point of the mixture, it can be observed from Figure 5.2 that the largest eigenvalue of the iteration matrix calculated by rigorous method decreases slightly at the early stages of iteration and then remains constant. The eigenvalue calculated by the DEM also decreases with successive iterations but, to a greater degree than that calculated by the rigorous method. The fact that the eigenvalues of the iteration matrix are decreasing with successive iterations, is the contrary to that observed in Figure 5.1. However, the eigenvalues calculated by the DEM also approach the eigenvalues calculated by the rigorous method which is also observed in Figure 5.1. The number of iterations required for the eigenvalues, calculated by both of the methods, to be equal are much smaller in this case (Figure 5.2) than that required in flash calculations for point 3 (Figure 5.1). Figure 5.2 shows that the average change of eigenvalues with each iteration is approximately 0.1%. This observation is similar to that observed in Figure 5.1.

In short, it can be said that the eigenvalue calculated by the DEM becomes equal to the largest eigenvalue calculated by the rigorous method after a few number of iterations when the flash calculations are performed removed

from the critical point of the fluid mixture. However, for flash calculations near the critical point of the mixture, a large number of iterations is required before the eigenvalues calculated by both of the methods become equal. The iteration matrix has two eigenvalues of almost similar magnitude for flash calculations near the critical point of fluid mixture. In this situation, the basic assumption of the DEM that there is only one dominant eigenvalue of the iteration matrix is violated and hence, the DEM will not be an efficient acceleration method for flash calculation near the critical point of the mixture. However, in both situations (away from critical point, close to critical point) the changes of eigenvalues with iterations are small. This characteristic of the iteration matrix supports one of the assumptions of the DEM.

5.1.2 Performance of the Coupled Algorithm

The performance of the coupled algorithm which is implemented by two schemes, Scheme 1 and Scheme 2 (see 4.2.1.3) is illustrated by four examples and is compared with that of other acceleration methods for flash calculations. Acceleration methods considered for comparison are the general dominant eigenvalue method (GDEM) followed by Newton's method as proposed by Michelsen (1982), GDEM only, DEM-xy (liquid and vapour mole fractions as iteration variables) as proposed by Gupta et al. (1988), algorithms 1, 2 and 3 of Mehra et al. (1983), and Risnes's (1981) method. For all the calculations

the convergence criteria is set as :

$$E < 10^{-12} \quad (5.1)$$

where $E = (S^T S)/N_c$ (5.2)

and $S_m = (f_m^l/f_m^v - 1)$ (5.3)

The compositions of the four mixtures which are the examples of the typical fluid mixtures encountered in the petroleum industry, are shown in Table 5.2.

Table 5.2: Compositions of the Example Mixtures

Component	Compositions in Mole Percent			
	Mixture 1	Mixture 2	Mixture 3	Mixture 4
CO_2	10.000	-	-	-
C_1	86.080	-	80.000	64.360
C_2	2.470	39.842	5.660	7.520
C_3	0.670	29.313	3.060	4.740
nC_4	0.450	20.006	-	4.120
nC_5	0.240	7.143	4.570	2.970
nC_6	0.090	3.696	-	1.380
nC_7	-	-	3.300	3.030
nC_8	-	-	-	3.710
nC_9	-	-	-	4.150
nC_{10}	-	-	2.440	4.020

Example 1

Mixture 1 is a seven components mixture which has a critical temperature of 213.62 K and a critical pressure of 6408.33 KPa. Flash calculations for this mixture were performed at four points in the vicinity of the critical point. The number of iterations required for all the methods except the DEM-xy method at four points are shown in Table 5.3. The

Table 5.3: Comparisons of Number of Iterations Required for Flash Calculations of Mixture 1

Points	T K	P MPa	Vap. frac.	Scheme 1 SS+NR	Scheme 2 SS+NR	Mehra's Algorithms # 1	# 2	# 3	Michelsen SS+NR	Risnes
1	214.0	6.41	0.655	7+3	12+3	25	30	75	10+4	25
2	214.0	6.43	0.652	7+4	12+4	25	30	30	10+5	25
3	212.0	6.20	0.361	7+3	12+2	21	21	39	10+3	28
4	212.0	6.10	0.562	9+3	9+2	16	20	25	10+3	25

Table 5.4: Comparisons of Number of Iterations Required for Flash Calculations of Mixture 2

Points	T K	P MPa	Vap. Frac.	Scheme 1 SS+NR	Scheme 2 SS+NR	Mehra's Algorithms # 1	# 2	# 3	Michelsen SS+NR	Risnes
1	387.5	5.57	0.116	6+4	11+2	17	21	21	10+4	25
2	390.0	4.50	0.976	6+2	6+2	7	7	7	10+0	14
3	388.9	5.57	0.536	6+5	11+3	18	22	22	10+4	30
4	385.9	5.55	0.037	6+3	10+2	16	16	16	10+2	16
5	391.0	5.52	0.966	6+3	10+2	17	16	16	10+2	20

calculations using the DEM-xy method do not converge for all the four points. Table 5.3 shows that the use of algorithm 3 of Mehra requires a large number of iterations for point 1. Table 5.3 also shows that the use of scheme 1 requires fewer iterations to converge at all the points studied compared to Michelsen's method and scheme 2. The number of iterations required for the use of algorithms 1 and 2 of Mehra, and Risnes's method at all the points are within 30.

Example 2

Mixture 2 is a five components mixture which was first used by Mehra et al. (1983) in their calulations, with a critical temperature of 388.95 K and a critical pressure of 5577.41 KPa. Flash calculations were performed at five points which are close to the critical point of the mixture. The calculations using the DEM-xy method fail to converge for any of the points, as in example 1. The number of iterations required for all other methods are shown in Table 5.4. Table 5.4 shows that the use of Scheme 1 requires fewer iterations than that required by Michelsen's method. The number of iterations required by Scheme 2 is comparable to that required by Michelsen's method. However, the computational load involved in taking acceleration steps by the GDEM method is much higher than that required by the DEM. The number of iterations required by Mehra's algorithms 1, 2 and 3, and Risnes's are less than 25.

Example 3

Mixture 3 is a typical six component dry gas mixture with critical temperature and pressure of 293.21 K and 21204.72 KPa, respectively. This mixture was first experimentlly studied by Yarborough (1972). Table 5.5 depicts the number of iterations required for flash calculations at four points near the critical point of the mixture. Apart from the DEM-xy and Risnes's methods, calculations by all other methods converge to obtain solution at all points. Scheme 1 performs better than Michelsen's method considering the number of iterations required for convergence. Comparing the performance of scheme 1 with that of scheme 2, it is observed that scheme 2 on average, reduces the requirement of additional Newton's step at the cost of SS steps. The number of iterations required by the use of both scheme 1 and scheme 2 are less than those required by Mehra's algorithms 1, 2 and 3, at all the points.

Example 4

Mixture 4 is a ten components mixture with critical temperature and critical pressure of 425.14 K and 19170.42 KPa, respectively. This mixture was initially used by Nghiem et al. (1983) in the calculations to test the hybrid algorithm for flash calculations. The number of iterations required to converge for all the methods except the DEM-xy are shown in Table 5.6. Calculations using the DEM-xy do not converge to solution for all the points. The number of iterations and computation load required for scheme 1 are less than those

Table 5.5: Comparisons of Number of Iterations Required for Flash Calculations of Mixture 3

Points	T K	P MPa	Vap. Frac.	Scheme 1 SS+NR	Scheme 2 SS+NR	Mehra's Algorithm # 1	# 2	# 3	Michelsen SS+NR	Risnes
1	292.5	21.14	0.461	6+7	14+4	25	34	30	10+6	NC*
2	293.0	21.15	0.509	6+6	11+4	22	30	25	10+5	NC
3	293.5	21.20	0.526	6+6	11+5	22	30	28	10+5	NC
4	293.2	21.20	0.504	6+9	16+4	24	39	34	10+7	Nc

NC* - No Convergence to obtain solution

Table 5.6: Comparisons of Number of Iterations Required for Flash Calculations of Mixture 4

Points	T K	P MPa	Vap. Frac.	Scheme 1 SS+NR	Scheme 2 SS+NR	Mehra's Algorithm # 1	# 2	# 3	Michelsen	Risnes
1	424.5	19.18	0.476	6+6	11+4	22	28	28	10+5	35
2	425.1	19.16	0.516	6+7	16+4	27	30	30	10+6	40
3	425.0	19.15	0.505	6+6	11+4	24	28	28	10+6	35
4	425.5	19.14	0.558	6+7	16+4	28	30	30	10+7	40
5	426.0	19.10	0.594	6+7	14+4	25	30	28	10+6	40

the Michelsen's method. Comparing the performance of Scheme 2 with that of Scheme 1, it is observed that calculations using scheme 2 reduce, on average, one Newton's step at the expense of 2.5 SS steps.

5.1.2.1 Comparison of Convergence Speed

To show the approach of convergence to solution for all the methods, $\log_{10}$ E and vapour fraction are plotted with iteration numbers for point 3 of mixture 4. The plots are shown in Figures 5.3 and 5.4, respectively. The convergence of Mehra's algorithms 3 and 2 are not included in Figures 5.3 and 5.4 to maintain its clarity. Figure 5.3 shows that scheme 1, scheme 2 and Michelsen's method converge much faster than other methods because of the superlinear convergence scheme of the Newton's method. However, calculations using Mehra's algorithm 1 show large oscillations in reducing the error ($\log_{10}$E). Alyhough, the error calculated by the DEM-xy method gradually approaches to convergence, the vapour fraction converges to a single phase, which is shown in Figure 5.4. Figure 5.4 shows that the vapour fraction converges close to the solution value within a few iterations, for all the methods except DEM-xy, and there is not much change in the vapour fraction values in the later stages of iteration. The convergence characteristic of the vapour fraction may be explained by the fact that the error is strongly dependent on phase composition near the critical point.

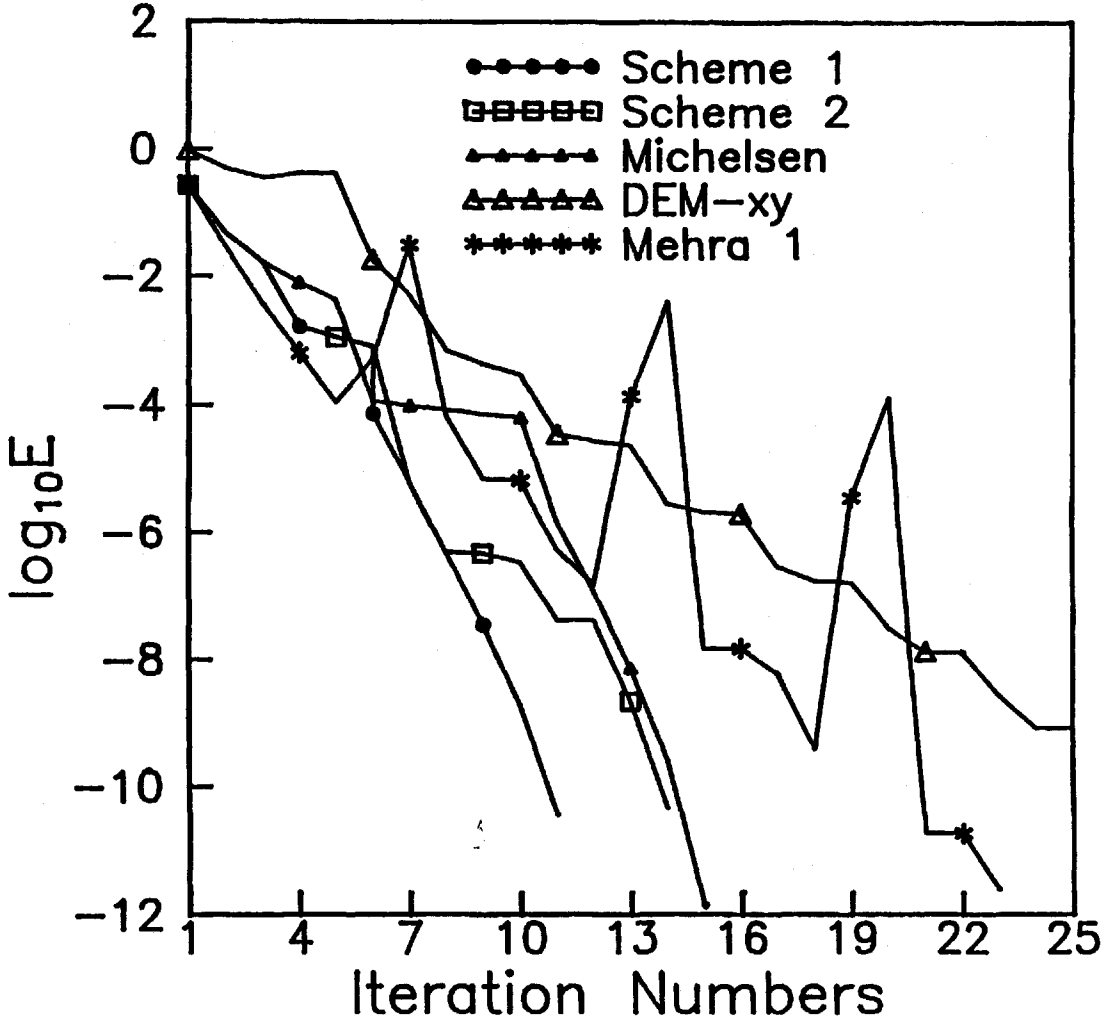

Figure 5.3 Convergence Behaviour of Calculations for Mixture 4 at 19.5 MPa and 425 K

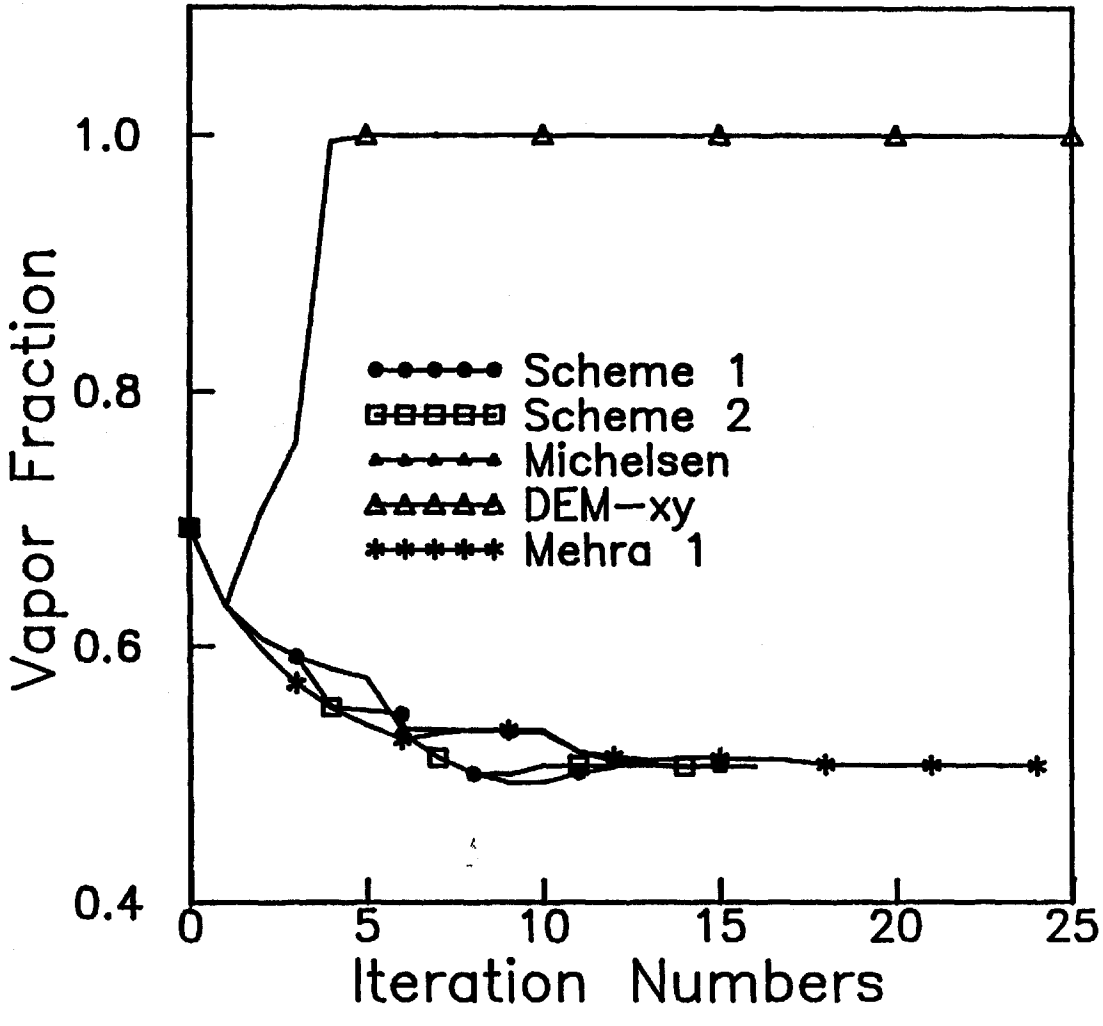

Figure 5.4 Convergence Behaviour of Calculations for Mixture 4 at 19.5 MPa and 425 K

5.1.2.2 Discussion

Flash calculations using Scheme 1, Scheme 2, Michelsen's method and Mehra's algorithms 1, 2 and 3 converge at all the points considered in this study. Michelsen's acceleration algorithm for the SS method is based on the GDEM. To illustrate the performances of DEM and GDEM in aiding the convergence speed, the error norms (δ^n) calculated by both of those methods are compared in Figure 5.5. The error norm is defined as the following (Crowe et al., 1975);

$$\delta^n = |\Delta u^n| \; / \; |u^n| \qquad (5.4)$$

where u is the vector of iteration variables. Iteration variables are the logarithm of the K-factors. The logarithm of the norm (δ_n) versus iteration number is plotted for flash calculation at point 4 of mixture 1. In both the acceleration methods of DEM and GDEM, one acceleration step has been taken after every 5 SS steps. Figure 5.5 shows that the improvement in convergence promotion by GDEM is very insignificant over that of DEM for the second acceleration step. At the third acceleration step the DEM is more effective in reducing the error norm than is the GDEM. Moreover, GDEM requires 3 times more storage of variables and 3.5 times more multiplication than does the DEM. Thus, it may not be an advantage to use the GDEM as an acceleration method for the particular application in flash calculations.

Mehra's algorithm 1 requires additional N_c^2 multiplication over SS and additional calculations for

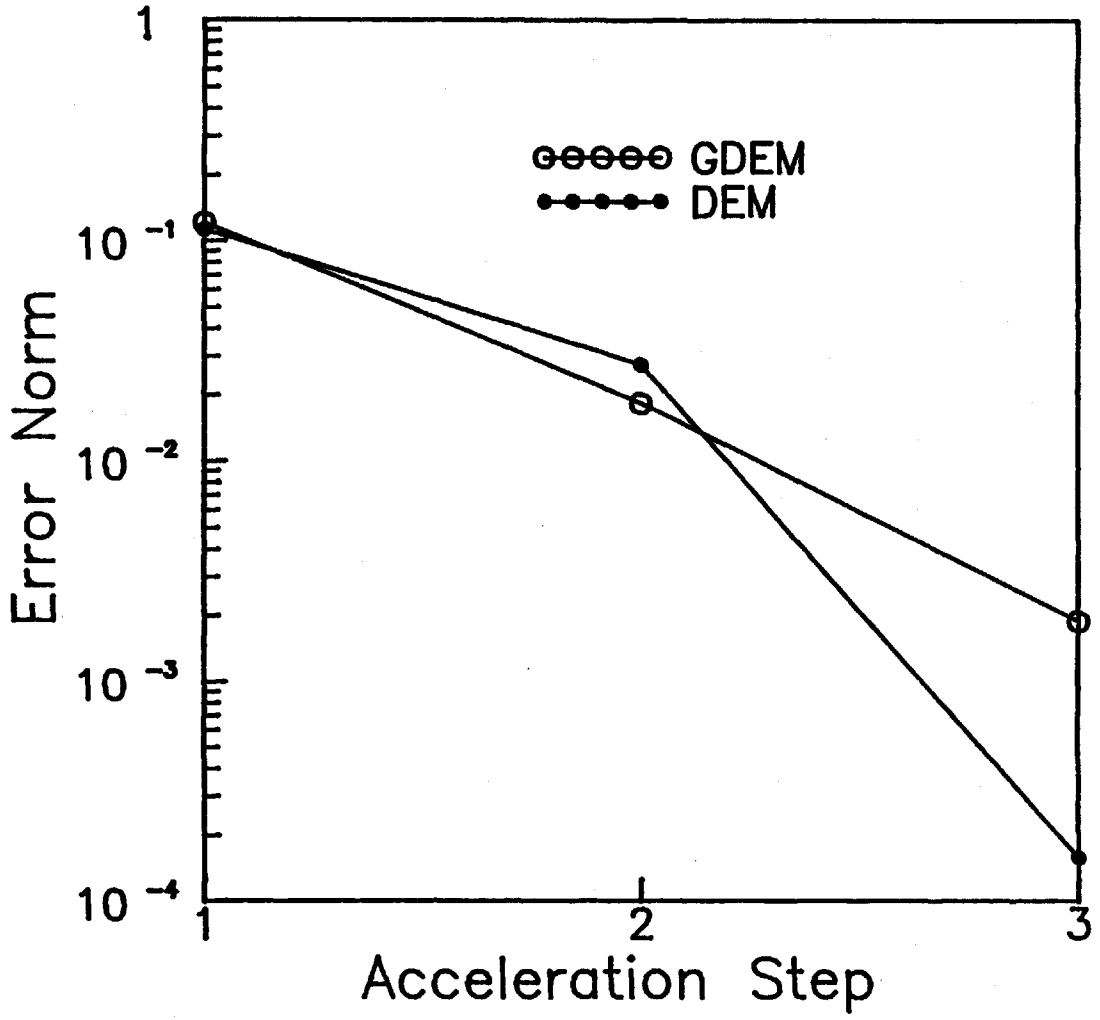

Figure 5.5 Convergence Behaviour of DEM and GDEM

computing the analytical matrix inverse. This method has step size limitation whereas acceleration based on DEM does not have any limit on step size. The oscillating convergence behaviour of Mehra's algorithm is not desirable. The CPU time requirement to perform flash calculations for mixture 1 at all the four points by Mehra's algorithm 1, Michelsen's method and scheme 1 are shown in Table 5.7. The calculations are performed with a VAX-8650 computer. Table 5.7 shows that scheme 1 requires about the same computing time as that required by Michelsen's method and Mehra's algorithm 1. It

Table 5.7: Comparisons of CPU Time Requirement

	CPU Time Requirement in seconds		
Points	Mehra's Algo. 1	Michelsen	Scheme 1
1	3.89	3.75	3.49
2	3.89	3.84	3.58
3	3.82	3.73	3.49
4	3.77	3.73	3.61

is found in this study that the DEM-xy method may not be a reliable method to use for acceleration of flash calculations. The problem with the DEM-xy method is that, near the critical point, the vapour fraction converges to unity while the mole fractions of the components in the vapour phase do not.

Risnes's method is not robust. The iterations performed by Risnes's method fail to converge in some points. The other drawback of the Risnes's method is that the application of this method sometimes takes too few

acceleration steps. It is due to the limitation that the acceleration step has to be rejected if the convergence criterion is not reduced in the subsequent iteration steps. Each acceleration step by Risnes's method is applied after 5 SS steps. This procedure is found to be optimum for the convergence of the calculations.

5.2 Results of Saturation Pressure Calculations

To illustrate the performance of Newton's method and that of the developed algorithm for saturation pressure calculations, the calculated results for a gas condensate mixture are presented. The composition of the gas condensate mixture is shown in Table 5.8. The experimental vapour-liquid equilibrium data for this mixture have been reported by Yarborough (1972). The critical point of this mixture is calculated from the Peng-Robinson equation state to be 315.6 K and 22.84 MPa.

Table 5.8 Composition of the example mixture

Components	Composition in Mole Percent
C_1	72.270
C_2	4.551
C_3	2.474
nC_5	5.205
nC_7	3.650
nC_{10}	2.814
N_2	3.020
CO_2	3.015
H_2S	3.001

A bubble-point pressure calculation and a dew-point pressure calculation in the vicinity of the critical point are made. The initial values of the unknowns (saturation pressure and the composition of the incipient phase) were obtained from an empirical procedure which is largely based on Wilson's equation (Wilson, 1969). Three SS iterations are applied before Newton's method is begun in the bubble-point calculation. However, only one SS iteration is used before Newton's method is applied in the dew-point calculation. The initialization procedure and the SS schemes are the same as those which were described by Peng (1990).

The convergence behaviour of the calculated pressures are shown in Figures 5.6 and 5.7. It is seen that in both Figures 5.6 and 5.7 the calculated pressures converge toward the final solutions in a monotonic manner after two or three Newton steps. The behaviour of the calculated mole fractions in the dew-point calculation is shown in Figure 5.8. For clarity, only the results for five selected components are shown. It is evident that the compositional variables also converge smoothly toward the final values.

The performance of the proposed acceleration scheme in the dew-point calculation is shown in Figures 5.9 and 5.10. It can be seen that the proposed scheme has reduced the number of iterations required from sixteen to eleven, or from fifteen Jacobian evaluations to ten Jacobian evaluations.

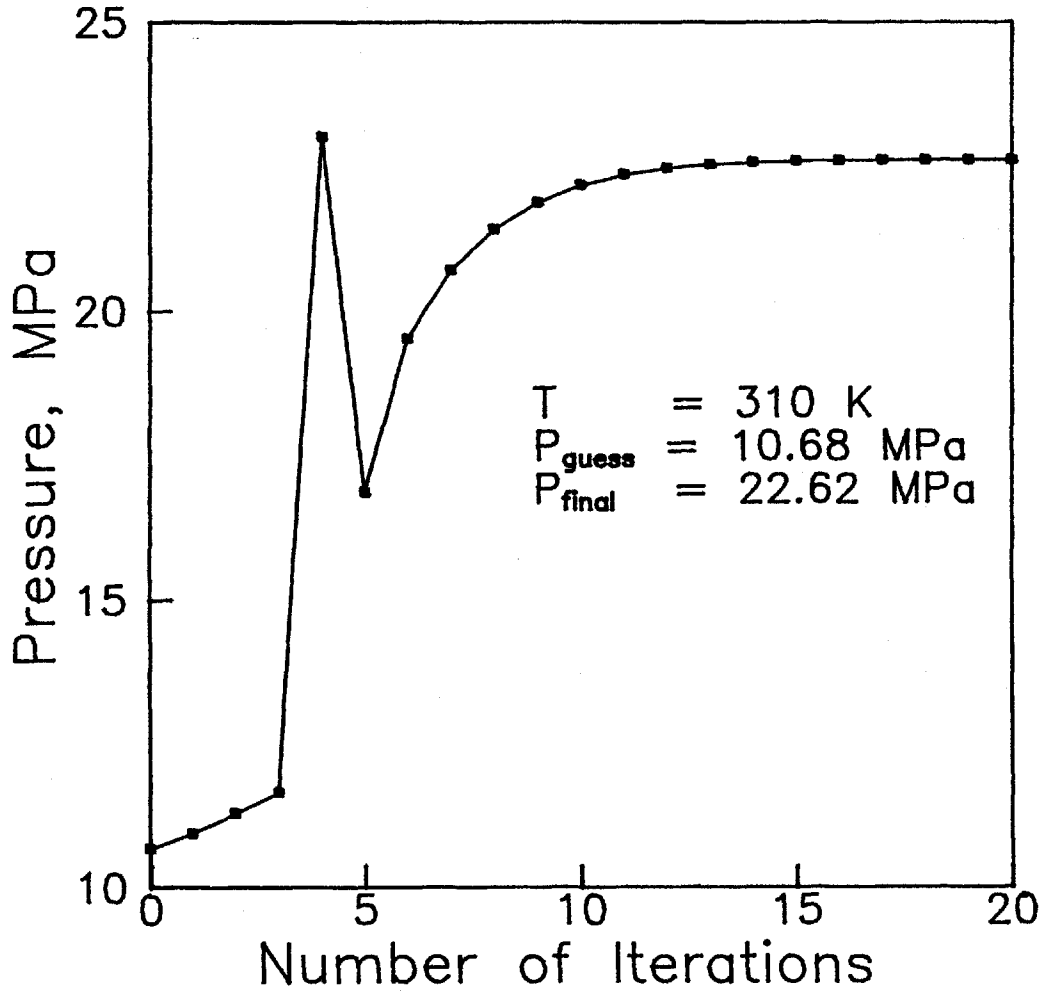

Figure 5.6: Performance of Newton's method in a bubble–point calculation

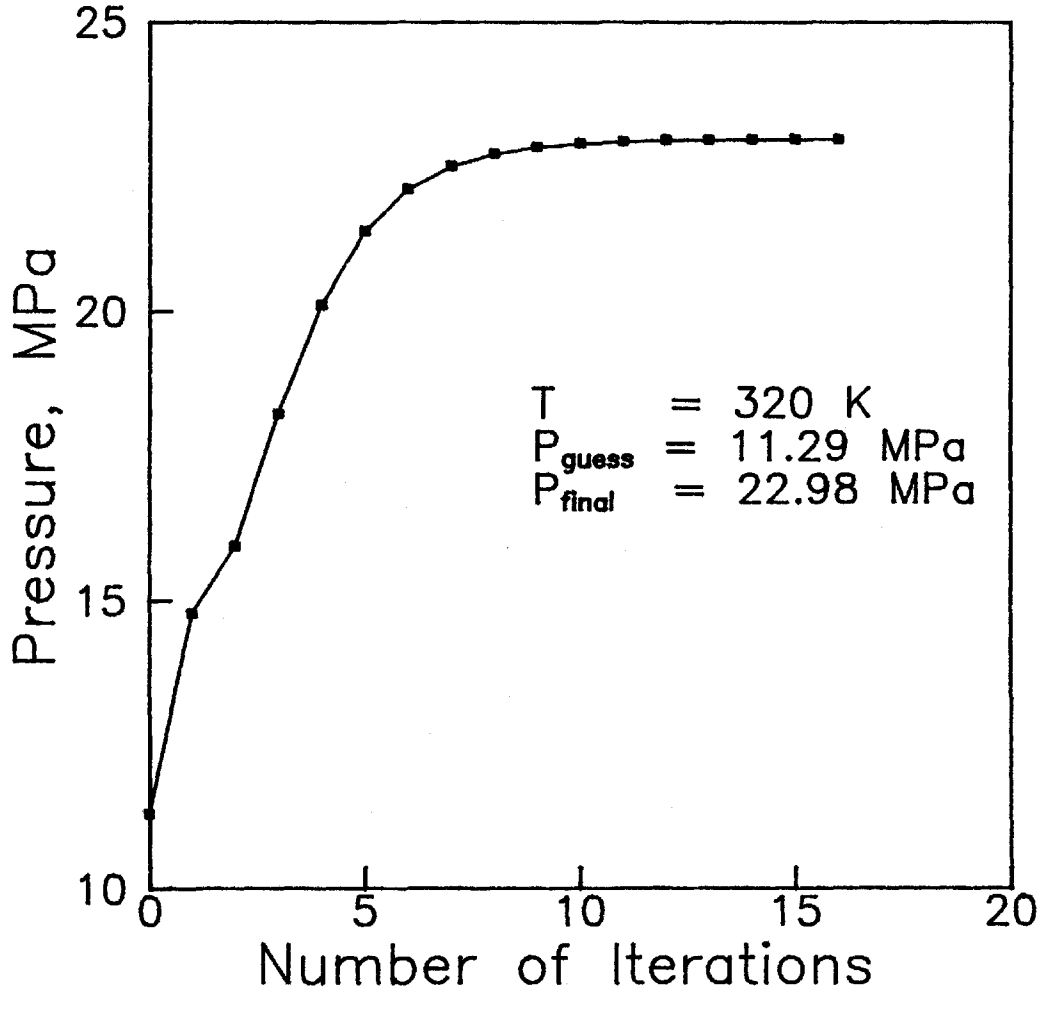

Figure 5.7: Performance of Newton's method in a dew-point calculation

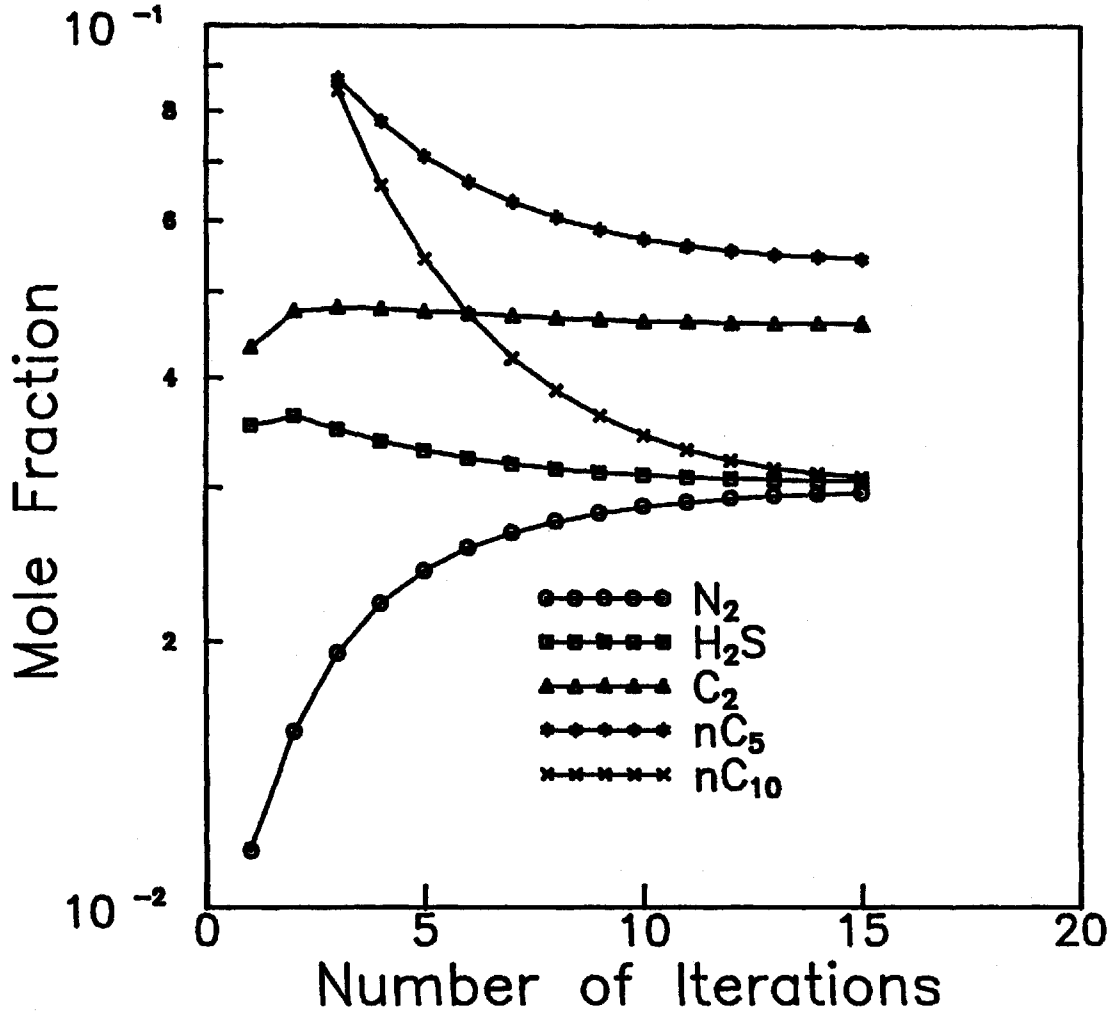

Figure 5.8 Behaviour of mole fractions in a dew–point calculation using Newton's method

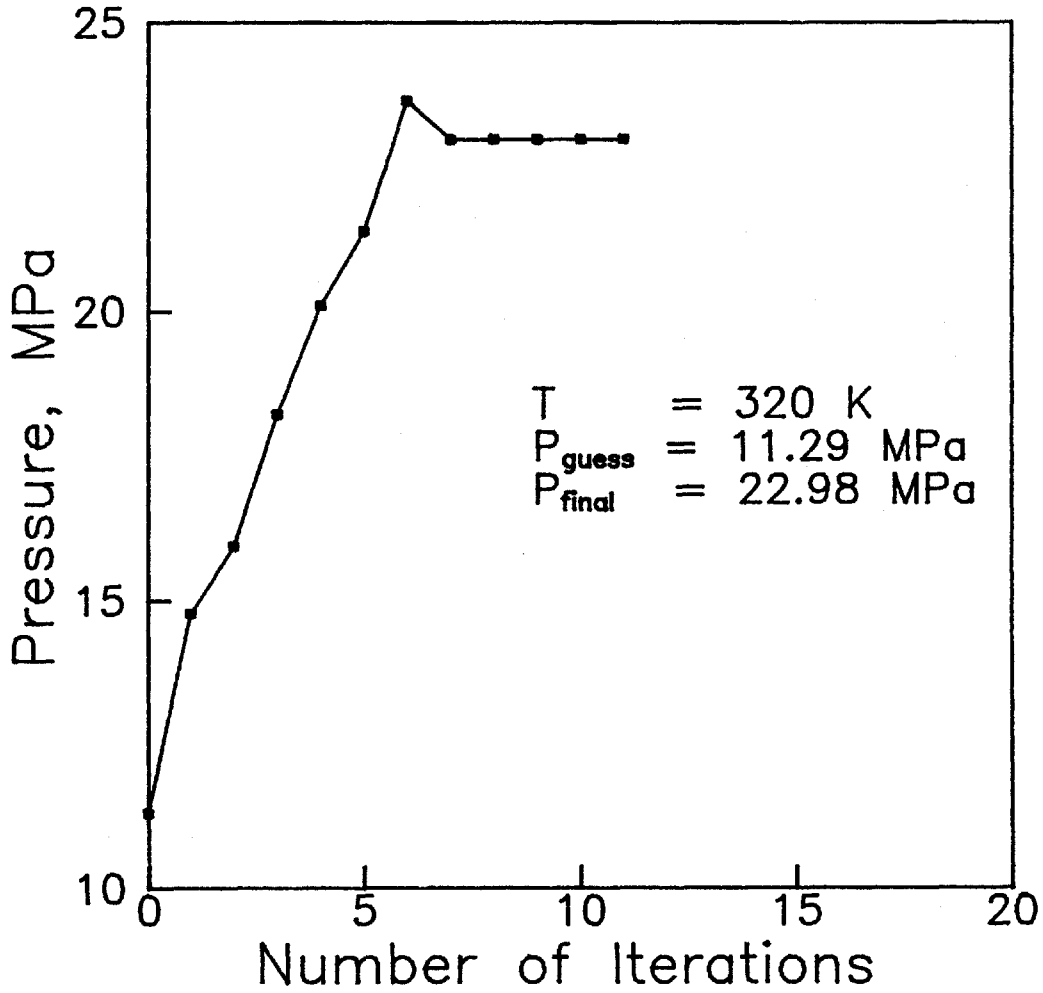

Figure 5.9: Performance of the proposed scheme in a dew–point calculation

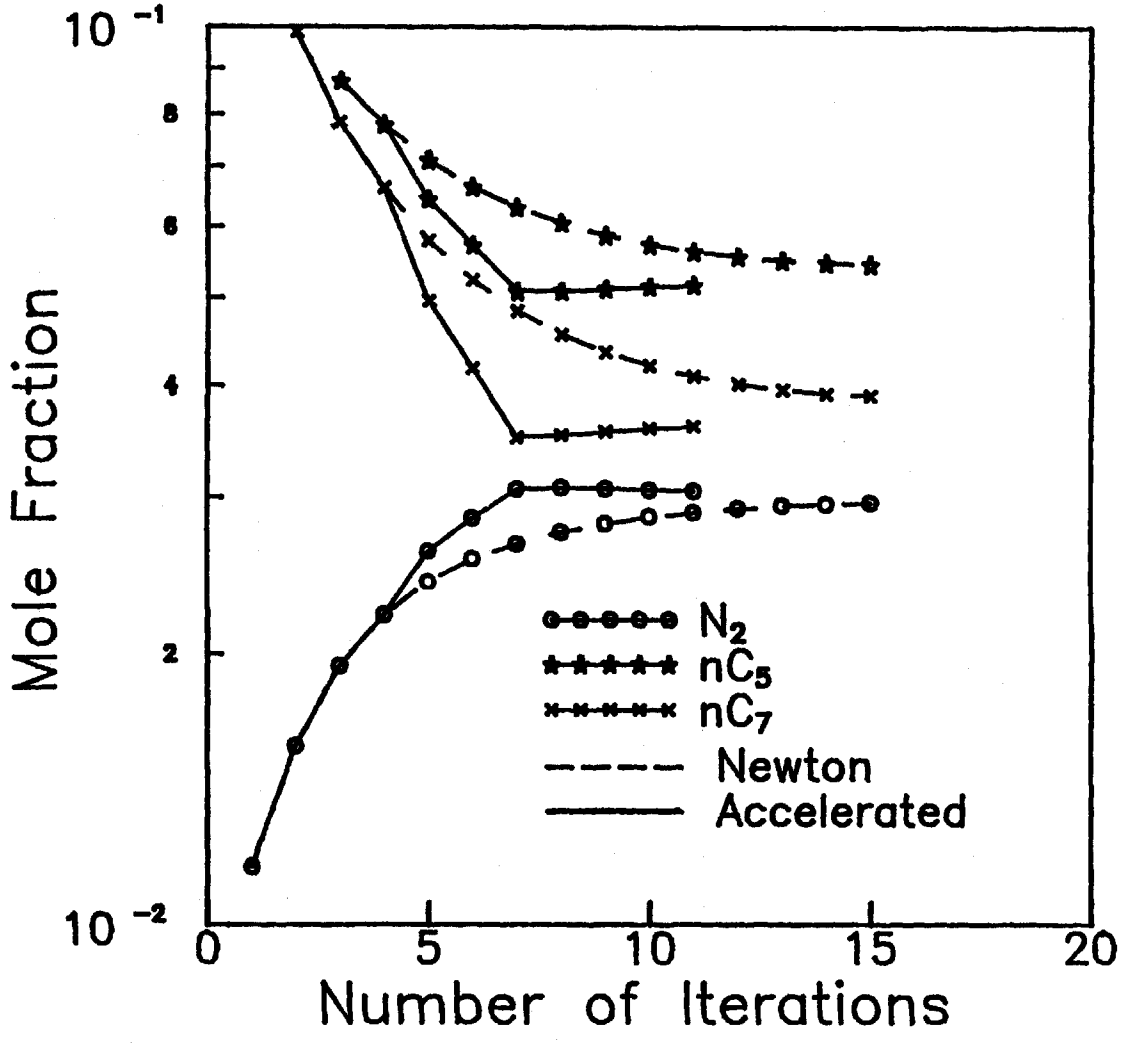

Figure 5.10 Comparison of the performances of Newton's method and the proposed method

5.2.1 Comparison with Other Acceleration Methods

The performance of the proposed algorithm for the saturation pressure calculation is compared with that of the other two acceleration schemes (Richardson Extrapolation and the overrelaxation method of Kelly et al., 1983) for Newton's method. The application of these two acceleration schemes of the Newton's method in saturation pressure calculations have never been attempted before by other researchers. The performance of the Newton's method is also compared with that of the acceleration methods.

Bubble-point pressures of the example mixture (Table 5.8) at nine temperatures, in the vicinity of the critical point, are calculated by using the accelerated

Table 5.9 : Comparison of the performances for bubble-point calculations

T	Calc.	Number of Iterations			
K	Pressure MPa	Extra-polation Method	Overrel-axation Method	Proposed Method	Newton's Method
300	22.09	11	13	12	NC*
301	22.15	11	13	12	NC
302	22.21	11	14	12	NC
303	22.27	11	14	12	NC
304	22.32	11	14	11	NC
305	22.38	12	14	13	NC
306	22.43	12	15	13	NC
307	22.48	12	15	13	NC
308	22.53	13	16	14	NC

*NC means not converged

methods and Newton's method. Each accelerated step is taken in all the three acceleration methods after three iteration steps by Newton's method and the same initialization procedure is used in all the accelerated methods and in Newton's method. The number of iterations required by the three acceleration methods and Newton's method are shown in Table 5.9. The results show that the number of iterations required by all the accelerated methods are almost the same. However, of all the accelerated methods, the overrelaxation method requires the largest number of iterations. Iterations using Newton's method do not converge at all the nine temperatures.

The comparison of the performances of the three acceleration methods with those of the Newton's method for dew-point pressure calculations of the same example mixture at nine temperatures is shown in Table 5.10. Calculations using the Richardson extrapolation method and the overrelaxation method fail to obtain solution at seven different temperatures. The problem encountered in calculations using these two acceleration methods is that dew-point pressures converge to the solution value, but the K-factors of all the components converge to values near unity. In such cases, the compositions of the incipient phases may not be calculated accurately. However, Table 5.10 shows that the calculation using Newton's method, without any acceleration, converge at all the nine temperatures. It can be observed from Table 5.10 that, for convergence of the accelerated methods, the number

of iterations required is almost equal for all the methods, except at the temperature 324 K where the overrelaxation method requires 11 iterations and the proposed method requires 6 iterations to converge. Table 5.10 also shows that the proposed method significantly reduces the number of iterations required for convergence compared to that required in Newton's method, especially near the critical point.

Table 5.10: Comparison of the performances for dew-point calculations

T K	Calc. Pressure (MPa)	Number of Iterations			
		Extra-polation Method	Overre-laxation Method	Proposed Method	Newton's Method
320	22.98	NC	NC	9	15
321	23.00	NC	NC	9	15
322	23.03	NC	NC	9	14
323	23.05	8	8	8	14
324	23.07	NC	11	6	14
325	23.09	NC	NC	7	13
326	23.11	10	NC	8	13
327	23.13	NC	NC	9	13
328	23.14	NC	NC	11	13

5.2.2 Discussion

The acceleration algorithm developed in this study is simple to use and requires an insignificant amount of computing effort. The calculation of saturation pressures for

the example mixture at different temperatures has shown that, by using the proposed algorithm, the number of iteration is reduced by 35 percent. Calculations for other mixtures have shown savings ranging from 2 to 6 iterations, depending on the complexity of the mixture and the region for which the calculations are made. In view of the computing effort required for each Newton iteration, the saving of computing cost and time is significant even with a reduction of only two or three iterations. In general, a saving of 20 percent can be expected for calculations in the vicinity of a critical point.

The comparison of the performance of the proposed algorithm with that of the Richardson extrapolation and the overrelaxation method shows that, in general, the Richardson extrapolation performs slightly better than the proposed method and the overrelaxation method for bubble-point pressure calculations. However, the use of the Richardson extrapolation method is not reliable because, for dew-point pressure calculations, the acceleration based on the Richardson extrapolation method does not converge for some points. This finding is also evident when the overrelaxtion method is used for dew-point pressure calculations. Overall, the performance of the overrelxation method is not better than that of the proposed method.

In this study, the relaxation parameters used in the proposed method are 0.7 for bubble-point pressure and 1.2 for

dew-point pressure calculations. It is possible that the performance of the proposed method may be further enhanced by the use of a variable relaxation parameter. However, the effects of various relaxation parameters on the proposed method were not explored in this study.

5.3 Results of Compositional Simulations

5.3.1 Parameter Adjustments

In the compositional simulation, the physical properties of the fluid mixtures such as densities and viscosities are calculated by an equation of state and viscosity correlation of Lohrenz et al. (1964), respectively. The adjustable prameters used in the correlations, have to be tuned for accurate predictions of the physical properties of the fluid mixtures.

5.3.1.1 Tuning of Interaction Parameters

The binary interaction parameters used in the Peng-Robinson equation of state are tuned to obtain an improved prediction of phase compositions and densities of fluid mixtures. Four hydrocarbon components, i.e., C_1, C_3, nC_4 and nC_{10} are used in the slim-tube experiments. Phase equilibrium data were collected from the literature involving the combination of these four components at 160^{o} F and in the pressure range close to the range of displacement pressures used in the experiments.

Fourteen data points were collected for the C_1-nC_4-

nC_{10} system at 160° F and in the pressure range of 1000-3500 psia (Reamer et al., 1949 and Sage et al., 1951). Eight data points were collected for the C_1-C_3-nC_{10} system at 160°F in the pressure range of 1000-3000 psia (Weise et al., 1970). Seven data points were collected for the C_1-C_3-nC_4 system at 160°F in the pressure range of 1000-1500 psia (Weise et al., 1970).

The binary interaction parameters for the four components are tuned by comparing the calculated phase equilibrium results with the experimental data. Tuned binary interaction parameters are shown in Table 5.11.

The average absolute percent deviation of K-(equilibrium constant) factors obtained by the use of tuned binary interaction parameters, for C_1, C_3, nC_4 and C_{10} are 2, 3, 6 and 13, respectively. If no interaction between the components is assumed, then the deviation of K-factor for C_{10} can be as high as 40%. These tuned interaction parameters are used in the compositional simulation.

Table 5.11: Tuned interaction parameters

	Interaction Parameters		
	C_1	C_3	nC_4
C_3	0.012	-	-
nC_4	0.013	0.001	-
nC_{10}	0.041	0.018	0.017

5.3.1.2 Modification of Viscosity Correlation

The Lohrenz, Bray, Clark (Lohrenz et al. 1964) correlation is used to calculate the viscosities of liquid and gas phases so that viscosities of both phases converge to a common value as phase compositions converge near the critical point. This correlation uses the value of reduced density of the mixture to calculate the viscosity of the mixture. Hence, to calculate reduced density one needs to know the critical volume of the mixture. The following equation was suggested by Lohrenz et al. (1964) for the calculation of psuedocritical volume of the mixture:

$$V_c=\sum x_j V_{cj}^m \qquad (5.5)$$

where j= component index, V_{cj} = critical volume of component j and m= exponent.

Lohrenz et al. (1964) considered different values of the exponent, m=1, suited best for their test results. Considering the hydrocarbons used in the slim-tube experiments, two binary systems C_1-C_{10} and C_1-nC_4 are used for tuning the parameter m. For the C_1-C_{10} system, 23 experimental data points were considered with a C_1 mole fraction range of 0.3-0.7, a temperature range of 160°-340° F and a pressure range of 1500-6000 psia (Lee et al., 1966). For the C_1-nC_4 system, 5 data points were considered with a C_1 mole fraction range of 0.2-0.7, a temperature range of 160° - 220° F and a pressure range of 2000-3000 psia (Dolan et al.

1964). The best value for m was found to be 0.87 for all the viscosity data considered in this study. The average absolute percent deviation obtained with the modified 'm' value for the C_1-C_{10} system in the pressure range of 1500-3000 psia is 2.7 and the overall deviation for 23 data points is 7.3. The average absolute percent deviation obtained for the C_1-nC_4 system is 9.8. The sensitivity of the exponent to the viscosity can be explained by the fact that approximately 1.5% increase of m reduces the viscosity of mixture by 10%. The modified exponent value (m=0.87) was used in the compositional simulation.

5.3.2 Simulation Using Phase Behaviour Models

A numerical simulation of an oil recovery process using gas injection was developed. In the numerical simulation, fluid phase behaviour was described by two models; i) the non-equilibrium model, which is developed in this study and ii) the equilibrium model, which is commonly used in a compositional simulator. In the following, an example of the simulation results with the two phase behaviour models is presented. The physical data used in the simulation is equivalent to the physical dimensions of the slim-tube apparatus used in the experiments. The physical data of the slim-tube apparatus is presented in Table 5.12.

5.3.2.1 Non-Equilibrium Model

The oil consists of 49.8 mole percent n-C_4 and 50.2 mole percent n-C_{10}. C_1 is used as an injection gas. The

operating pressure is 3430 psia and the operating temperature is 160° F. The injetion rate of gas is 0.048 pore volume (PV) per hour. The pore volume of the slim-tube is represented by 81 grid blocks of equal volume. The time step is selected automatically based on the strategy discussed in section

Table 5.12 Physical Data of Slim-Tube

Length of Slim-Tube	2440 cm
Cross sectional area of Tube	0.1693 cm^2
Permeability	22.0 E-08 cm^2
Porosity	0.3798
Relative permeability of oil	$K_{ro} = S_o^3$
Relative Permeability of gas	$K_{rg} = S_g^{1.5}$

4.1.2.2 namely, that a saturation front cannot cross a single grid block in one time step. Numerical simulation is performed until 1.22 pore volume of gas has been injected. A total of 198 time steps are required for simulations with the non-equilibrium model and on an average 3 to 4 iterations are needed per time step for the convergence of pressures in the grid blocks. Each time step has a fixed value of 464 seconds.

The calculated recovery profile is shown in Figure 5.11. The calculated amount of oil recovered after 1.22 PV of gas injection is 89.33%. It is apparent from the recovery value that the displacement process may be considered as a near MCM process. The calculated breakthrough time obtained in terms of pore volume of gas injected is 0.998.

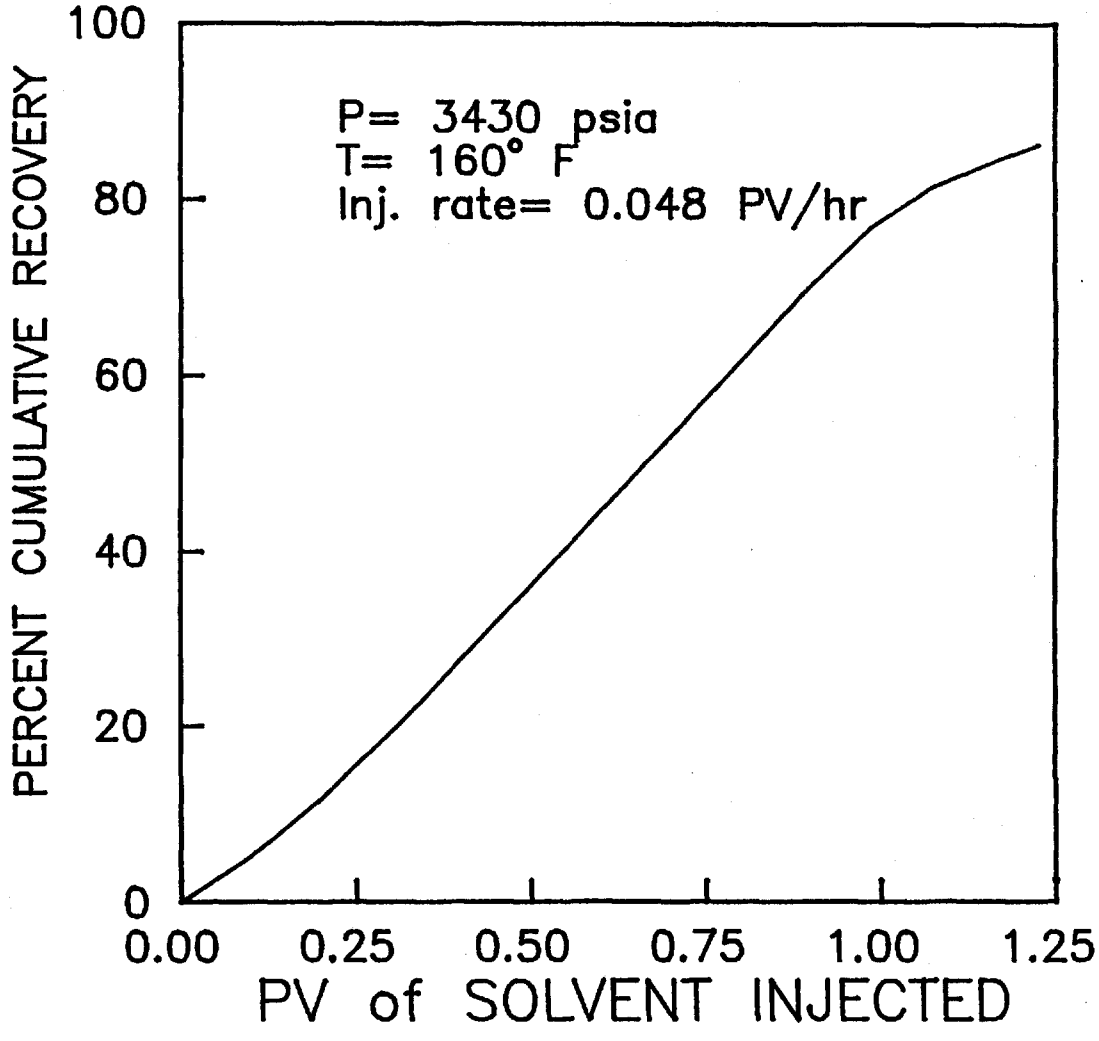

Composition in Mole fractions

	OIL	SOLVENT
C_1	0.000	1.000
nC_4	0.498	0.000
C_{10}	0.502	0.000

Figure 5.11: Recovery Profile Prediction by the Non–equilibrium Model

5.3.2.2 Equilibrium Model

Compositional data, physical data of the slim-tube and the operating conditions used in the simulation with the non-equilibrium model are also used in the simulation with the equilibrium model. The pore volume of the slim-tube is represented by 81 grid blocks system as in the non-equilibrium model simulation.

The total time steps required for 1.22 PV of gas injection are 198 and the length of each time step is also fixed at 464 seconds, as in the non-equilibrium model simulation. However, it is observed that for other systems of fluids and operating conditions, the number of time steps required in equilibrium model simulations are less than those that are required in non-equilibrium model simulations.

The calculated recovery profile is shown in Figure 5.12. The calculated ultimate recovery is 90.88%. The ultimate oil recovery calculated from the equilibrium model simulation is 4.5% higher than that calculated from the non-equilibrium model simulation. The breakthrough time (in terms of PV of gas injection) calculated from the equilibrium model simulation is 1.084 PV which is higher than that calculated from the non-equilibrium model simulation. In other case studies, which will be discussed in the following sections, higher recovery and late breakthrough times are obtained from the equilibrium model simulations compared to those obtained from the non-equilibrium model simulations.

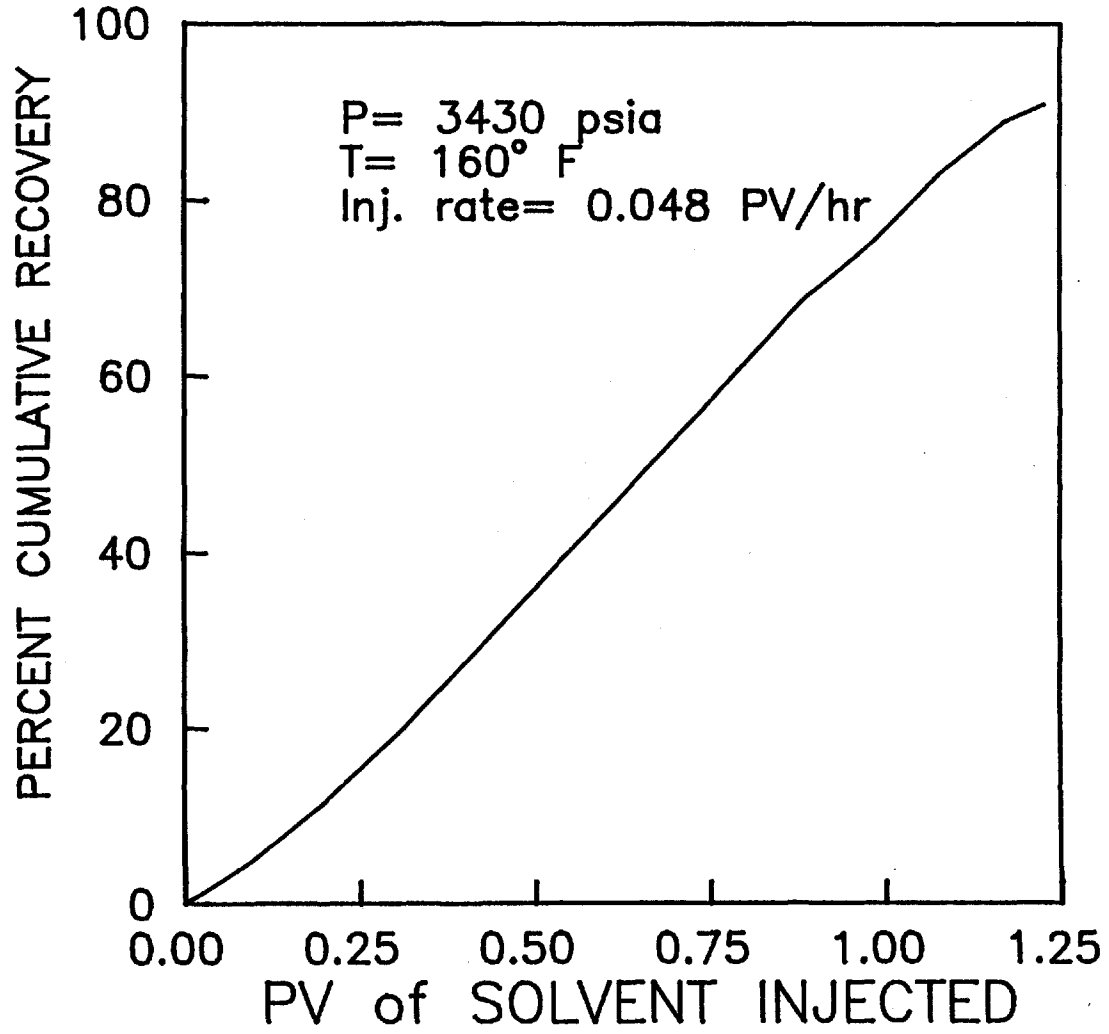

Composition in Mole fractions

	OIL	SOLVENT
C_1	0.000	1.000
nC_4	0.498	0.000
C_{10}	0.502	0.000

Figure 5.12: Recovery Profile Prediction by the Equilibrium Model

The recovery profiles (Figures 5.11 and 5.12) calculated from the use of both models are similar till the breakthrough time. A change in slopes of the recovery profiles after the breakthrough can be observed from Figures 5.11 and 5.12 . This phenomenon occurs because of the fact that, after breakthrough, gas production increases rapidly and oil production drops drastically. If gas injection is continued for considerable time after the breakthrough, the recovery profiles will be completely flat at the tail end.

5.4 Comparisons of Numerical Simulation Results with Experimental Data

The results obtained from the one dimensional reservoir simulator based on the non-equilibrium and equilibrium phase behaviour models are compared with the experimental data. Compositions of oil and gas mixtures used in the experiments and the operating conditions of experiments are shown in Table 3.1, Table 3.2 and Table 3.3, respectively. The ultimate recovery of oil and breakthrough time obtained from simulations based on the non-equilibrium model and the equilibrium model, and those obtained from experiments are presented in Table 5.13 and Table 5.14, respectively.

A displacement process is identified as an immiscible displacement process if less than 90% recovery is obtained at 1.2 PV of gas (solvent) injection. Based on this criterion, it can be inferred from Table 5.13 that experiment 2, and experiments 4 to 14 may be considered as immiscible

displacement processes, and experiments 1, 3 and 15 may be considered as MCM or near MCM processes.

5.4.1 Immiscible Displacement Processes

Table 5.13 and Table 5.14 show that for the immiscible displacement processes, calculated oil recovery

Table 5.13 : Comparison of ultimate recovery of oil obtained from numerical simulation based on the non-equilibrium model and the equilibrium model with experimental values.

				Ultimate Oil Recovery in %		
Experiment #	Oil #	Gas #	Pressure in psia	Non-Equi. Model	Experimental	Equi. Model
1	A	A	3430	86.34	89.55	91.25
2	A	B	2390	51.34	49.40	56.95
3	A	C	2700	91.95	94.32	97.20
4	A	D	2700	73.30	69.15	80.75
5	B	D	2700	55.60	52.62	66.30
6*	B	D	2700	66.36	61.78	66.63
7	B	C	2700	76.67	71.40	88.80
8	D	C	2940	54.33	54.81	54.97
9	A	B	2700	59.58	58.00	66.56
10	A	A	2700	56.48	56.41	63.02
11	A	A	3100	71.50	73.93	78.40
12**	A	A	3100	69.70	67.24	80.70
13	A	C	2390	55.20	59.60	59.16
14	C	A	3430	45.94	47.48	49.01
15	A	A	3430	86.33	91.20	90.88

* Injection rate=0.048 PV/hr, PV=Pore Volume
** Injection rate=0.127 PV/hr, else Injection rate=0.096 PV/hr

Table 5.14: Comparison of breakthrough times obtained from numerical simulation based on the non-equilibrium model and the equilibrium model with experimental values.

Experiment #	Total PV of Gas Injected	Breakthrough Time in PV of Gas Injected: Non-Equi. Model	Experimental	Equi. Model
1	1.270	1.010	1.120	1.041
2	1.074	0.895	0.878	1.076
3	1.220	1.076	1.138	1.131
4	1.195	1.096	0.781	1.146
5	1.174	0.924	0.781	1.090
6	1.171	0.708	0.785	0.908
7	1.220	1.031	0.910	N.O
8	1.270	N.O	N.O*	N.O
9	1.176	0.968	0.992	1.108
10	1.290	1.042	1.163	1.204
11	1.380	1.030	1.220	1.167
12	1.240	1.016	1.041	1.235
13	1.170	1.074	N.O	N.O
14	1.220	1.006	1.089	1.224
15	1.220	0.998	1.147	1.084

* N.O= Breakthrough not obtained.

values and breakthrough times obtained from simulations based on the non-equilibrium model and those obtained from experiments are in good agreement. Table 5.13 also shows that except for experiments 8 and 6, there are significant differences (4-12%) between the ultimate oil recovery values obtained from simulations based on non-equilibrium model and

equilibrium model.

In Experiment 8, almost identical ultimate oil recovery values are obtained from simulations based on both phase behaviour models. The identical predictions of oil recoveries obtained by using both models may be attributed to the lack of formation of a two-phase zone during the displacement of oil by gas. A similar argument may be made for experiment 6 where almost the same ultimate oil recoveries are obtained from simulations using both models. This explanation is supported by the fact that in experiment 8 breakthrough is neither observed after 1.27 PV of gas injection nor it is predicted by simulations based on both phase behaviour models.

The comparisons of the calculated recovery profiles for immiscible displacement processes from the non-equilibrium and the equilibrium model simulations with the experimental recovery profiles are shown in Figures 5.13 through 5.24. In all the case studies (experiment 2, and experiments 4-14), it can be seen from the corresponding figures that, until breakthrough, there is no significant difference between the recovery obtained from the use of the non-equilibrium and the equilibrium model simulations. This observation leads to the conclusion that phase behaviour mechanisms do not affect the recovery profiles but affect the mixing between oil and gas. The differences in describing the mixing behaviour between non-equilibrium and equilibrium model simulations cause

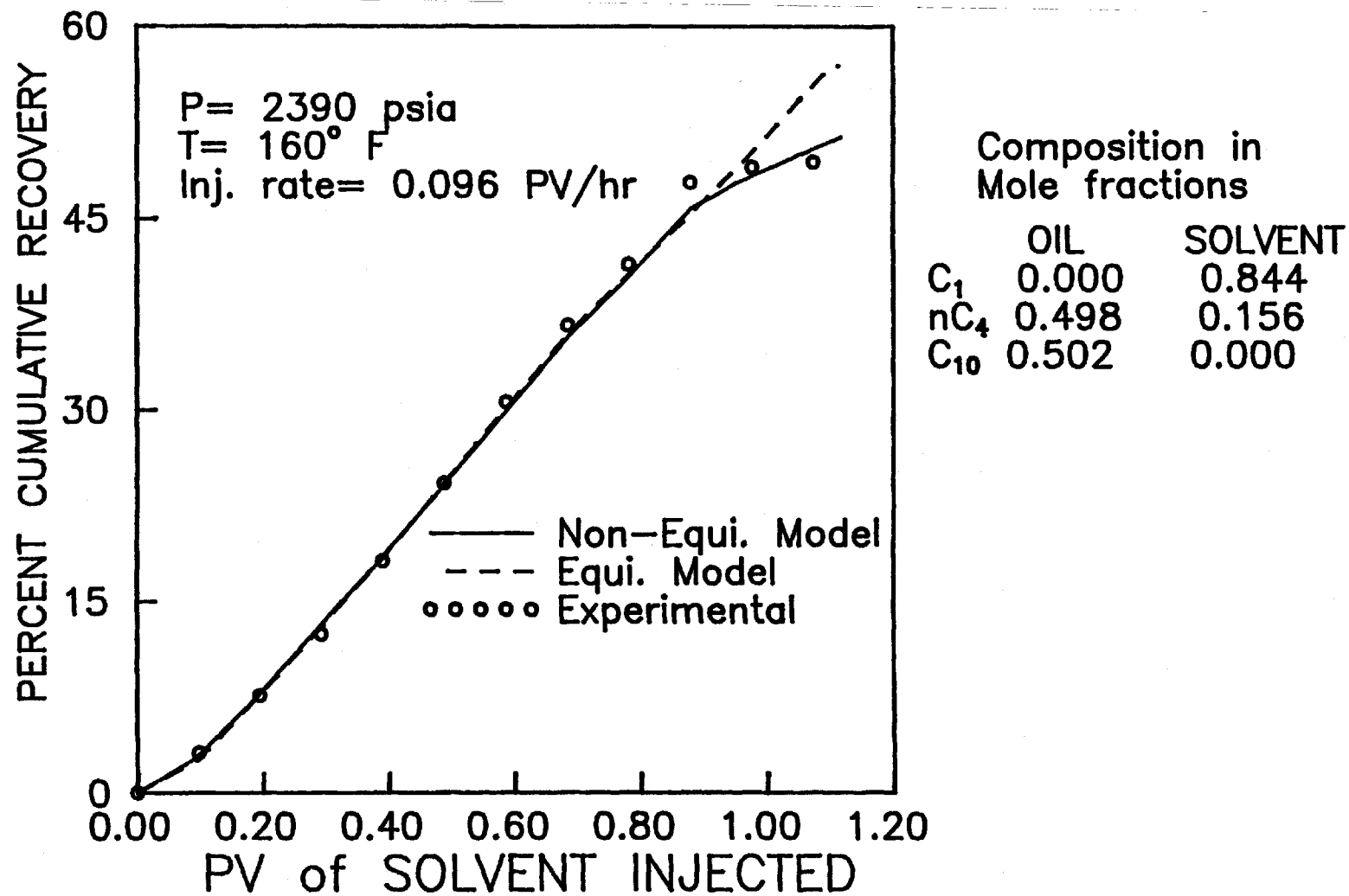

Figure 5.13: Comparison of Recovery Profile for Experiment 2

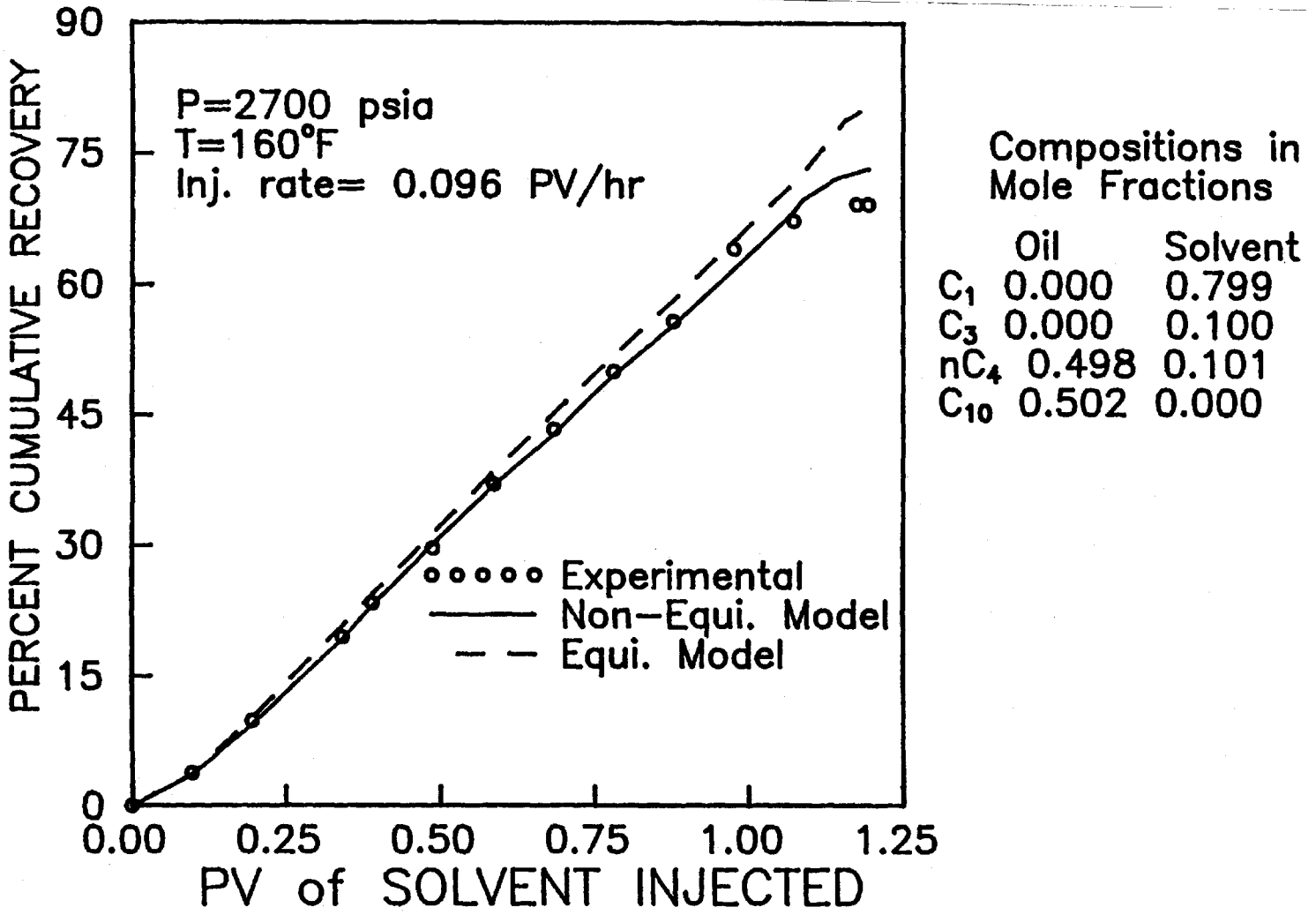

Figure 5.14: Comparison of Recovery Profile for Experiment 4

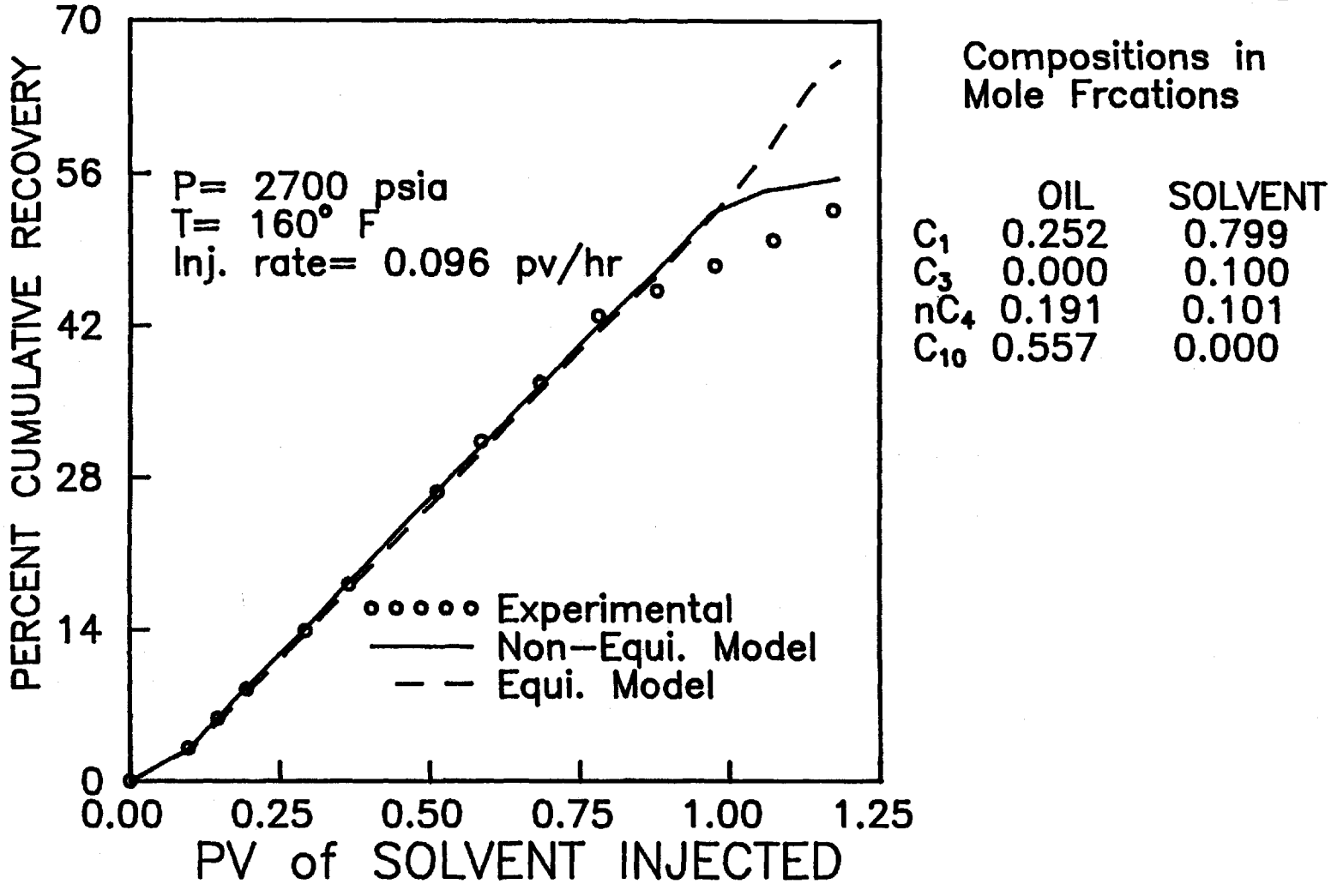

Figure 5.15: Comparison of Recovery Profile for Experiment 5

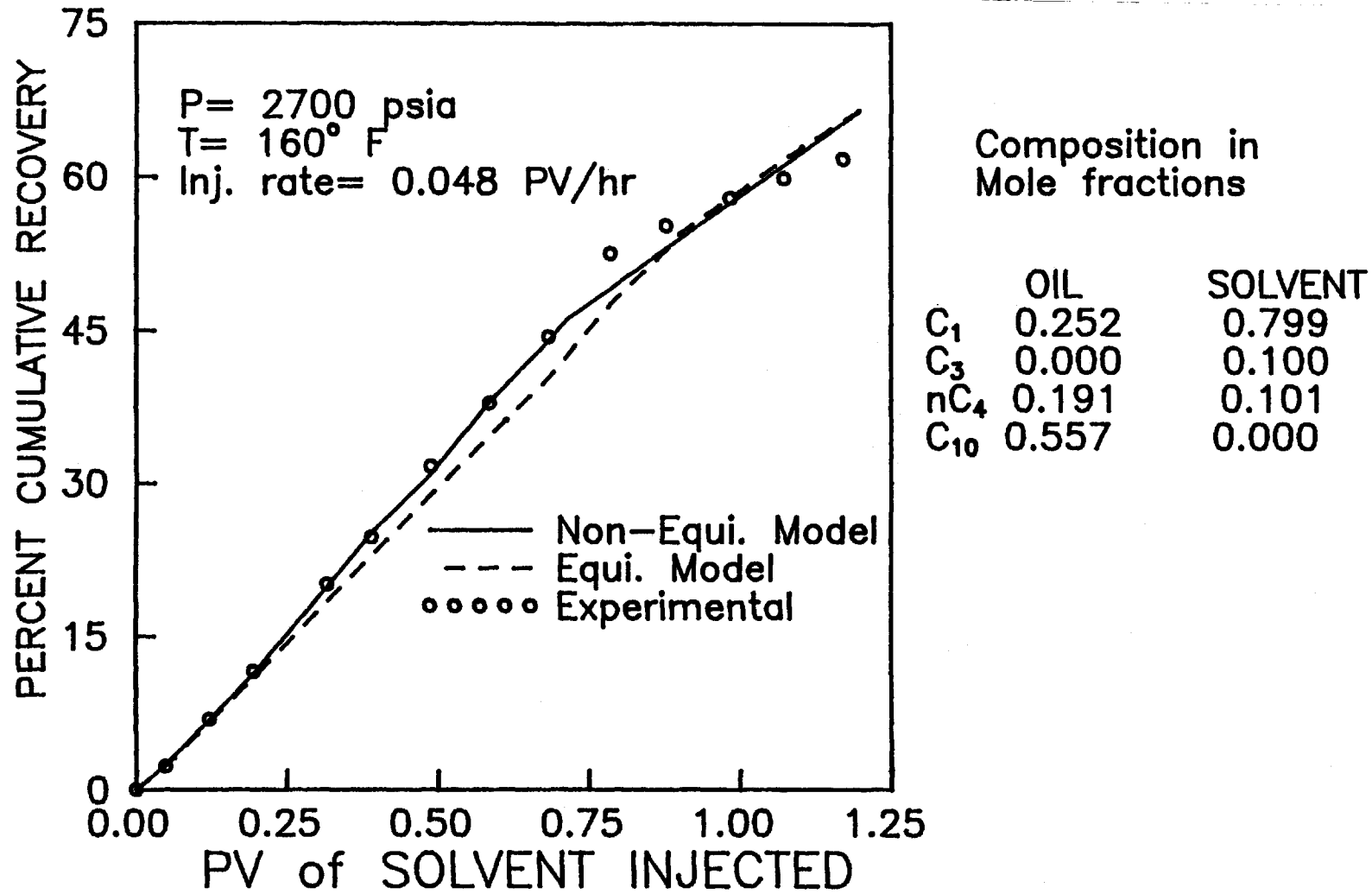

Figure 5.16: Comparison of Recovery Profile for Experiment 6

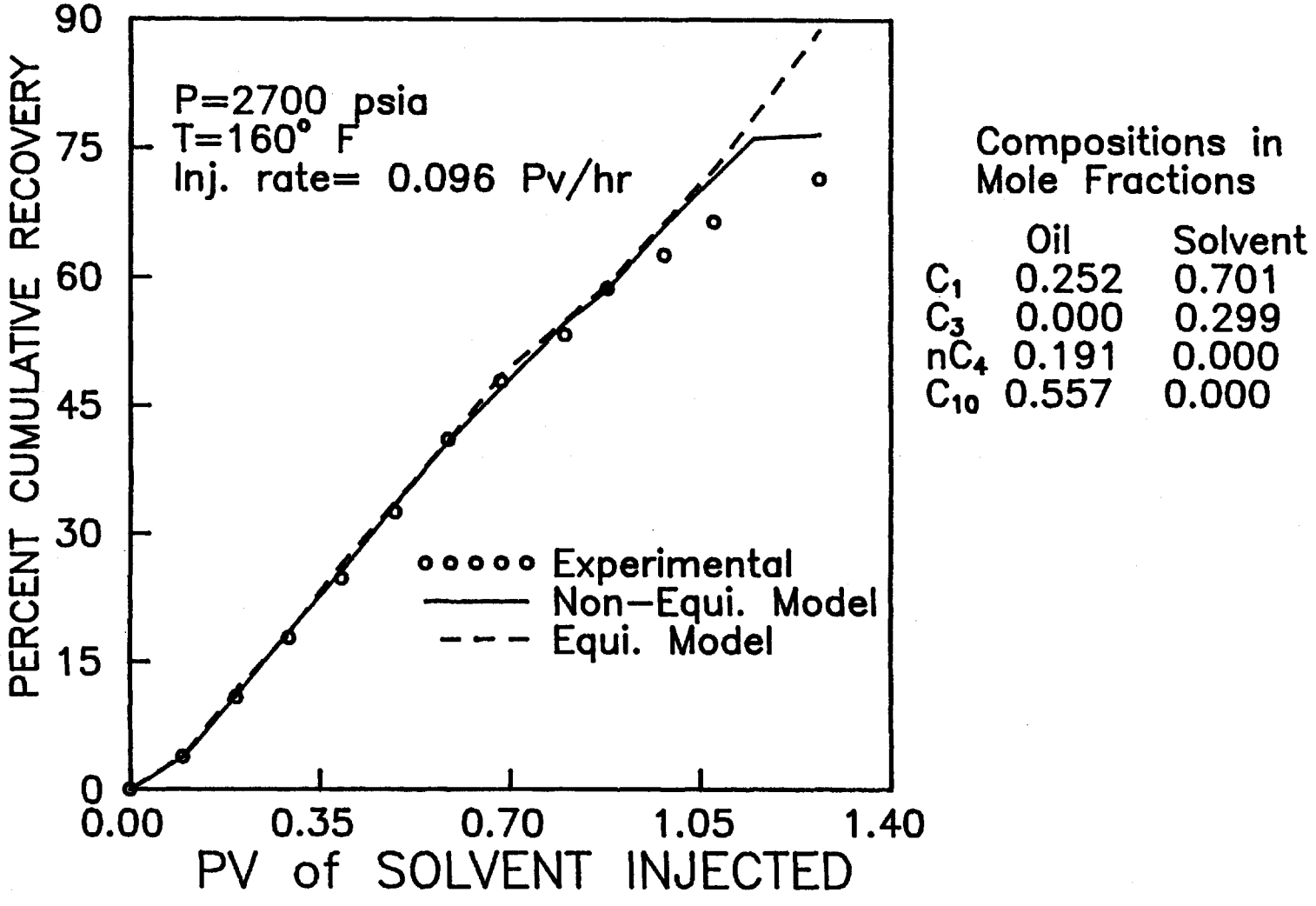

Figure 5.17: Comparison of Recovery Profile for Experiment 7

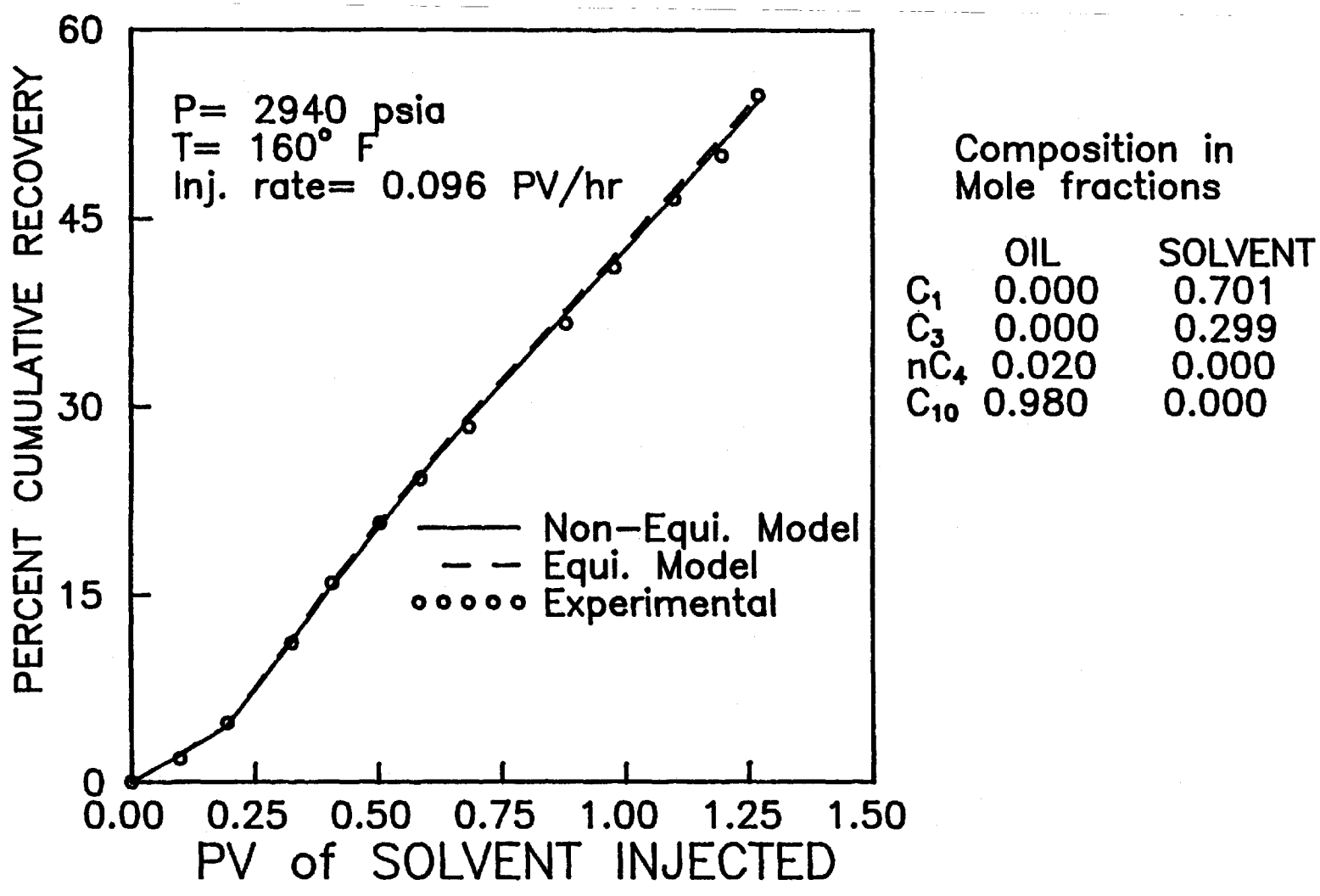

Figure 5.18: Comparison of Recovery Profile for Experiment 8

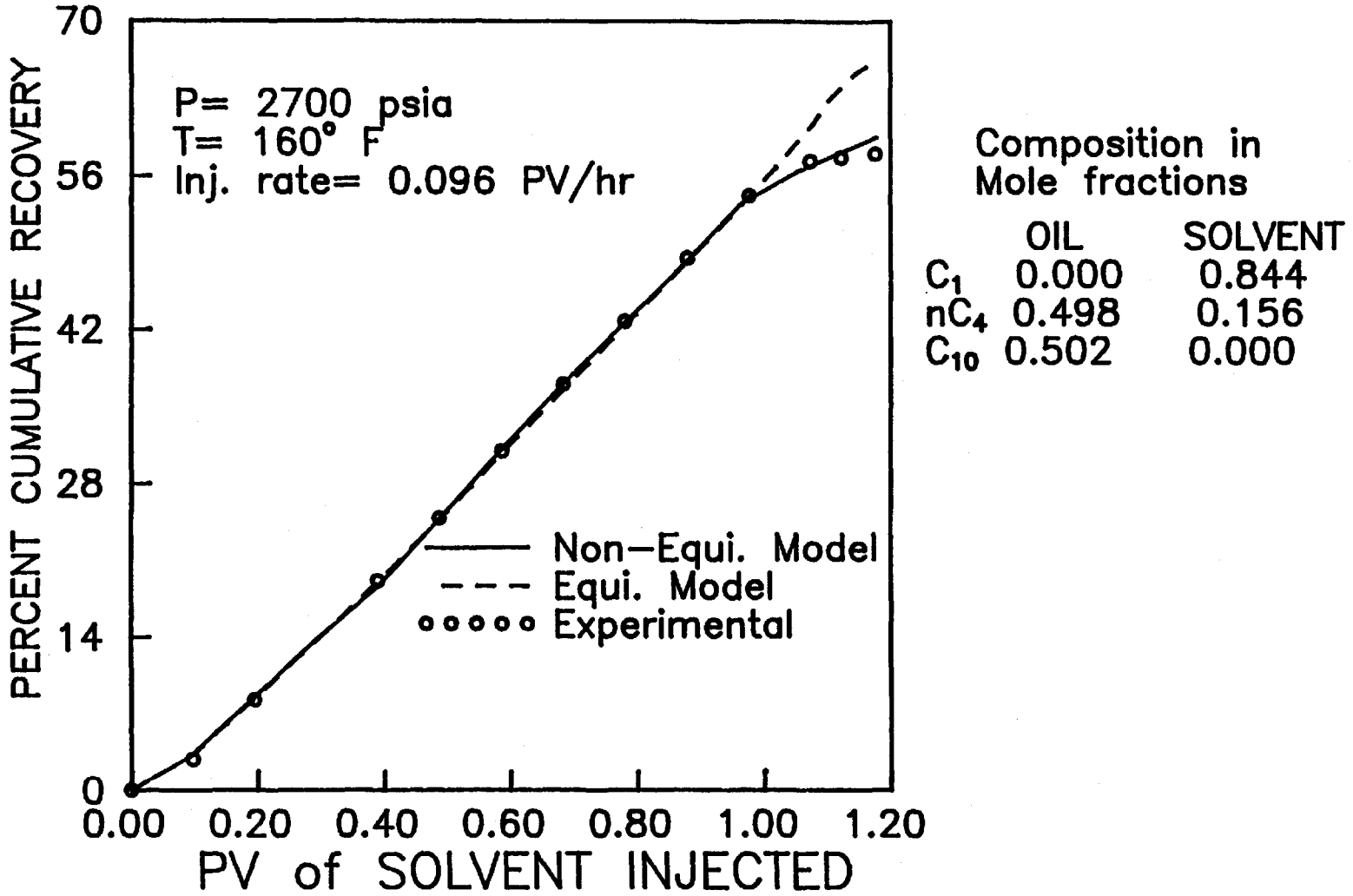

Figure 5.19: Comparison of Recovery Profile for Experiment 9

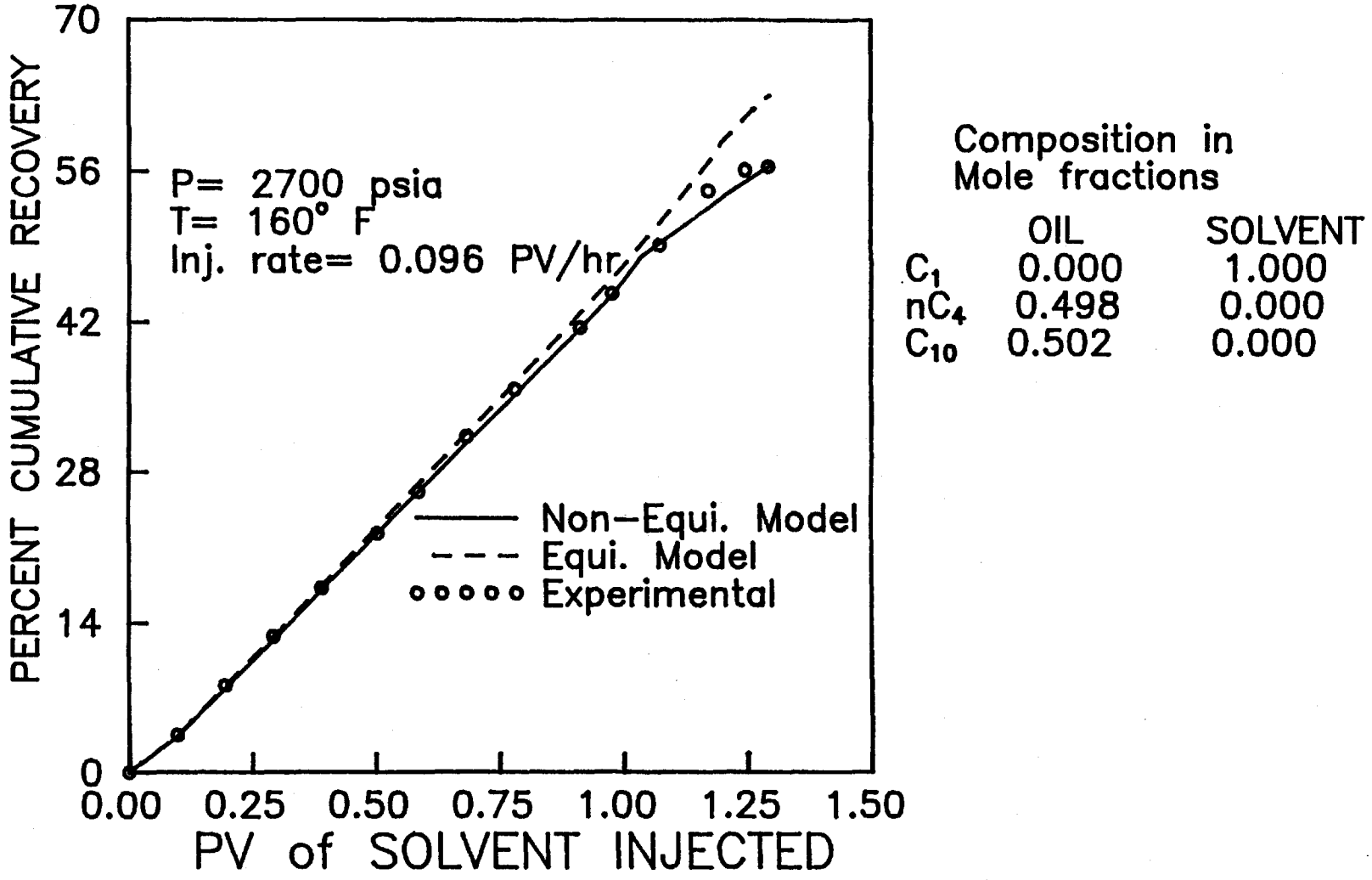

Figure 5.20: Comparison of Recovery Profile for Experiment 10

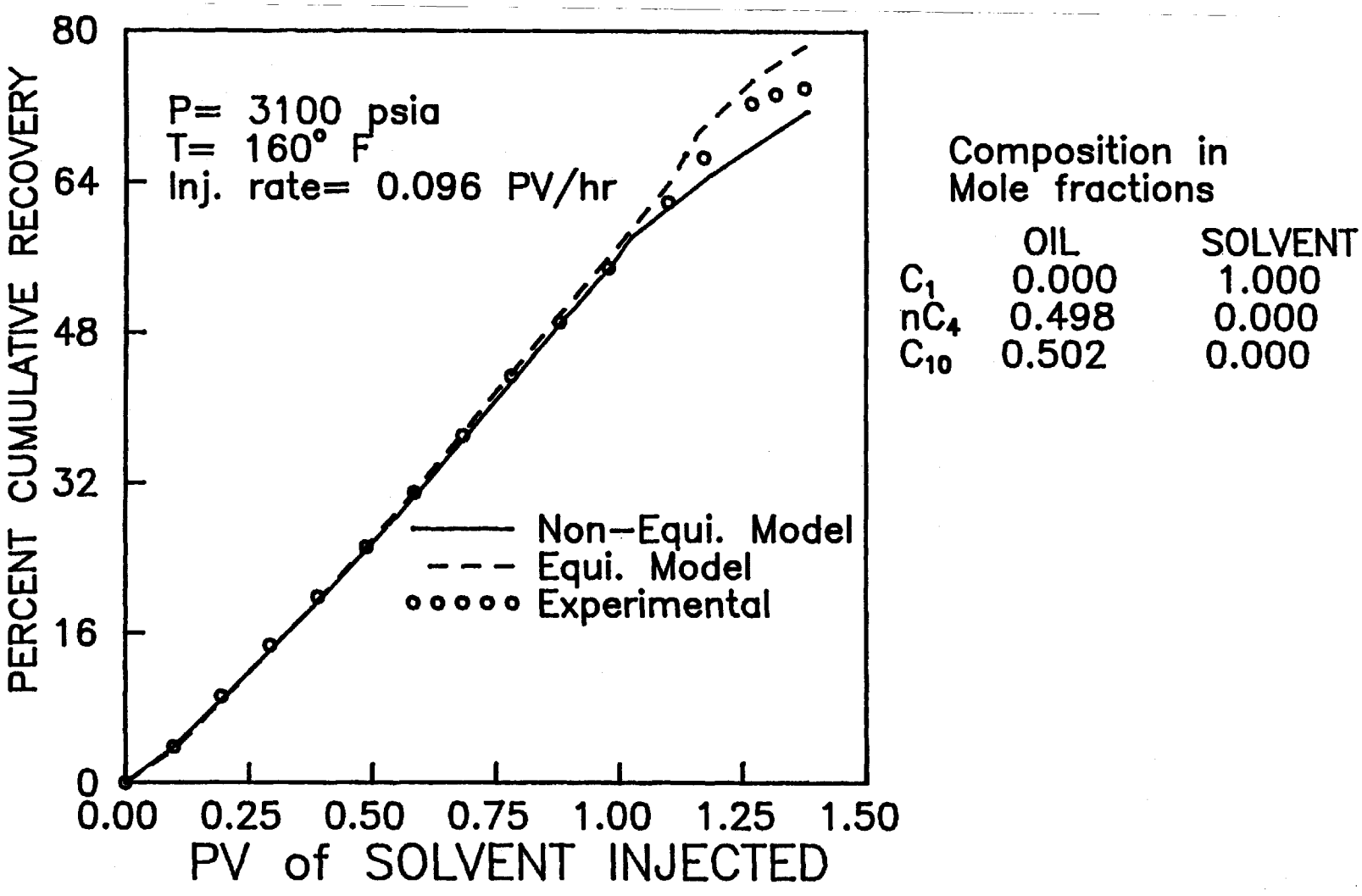

Figure 5.21: Comparison of Recovery Profile for Experiment 11

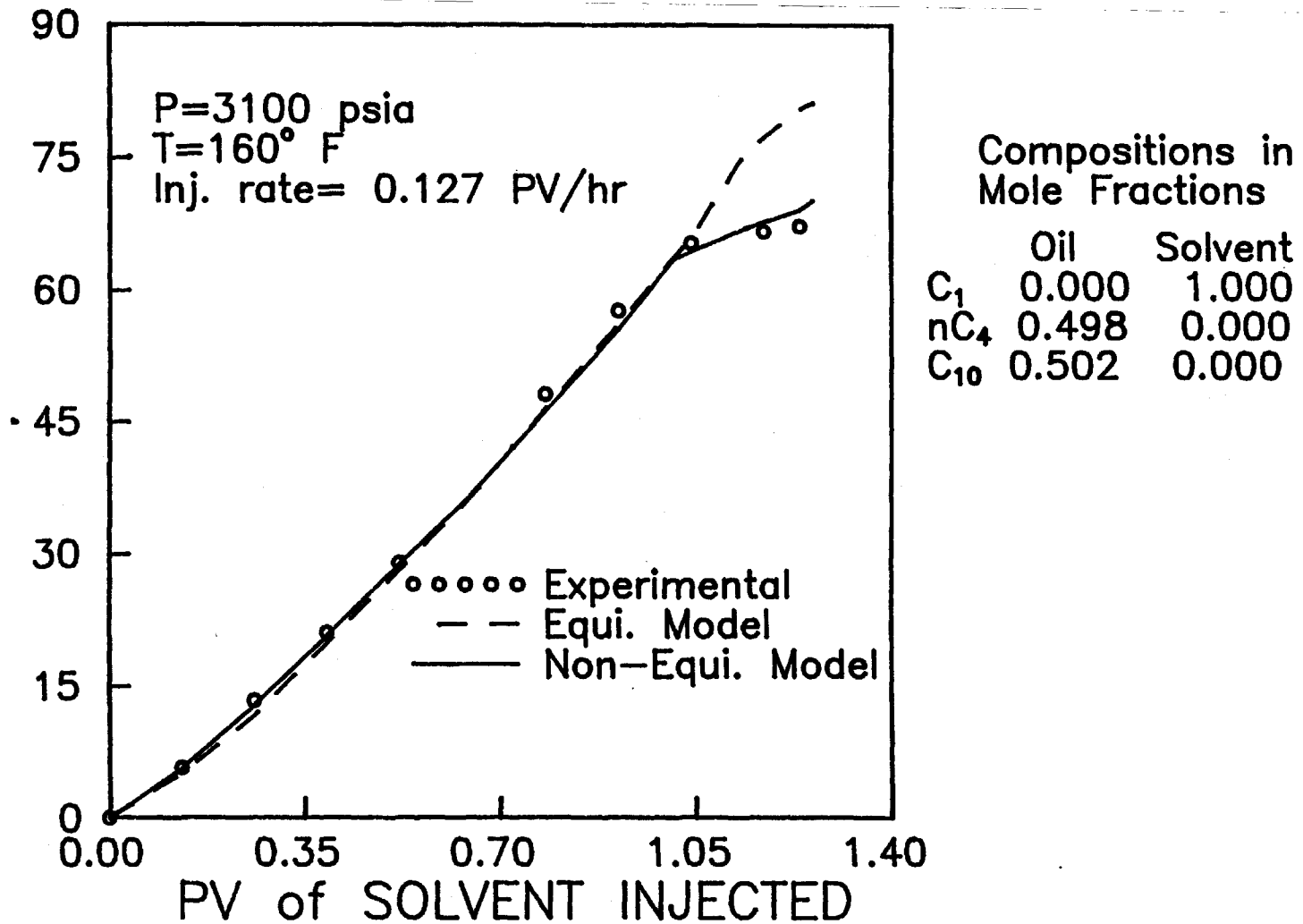

Figure 5.22: Comparison of Recovery Profile for Experiment 12

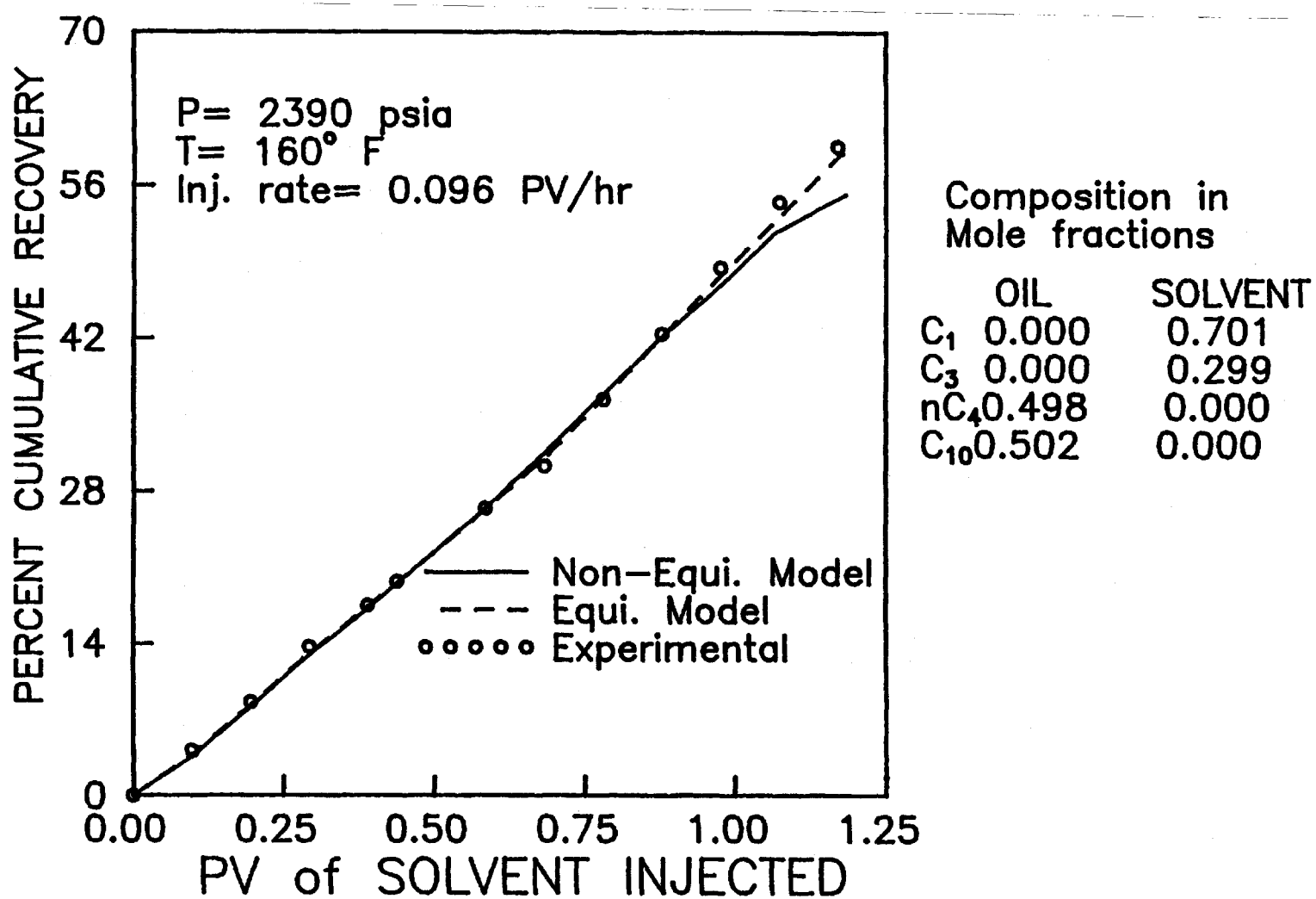

Figure 5.23: Comparison of Recovery Profile for Experiment 13

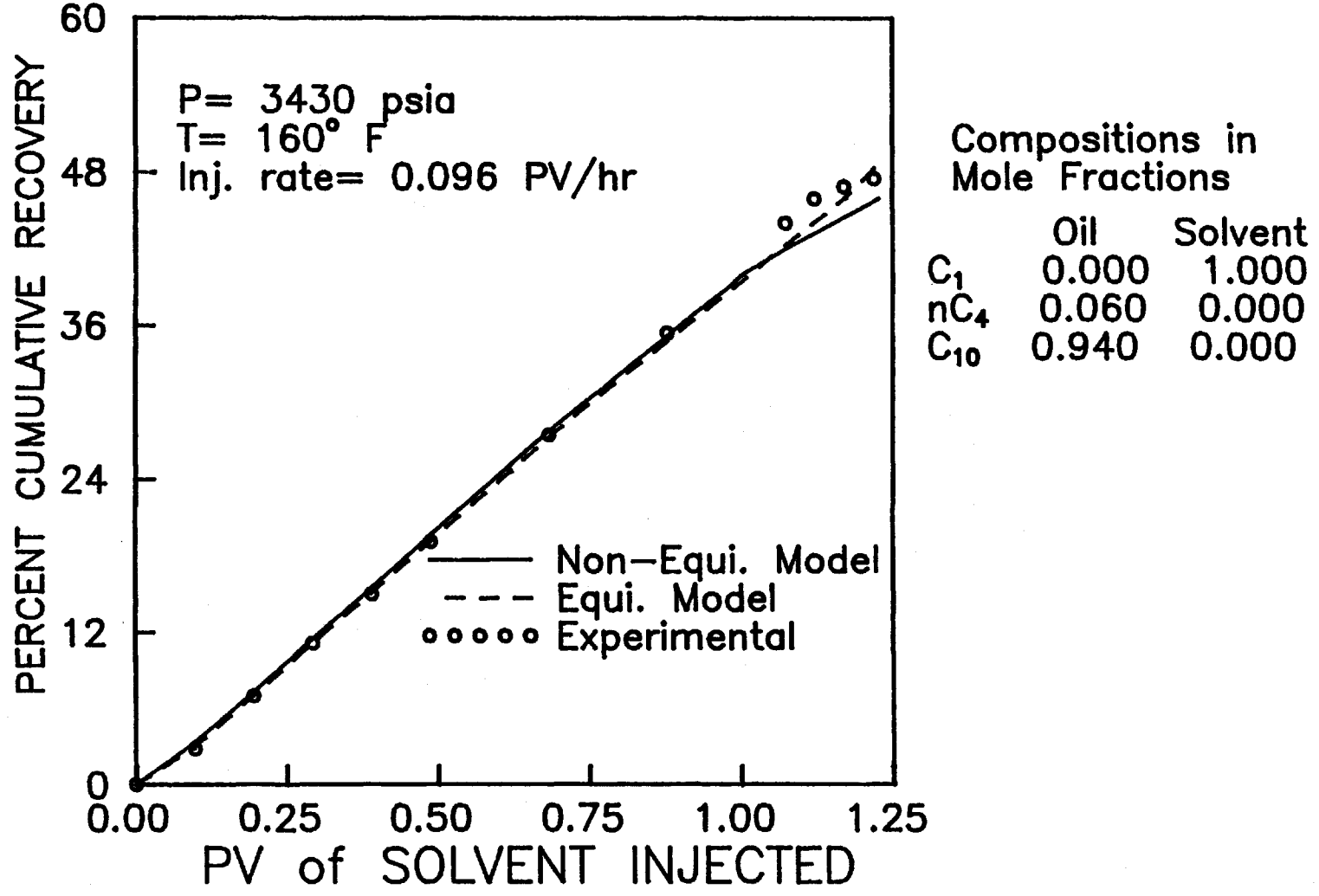

Figure 5.24: Comparison of Recovery Profile for Experiment 14

variations in the calculated breakthrough times (shown in Table 5.14). Non-equilibrium model simulations predict smaller breakthrough times than those calculated from equilibrium model simulations. This phenomenon causes smaller ultimate oil recovery values for the non-equilibrium model simulations than those calculated from the equilibrium model simulations.

In all the case studies, calculations of ultimate recovery values and breakthrough time from simulations based on the equilibrium model are significantly higher (recovery values differ 5-17%) than those calculated from simulations based on the non-equilibrium model and those obtained experimentally. On the other hand, the differences between the calculated recovery values from non-equilibrium model simulations and those obtained from experiments vary within (± 1.5-5%).

The largest variation (17.4%) between the calculated ultimate recovery value based on equilibrium model simulation and that obtained from experiment is observed for experiment 7. Figure 5.17 shows that the change in the slope of the recovery profile obtained from the non-equilibrium model simulation is similar to the experimental data. The simulation based on the equilibrium model does not predict the change in slope of the recovery profile as can be observed from Figure 5.17. Breakthrough is not obtained with the equilibrium model simulation whereas breakthrough is obtained

in the experiment and is calculated from the non-equilibrium model simulation.

Table 5.13 shows that a significant increase in the ultimate oil recovery value is obtained in experiment 6 compared with that in experiment 5 because of the lower injection rate of solvent or gas in experiment 6. A similar trend in the ultimate oil recovery value at the lower gas injection rate is calculated from the non-equilibrium model simulation whereas the equilibrium model simulation does not account for the effect of the lower injection rate on oil recovery. The same phenomena are observed when the results of numerical simulation and the results of experiment 11 are compared with those of experiment 12. In short, it can be said that the calculated results from non-equilibrium model simulations are consistent with the experimental data.

5.4.2 Miscible Displacement Processes

Experimental data indicate that experiments 1, 3 and 15 may be identified as MCM or near MCM processes. Comparisons of the calculated recovery profiles based on the non-equilibrium and equilibrium models with the experimental data are shown in Figures 5.25-27 for experiments 1, 3 and 15, respectively. It can be seen from Table 5.13 that for all the experiments considered in the miscible displacement processes, ultimate oil recoveries calculated from numerical simulation using the non-equilibrium model are slightly lower than the

experimental values. On the other hand, the ultimate oil recovery values obtained from numerical simulations based on the equilibrium model are slightly higher than experimental values. The conservative estimates of ultimate oil recovery values from the non-equilibrium model simulations may be explained by the fact that the breakthrough times calculated from non-equilibrium model simulations are smaller than those calculated from equilibrium model simulations and those obtained from experimental data.

Figure 5.25 shows that during the initial period of gas injection calculated recoveries from the equilibrium model simulation are smaller than both the experimental recovery and calculated recovery values from the non-equilibrium model simulation. This characteristic of the recovery profile is different from that are observed in Figures 5.26 and 5.27. It may be explained by the fact that the effect of mobility ratio is more pronounced on the non-equilibrium simulation for experiment 1 than other two experiments, 3 and 15. However, the ultimate oil recovery calculated from the equilibrium model is higher than the experimental ultimate recovery and ultimate recovery calculated from the non-equilibrium model simulation. This optimistic recovery estimation is a characteristic of the equilibrium model simulation and was also reported by Nghiem et al. (1989).

The differences between the experimental recoveries and the recoveries calculated from the equilibrium model are

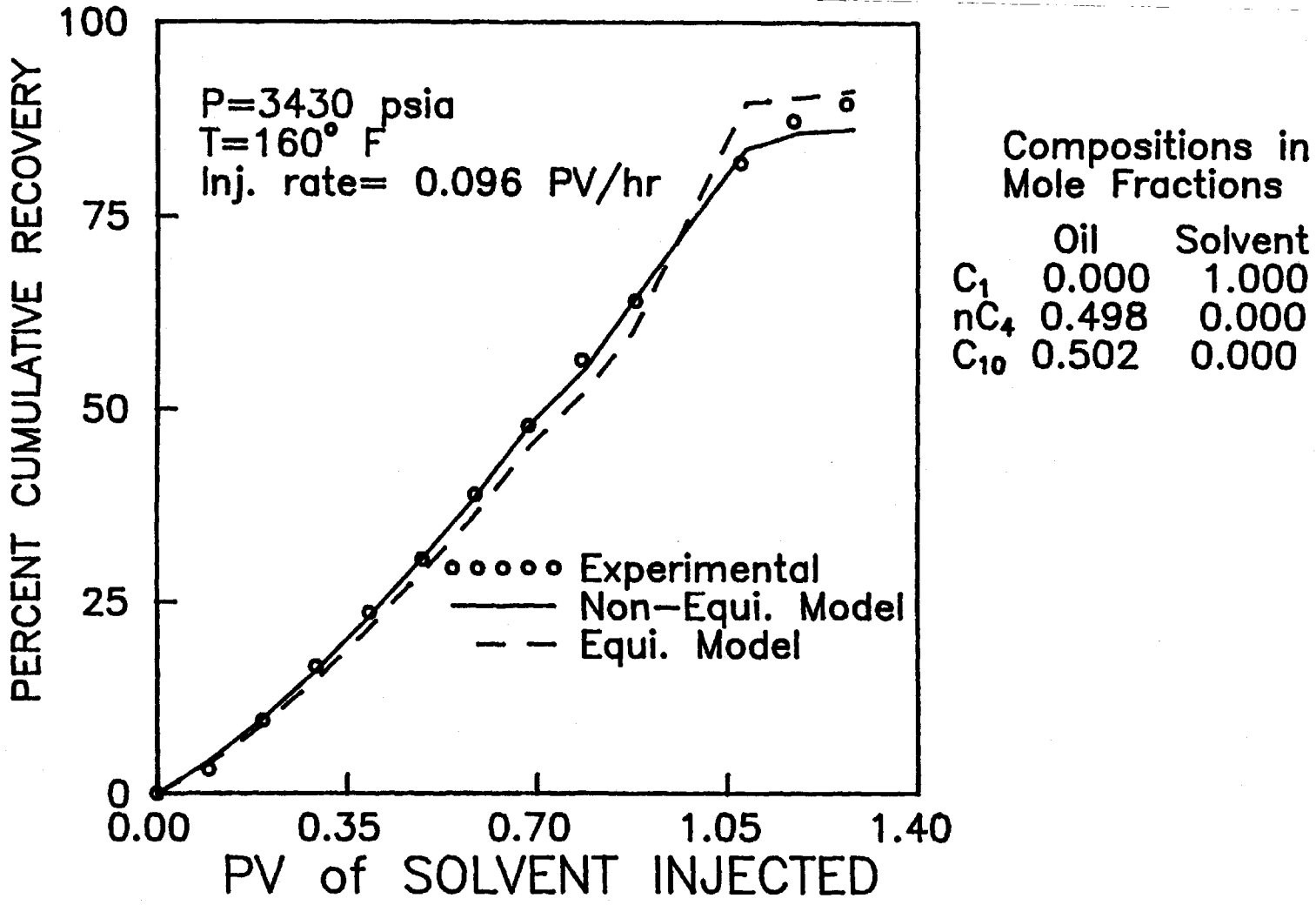

Figure 5.25: Comparison of Recovery Profile for Experiment 1

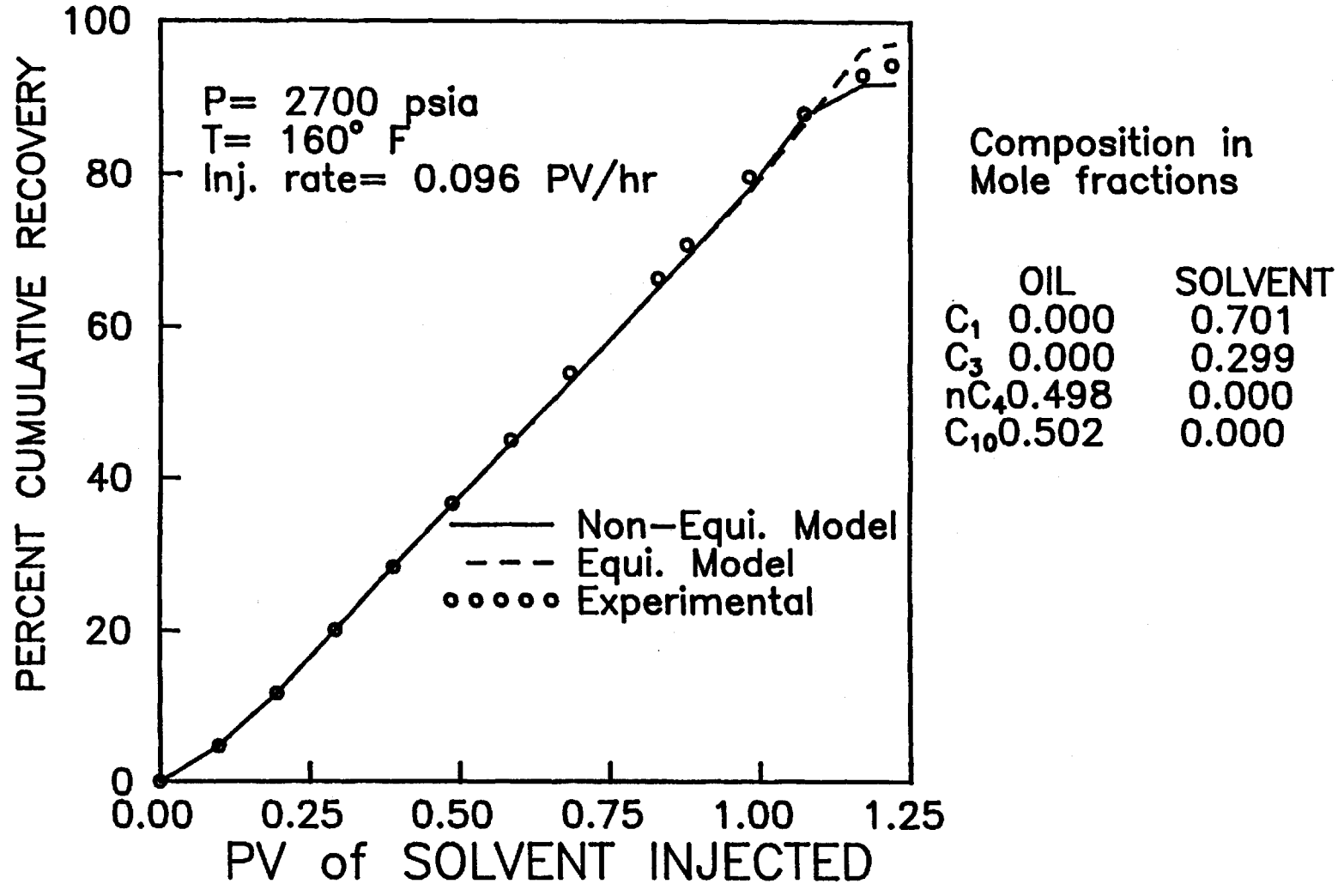

Figure 5.26: Comparison of Recovery Profile for Experiment 3

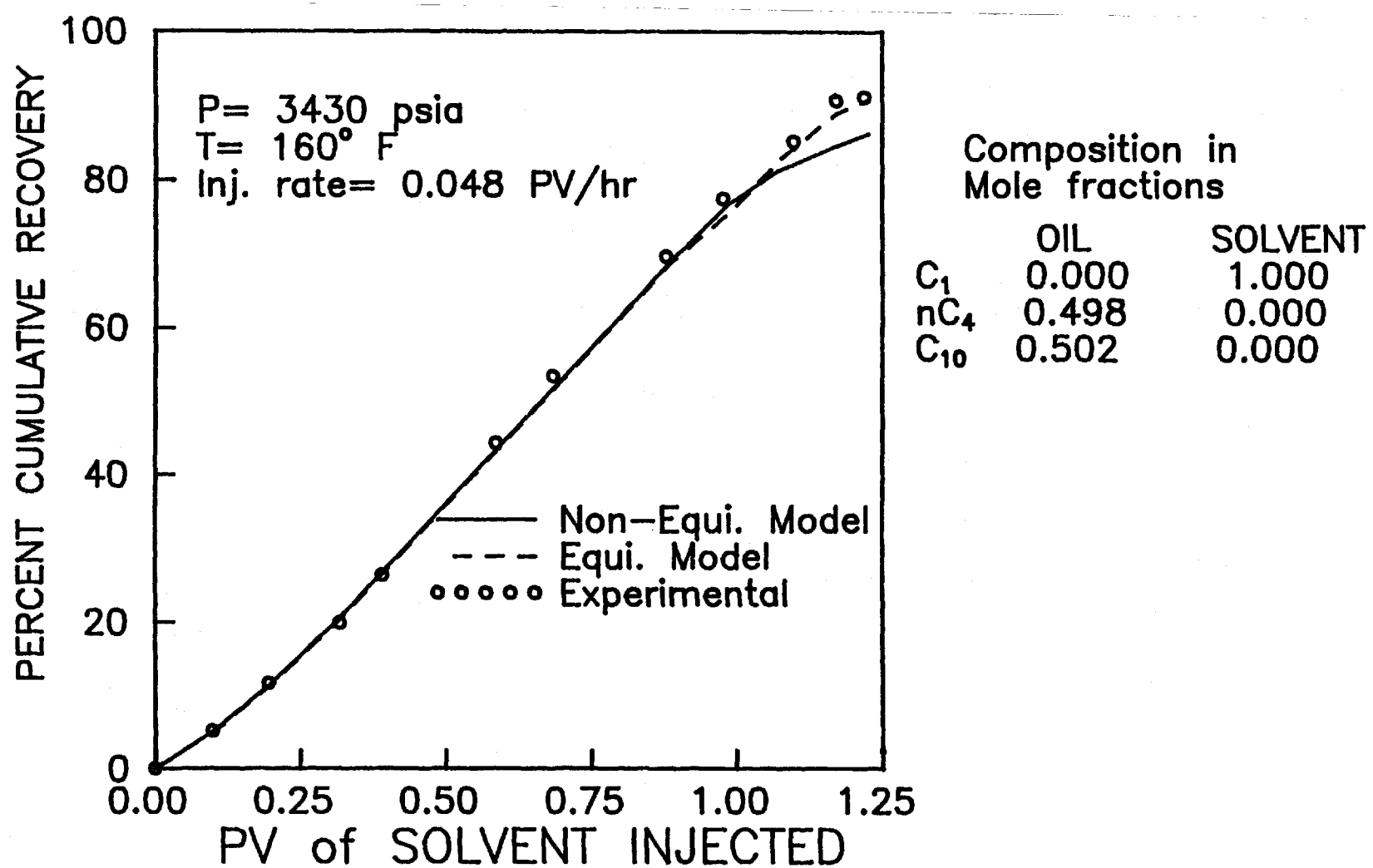

Figure 5.27: Comparison of Recovery Profile for Experiment 15

not significant for these particular experiments (1, 3 and 15) which are miscible displacement processes. This observation is consistent with the results reported by other researchers (Coats, 1980 and Crump, 1988) for the simulations of miscible displacement processes. Nevertheless, the fact that the results obtained from the non-equilibrium model are in good agreement with the experimental values indicate that the non-equilibrium model may be considered as an alternative to the equilibrium model in the numerical simulations of miscible displacement processes.

5.5 Comparisons of Calculated Saturation Profiles and Composition Profiles

There is a possibility that channelling or bypassing of the gas phase may occur in a displacement process due to the following reasons; i) viscosity difference between the displaced phase (oil phase) and the displacing phase (gas phase), ii) density difference between the oil phase and gas phase which will cause gravity segregation between the phases, iii) reservoir geometry and heterogeneity.

Channelling of the gas phase causes incomplete mixing between the oil and gas phases. This incomplete mixing reduces the recovery efficiency of the displacement process. To illustrate how non-equilibrium model simulation describes incomplete mixing compared with to that of the equilibrium model simulation, experiment 12 and experiment 4 are chosen as

examples.

Example 1

The calculated solvent or gas saturation profiles from the non-equilibrium model and the equilibrium model simulations at 0.4 PV and 0.8 PV of gas injection for Experiment 12 are shown in Figures 5.28 and 5.29, respectively. The differences between the saturation profiles calculated from the two models are more pronounced at 0.8 PV of gas injection than those at 0.4 PV of gas injection. Figure 5.29 shows that the mobility of the gas phase is higher in the non-equilibrium model simulation than in the equilibrium model simulation. The discrepancies between the saturation profiles obtained from the equilibrium model and the non-equilibrium model are comparable to those that exist between the saturation profiles calculated from the no-fingering model and the fingering model as reported by Nghiem et al.(1989).

The calculated concentration profiles of C_1 and n-C_4 at 0.8 PV of gas injection are shown in Figures 5.30 and 5.31, respectively. In comparison with the gas saturation profiles shown in Figure 5.29, Figure 5.30 clearly shows that the C_1 concentration profile is ahead of the gas saturation front. This can be considered as evidence that channelling or bypassing has occurred under the displacement conditions. The fact, as shown in Figure 5.31, that the n-C_4 concentration profile calculated from the non-equilibrium model lags behind that calculated from the equilibrium model substantiates this

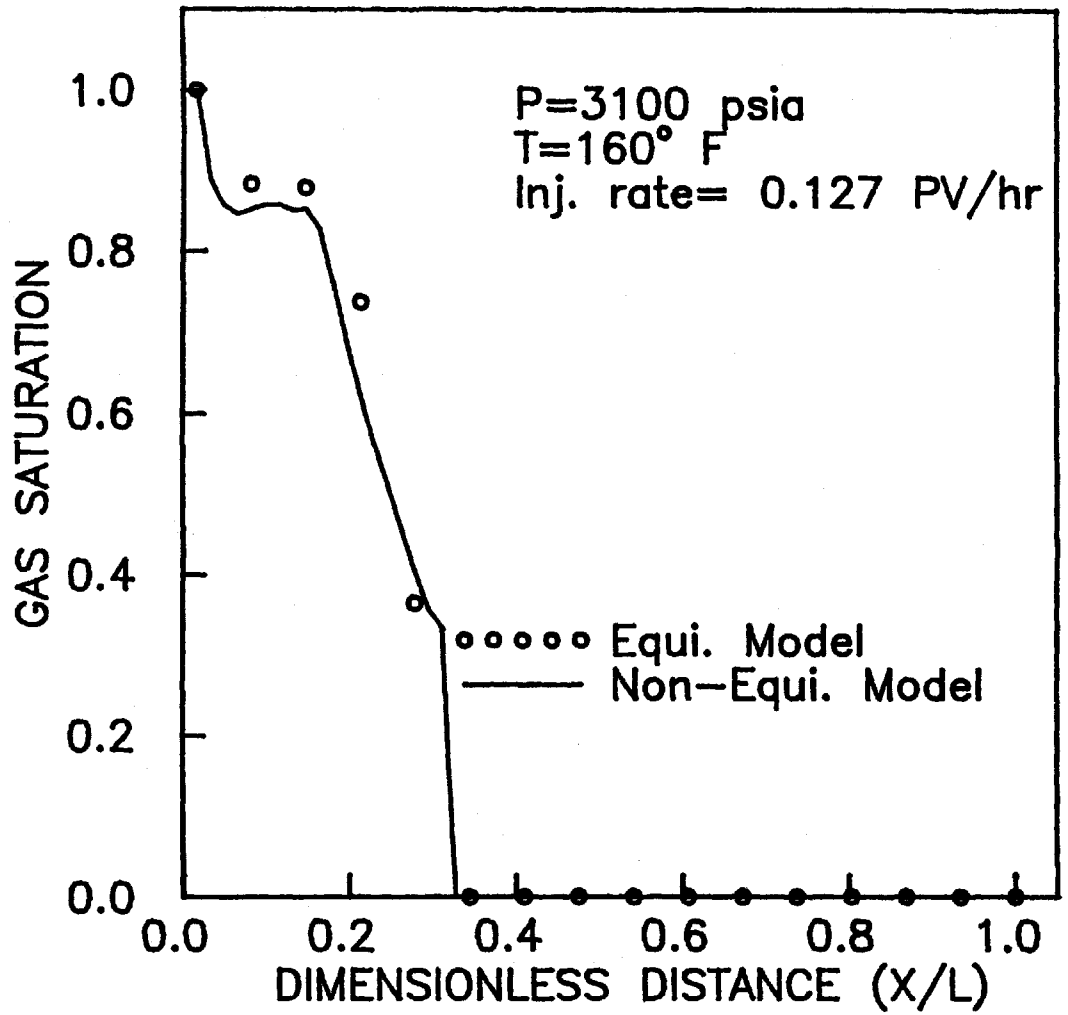

Figure 5.28: Calculated Gas Saturation Profile for Experiment 12 at 0.4 PV of Solvent Injected

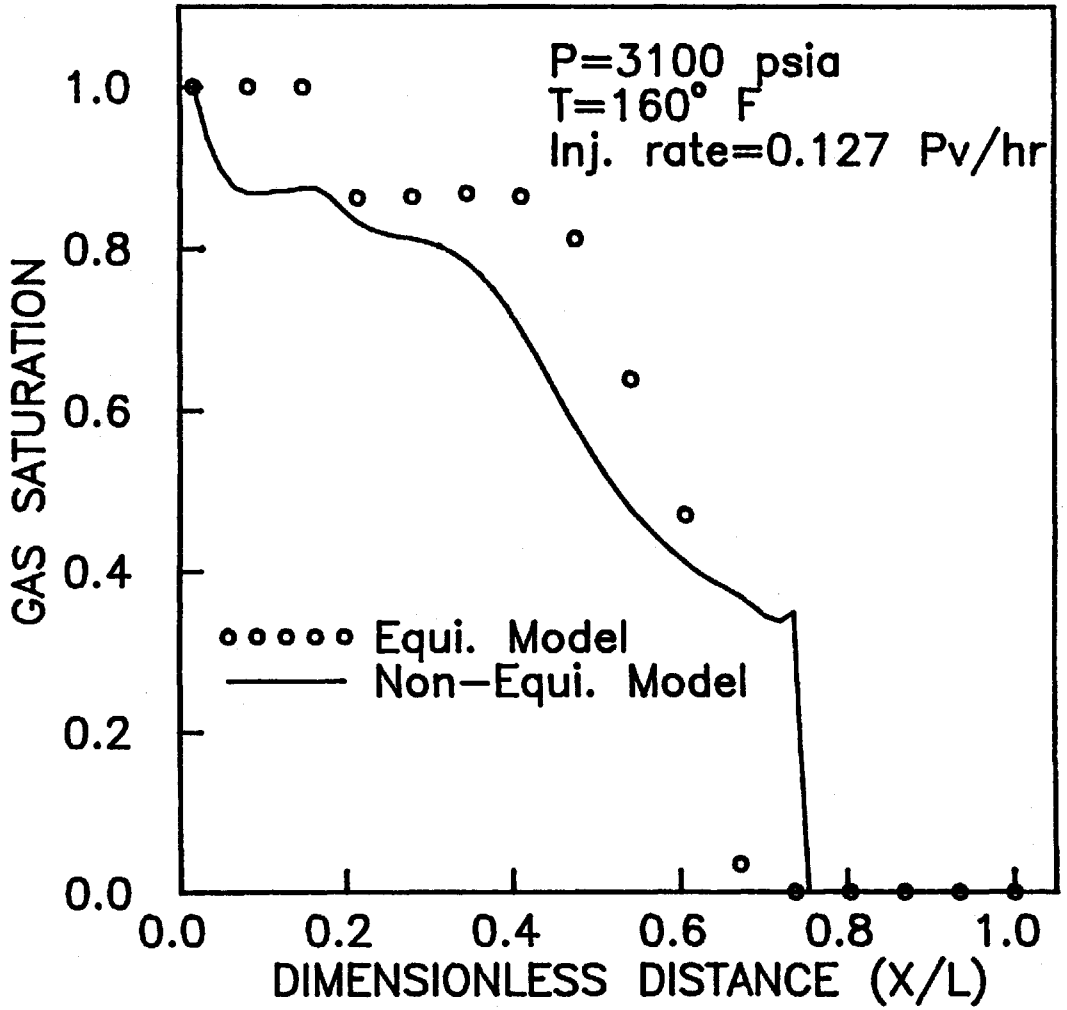

Figure 5.29: Calculated Gas Saturation Profile for Experiment 12 at 0.8 PV of Solvent Injected

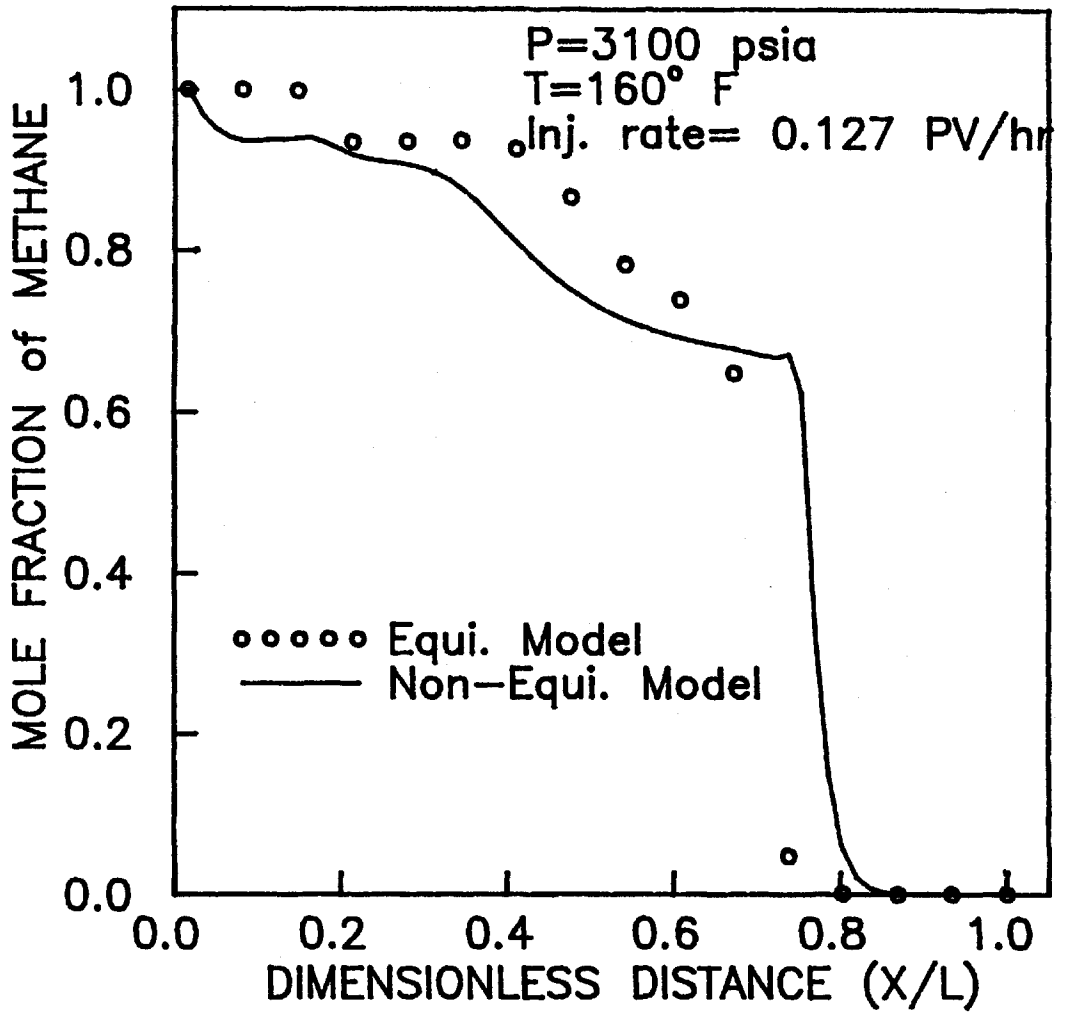

Figure 5.30: Calculated Composition Profile of Methane for Experiment 12 at 0.8 PV of Solvent Injected

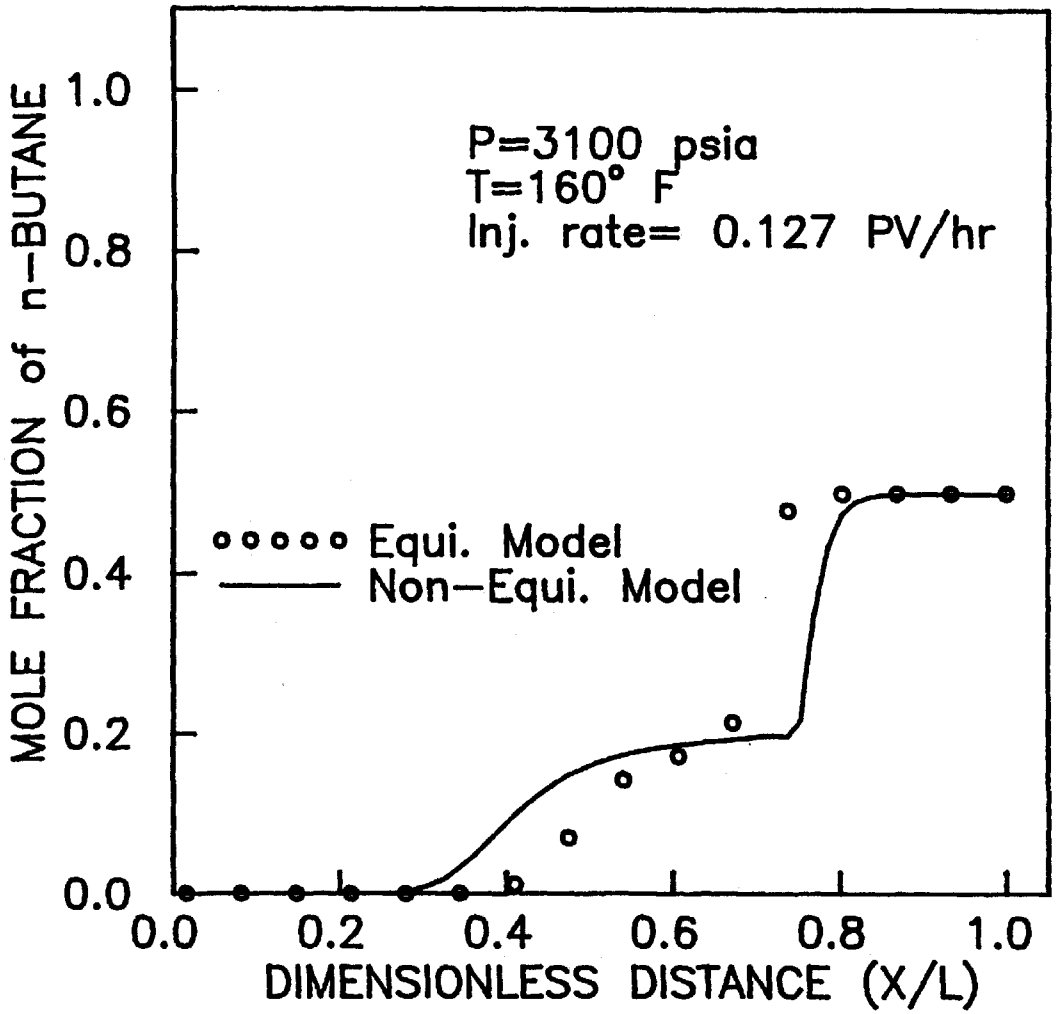

Figure 5.31: Calculated Composition Profile of n–Butane for Experiment 12 at 0.8 PV of solvent Injected

hypothesis.

Example 2

The calculated gas saturation profiles from the non-equilibrium simulation and equilibrium model simulation at 1 PV of gas injection for Experiment 4 are shown in Figure 5.32. The differences between the saturation profiles calculated from the equilibrium model and the non-equilibrium model simulations are similar to those observed in the previous case study (example 1).

The calculated concentration profiles of C_1 and n-C_4 at 1 PV of gas injection are shown in Figures 5.33 and 5.34, respectively. In comparison with the gas saturation profiles shown in Figure 5.32, the C_1 concentration profile shown in Figure 5.33, is clearly ahead of the gas saturation front.

Figure 5.32 shows that at the leading edge of the gas front, the calculated gas saturations from the non-equilibrium model are higher than those calculated from the equilibrium model. Similar phenomena are observed for the C_1 concentration profiles shown in Figure 5.33. On the other hand, Figure 5.34 shows that at the leading edge of the gas front calculated concentrations of n-C_4 from the non-equilibrium model are lower than those calculated from the equilibrium model. This can be interpreted by the fact that the gas phase and the lighter hydrocarbon are more mobile in the non-equilibrium model simulation than they are in the equilibrium model simulation.

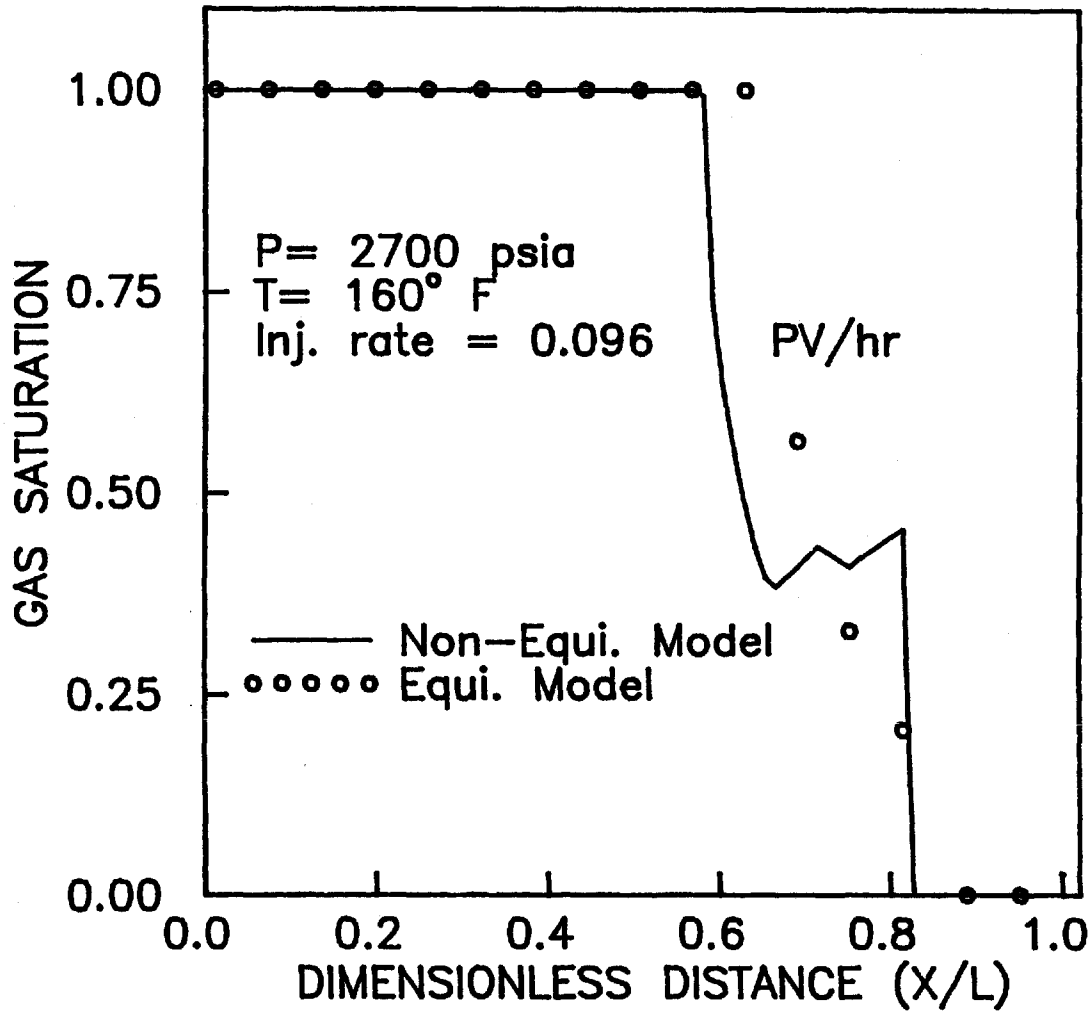

Figure 5.32: Calculated Gas Saturation Profile for Experiment 4 at 1 PV of Solvent Injected

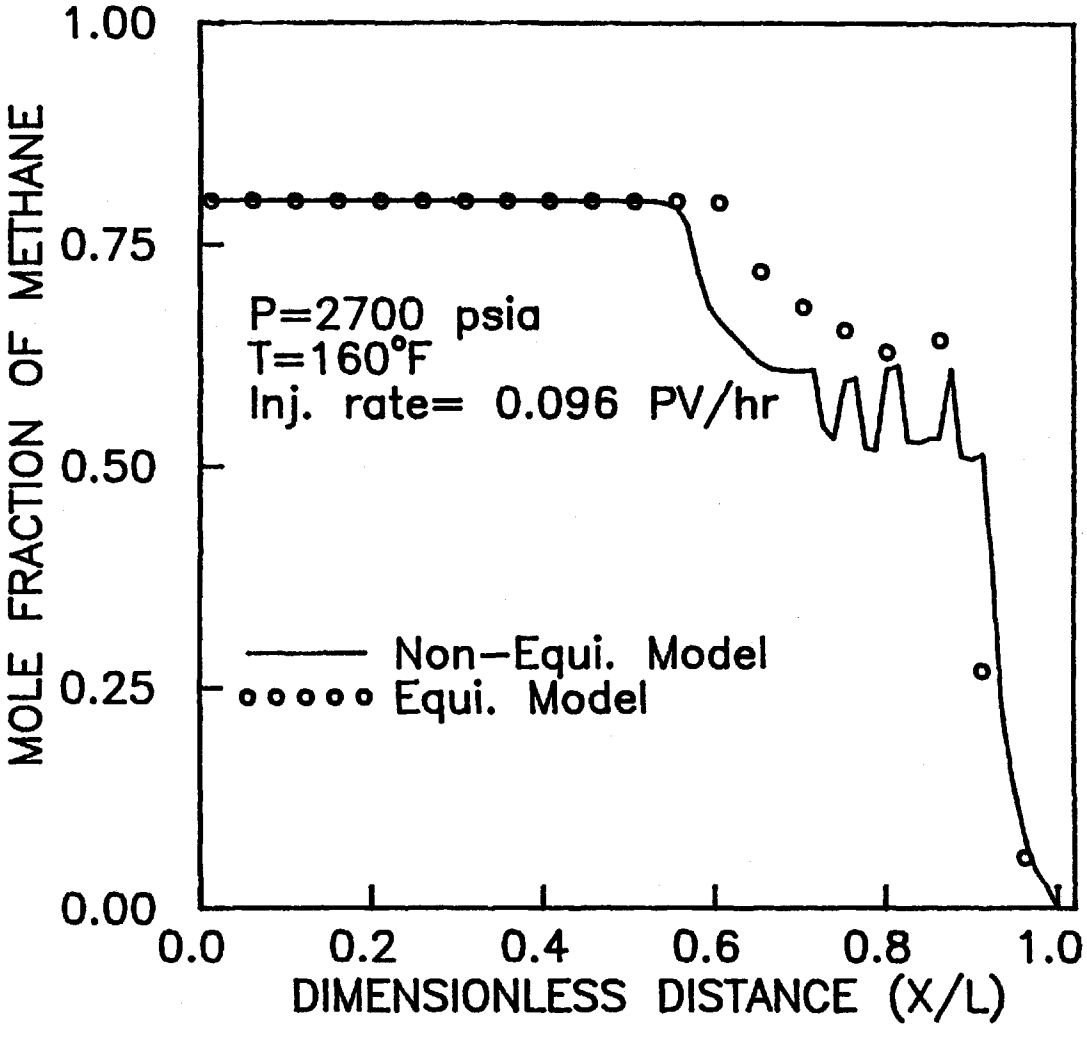

Figure 5.33: Calculated Composition Profile of Methane for Experiment 4 at 1 PV of Solvent Injected

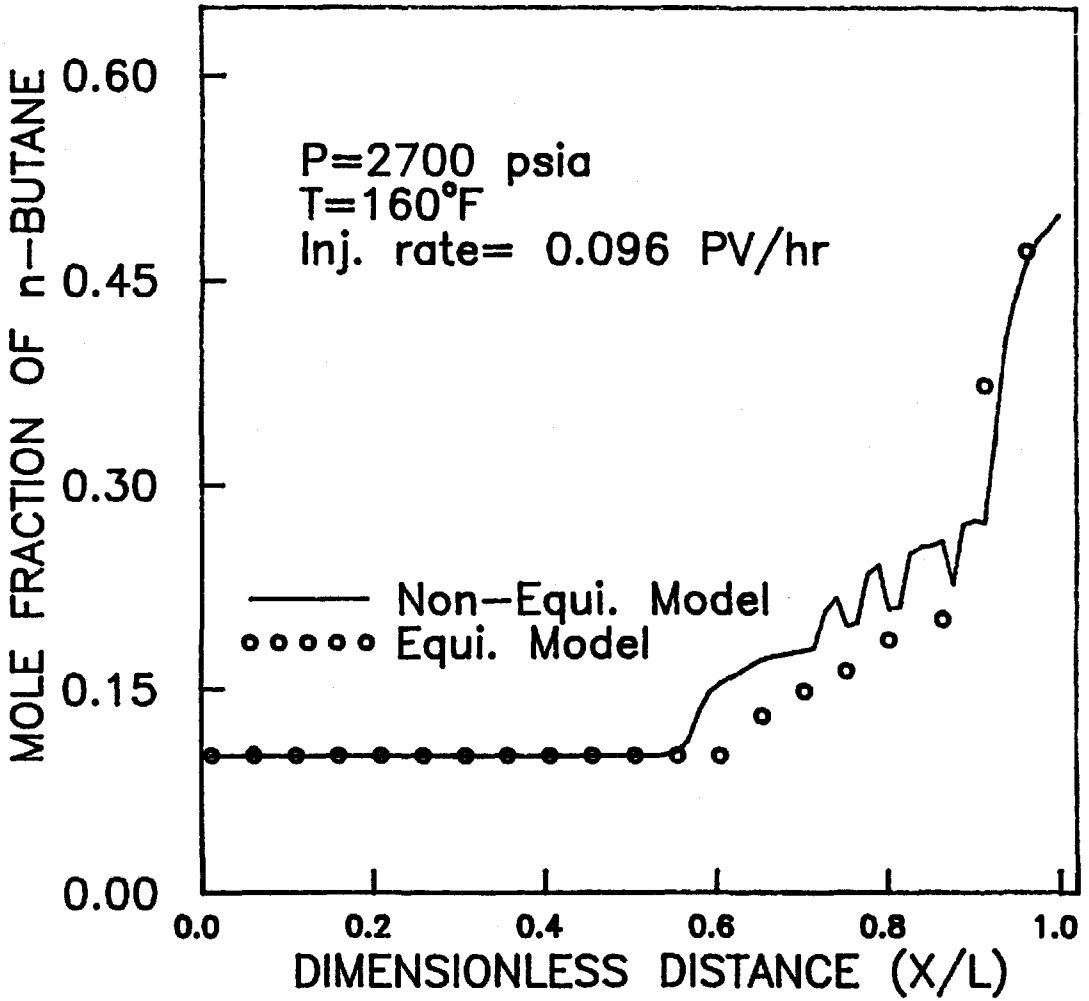

Figure 5.34: Calculated Composition Profile of n-Butane for Experiment 4 at 1 PV of Solvent Injected

The zigzag pattern of the saturation profile and the concentation profiles calculated from the non-equilibrium model (Figures 5.32, 5.33, 5.34) is observed at the interface of the two-phase and the oil phase. This phenomenon can be explained by the fact that at the interface, the transfer of the lighter components between the grid blocks is strongly dependent on the two independent variables (M_E and K-factors) which makes the distributions of the lighter components and in turn the saturation in the grid blocks, adjacent to the interface, uneven.

5.6 Comparison of Numerical Simulation Results with Blackwell's Experimental Data

Blackwell et al. (1959) reported the effects of the mobility ratio on the displacement process with equal density miscible fluids in a linear reservoir model. In particular, the effects of the mobility ratio on the breakthrough recovery, which were reported by Blackwell et al.(1959), are considered in this section. The height, width and length of the linear model used by Blackwell et al. (1959) were 3/8, 1/2 and 72 inches, respectively.

Breakthrough recoveries at three mobility ratios (10, 30 and 60) are calculated from the non-equilibrium and equilibrium model simulations. In the numerical simulations, C_1 is used as the injection gas or solvent at all three mobility ratios and the compositions of oils which were used in the simulations are shown in Table 5.15.

Table 5.15: Compositions of oils at different mobility ratios

Mobility Ratio	Mole Fraction	
	$n\text{-}C_4$	C_{10}
10	0.64	0.36
30	0.49	0.51
60	0.41	0.59

Mobility ratio is defined by the following relation:

$$M=\frac{\mu_{oil}}{\mu_{gas}} \qquad (5.6)$$

The viscosities of the oil and gas phases were calculated from the 1/4 power fluidity mixing rule (Nghiem et al., 1989);

$$\mu_j=[\sum y_{mj}\mu_m^{*-\frac{1}{4}}]^{-4} \qquad (5.7)$$

where m= component index, j= oil or solvent, μ_m^* = pure component viscosity.

Pure component viscosities which were used to calculate the mobility ratio are shown in Table 5.16:

Table 5.16: Pure Component Viscosities

	μ_m^* (cp)		
M	C_1	$n\text{-}C_4$	C_{10}
10	0.01	0.08	0.1538
30	0.01	0.23	0.3940
60	0.01	0.40	0.8160

The operating pressure is 2700 psia and temperature is 160° F. The injection rate of solvent is 40 ft/day (0.014 cm/s). These operating conditions were used in the experiments of Blackwell et al. (1959). Figure 5.35 shows the comparison of

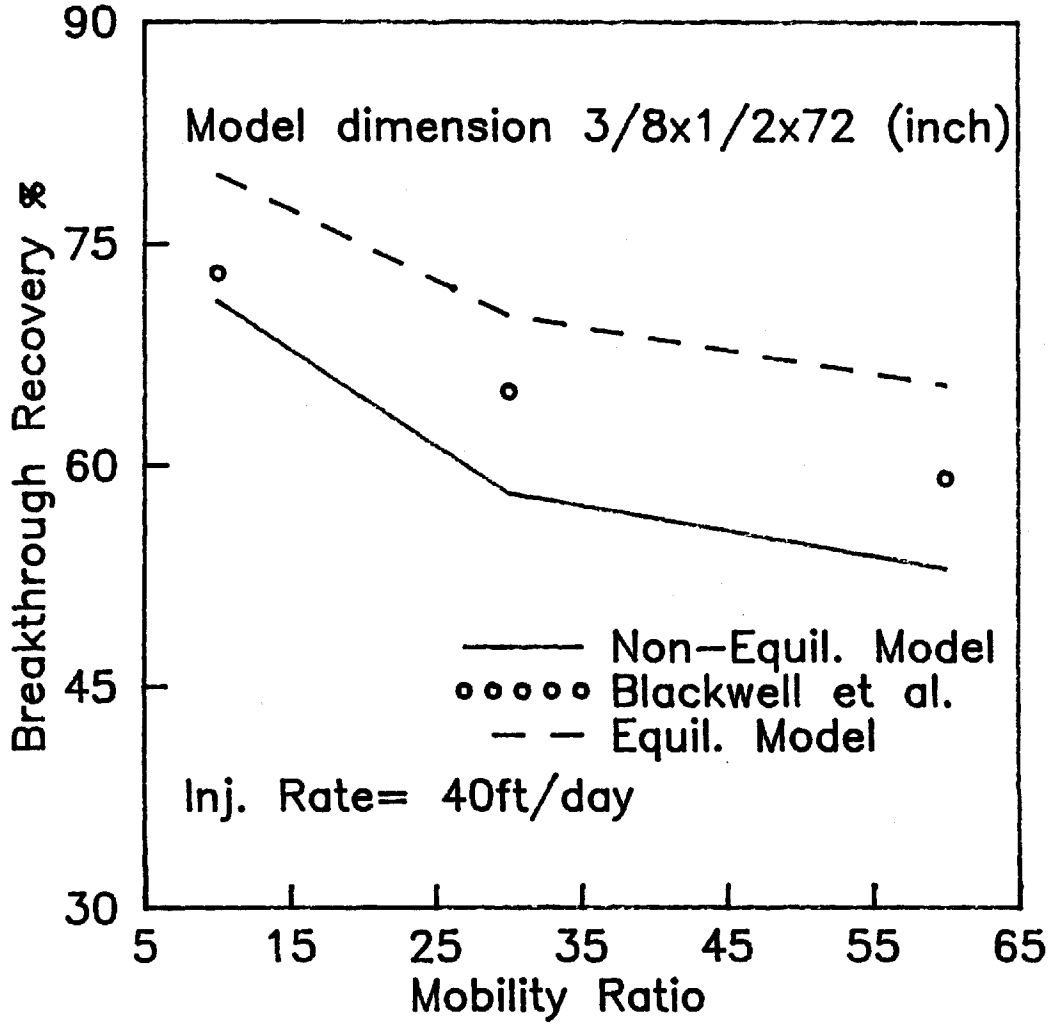

Figure 5.35: Comparison of the Effect of Mobility Ratio on Breakthrough Recovery

calculated breakthrough recoveries from the non-equilibrium and the equilibrium model simulations at the three mobility ratios with those obtained from experimental data. Figure 5.35 shows that the calculated breakthrough recoveries from non-equilibrium and equilibrium model simulations follow the same trend as that experimentally obtained by Blackwell et al. (1959). Breakthrough recoveries calculated from the non-equilibrium model simulations are smaller than the experimental data. These results are expected because Blackwell et al. (1959) used solvent and oil of equal density whereas in the numerical simulations there is a density difference between the oil and gas. However, the breakthrough recoveries calculated from the equilibrium model simulations are higher than those obtained from experimental data.

5.6.1 Simulation Results at Different Mobility Ratios

Calculated recovery profiles from the non-equilibrium model simulations at three mobility ratios (10, 30 and 60) are shown in Figure 5.36. There is a greater difference between the calculated ultimate recoveries obtained from the non-equilibrium model simulation for M=10 and M=30 than between M=30 and M=60. This observation is similar to that reported by Nghiem et al. (1989).

Calculated recovery profiles from both the non-equilibrium and the equilibrium model simulations for M=30 and M=10 are shown in Figures 5.37 and 5.38, respectively.

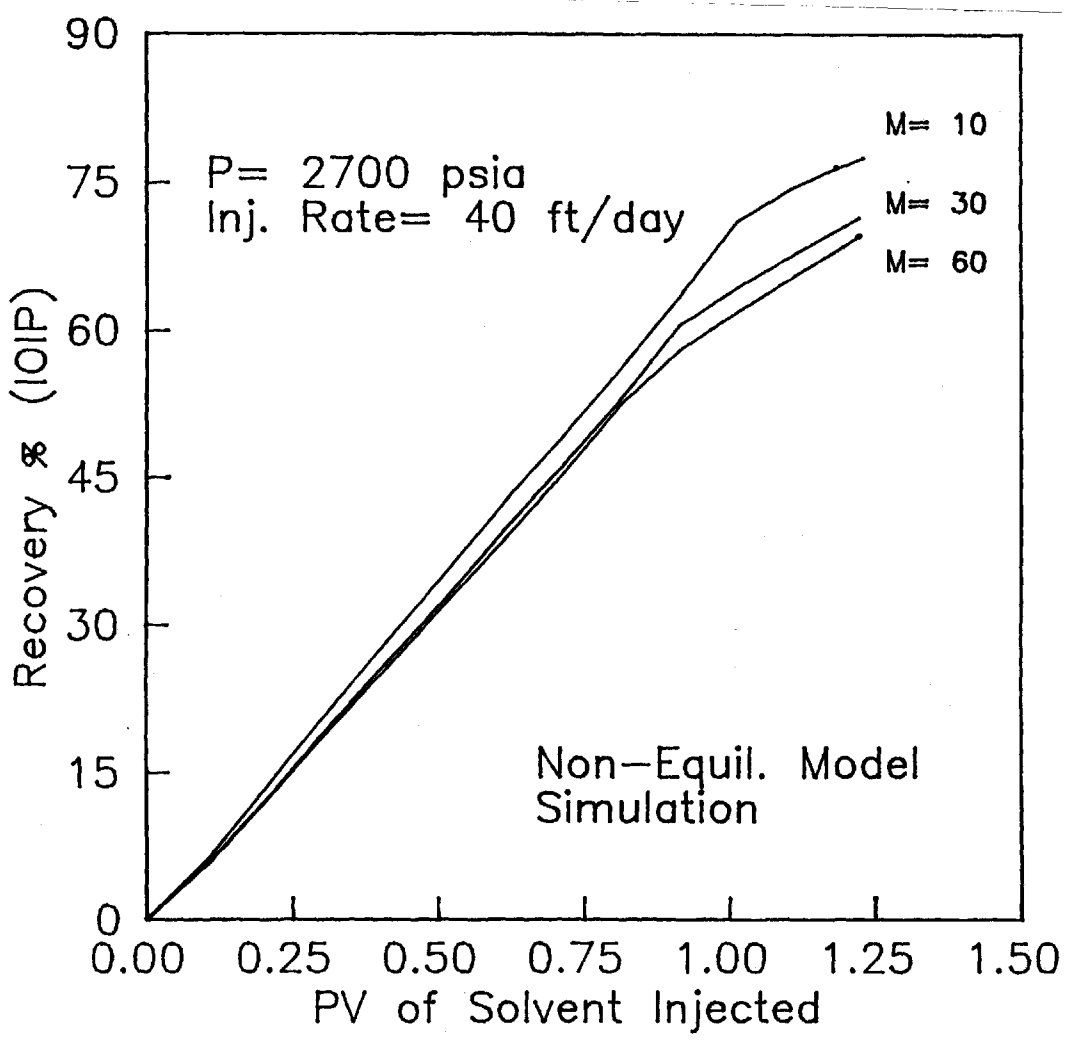

Figure 5.36: Effect of Mobility Ratio on Recovery

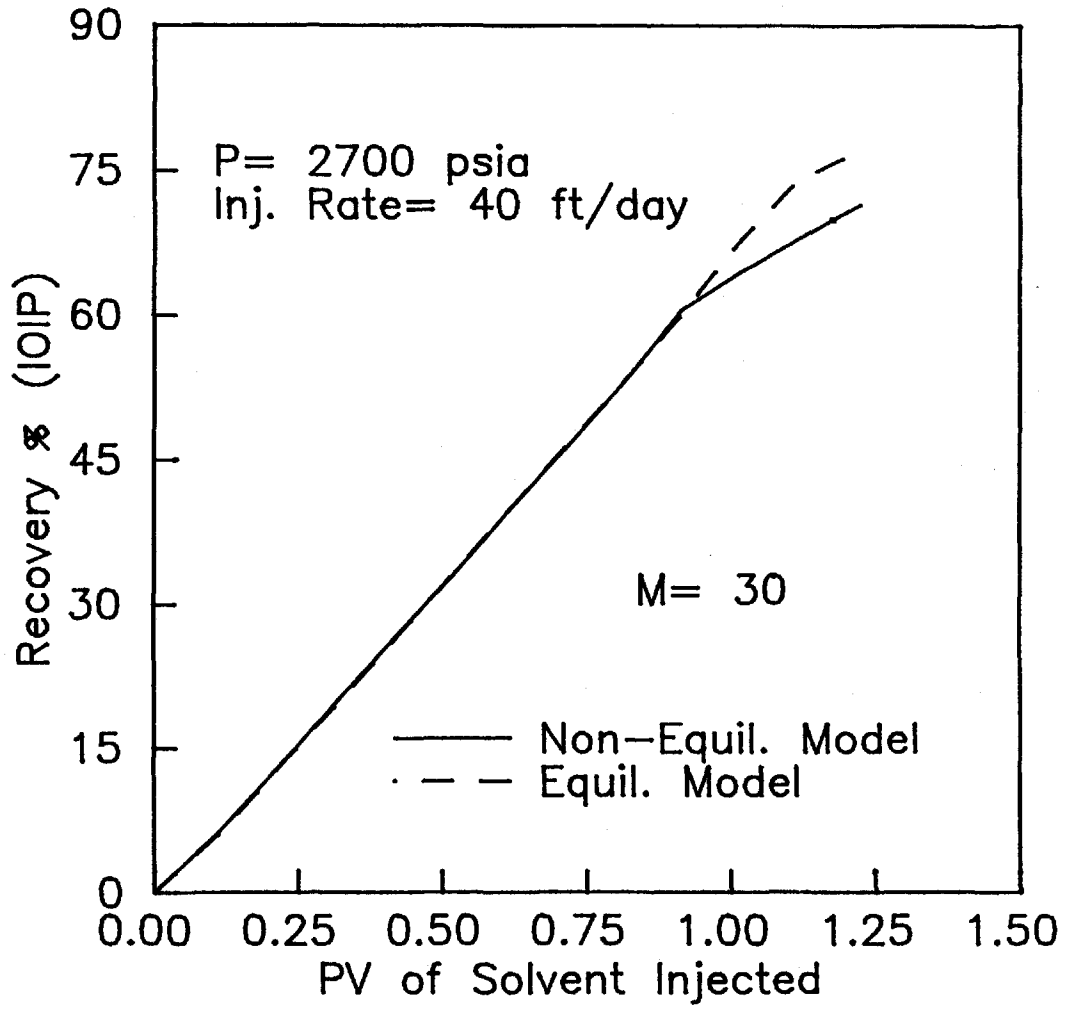

Figure 5.37: Comparison of Calculated Recovery Profiles for M= 30

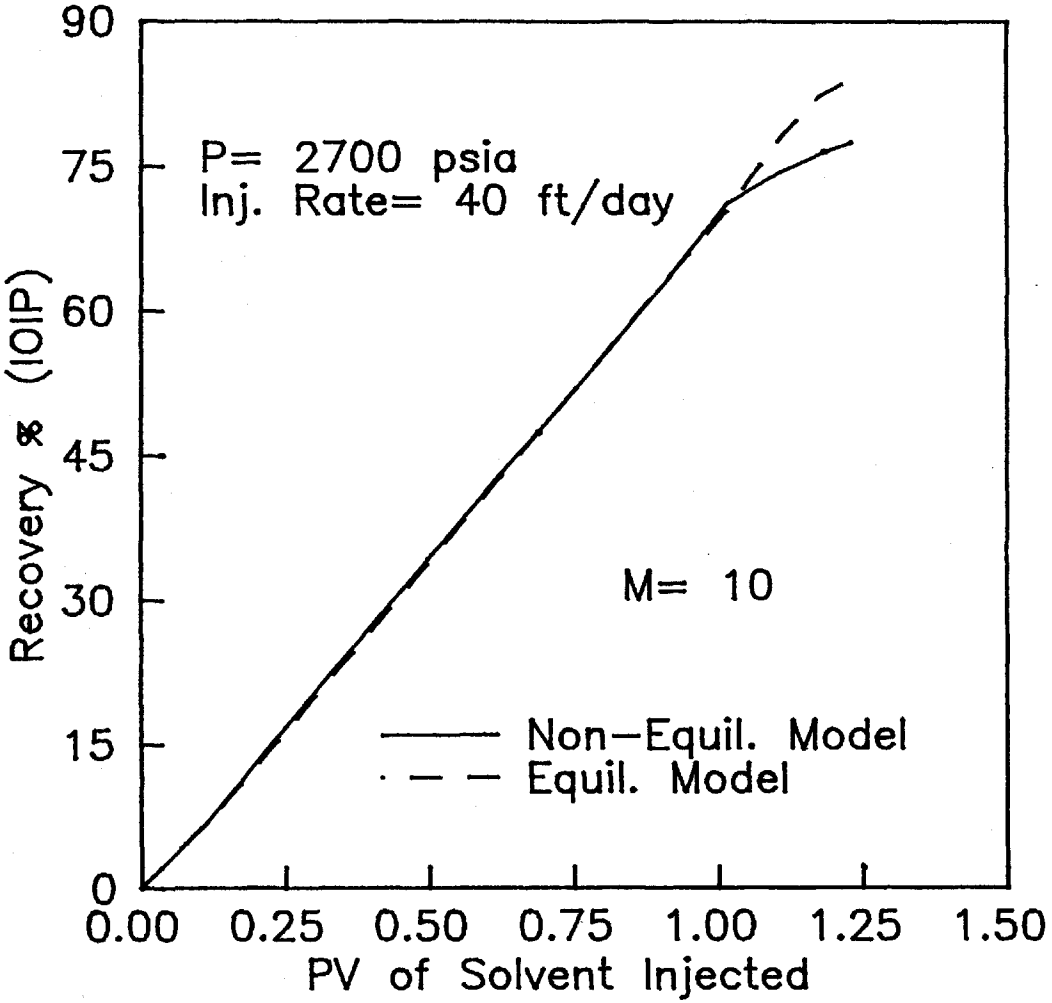

Figure 5.38: Comparison of Calculated Recovery Profiles for M= 10

Figures 5.37 and 5.38 show that calculated ultimate recoveries from the equilibrium model are higher than those calculated from the non-equilibrium model.

Calculated gas saturation profiles and C_1 concentration profiles for M=10 at 0.95 PV of gas injection, are shown in Figures 5.39 and 5.40, respectively. Figure 5.39 shows that the gas saturation front calculated from the non-equilibrium model simulation is ahead of that calculated from the equilibrium model simulation at the downstream end of the reservoir model. Figure 5.39 also shows that gas saturations calculated from the non-equilibrium model are lower than those calculated from the equilibrium model at the upstream end of the reservoir model. This observation indicates that more oil is trapped in the reservoir according to the calculations from the non-equilibrium model simulation than those calculated from the equilibrium model simulation. This hypothesis can also be substantiated by the fact that concentrations of C_1 calculated from the non-equilibrium model are lower at the upstream end than those calculated from the equilibrium model (shown in Figure 5.40).

5.7 Discussion on Simulation Results

It has been shown in the previous sections that the non-equilibrium model can be used to predict the results with reasonable accuracy for both the miscible displacement process and immiscible displacement process. The difference in

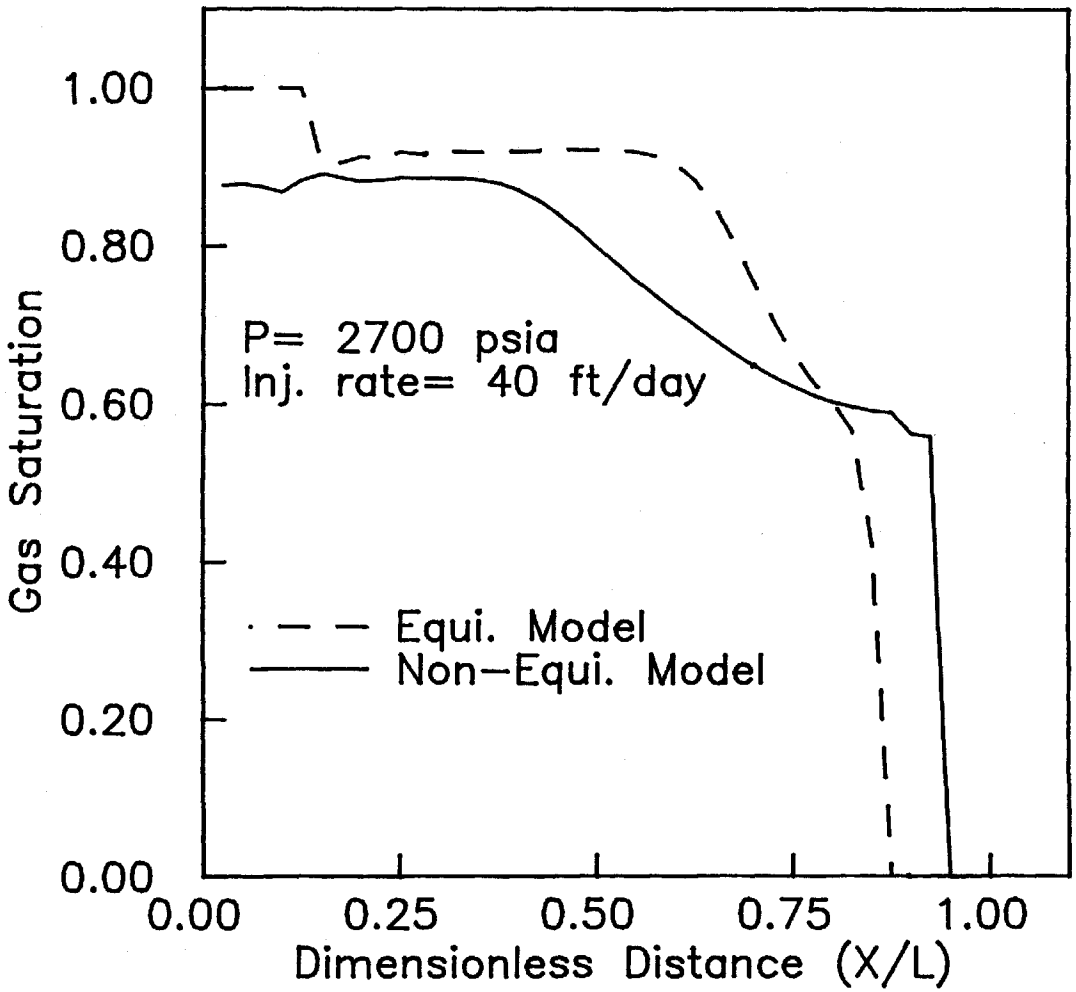

Figure 5.39: Saturation Profiles at 0.95 PV of Solvent Injection for M= 10

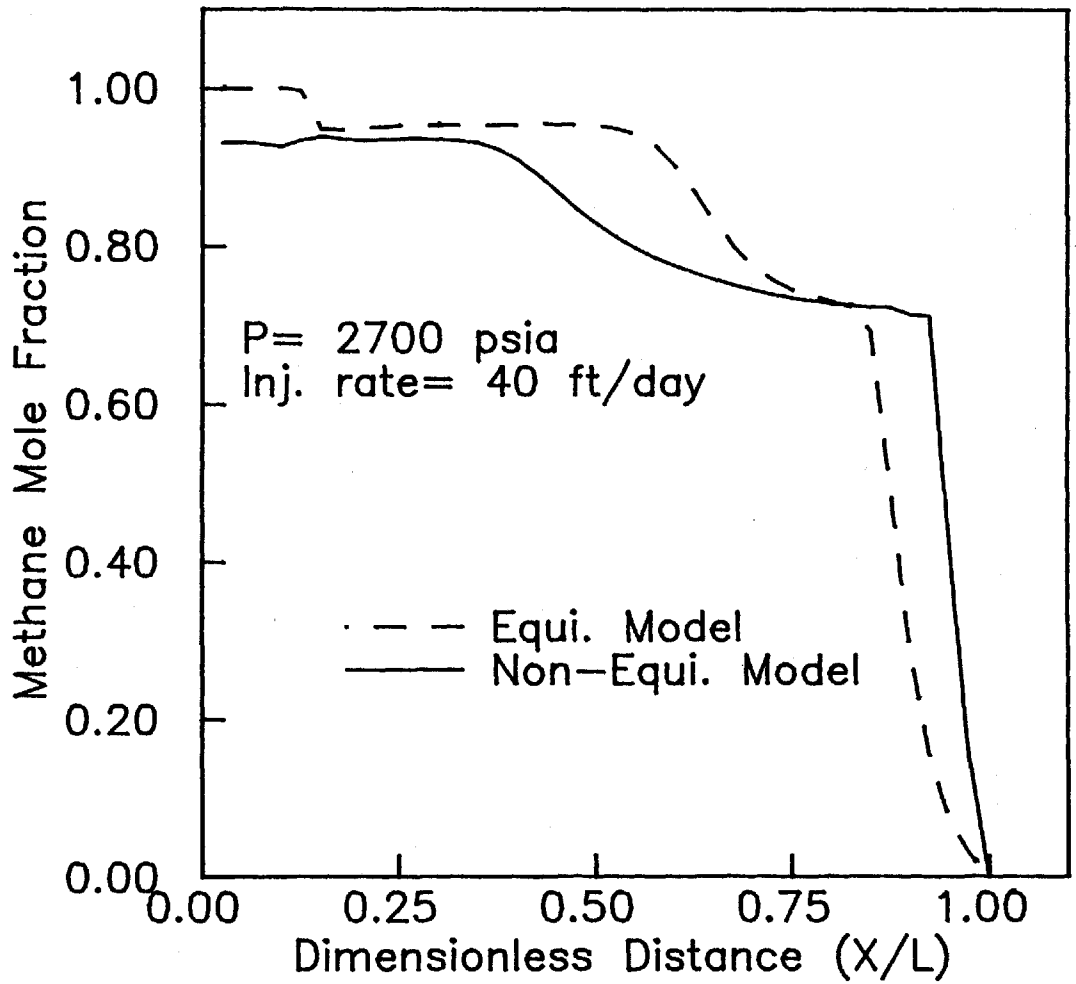

Figure 5.40: Composition Profiles of C_1 at 0.95 PV of Solvent Injection for M=10

results between the equilibrium model and the non-equilibrium model formulation are similar to those between the no fingering and fingering model. Predictions of simulations based on the non-equilibrium model are superior than the predictions based on the equilibrium model simulations when the results are compared with the experimental data obtained in this study and those reported by Blackwell et al. (1959). An adjustable parameter α is used in the non-equilibrium model. It is observed that the empirical relation used in this study to correlate α to M_E is of sufficient accuracy for matching the experimental data. Different linear relations were used to relate these two variables but no significant changes were observed in the calculated recovery or other results.

CHAPTER 6

CONCLUSIONS

6.1 Conclusions of the Experiments

A total of fifteen experimental runs were made with four oils and four solvents (gases) at different operating conditions. The conclusions obtained from the results of the experiments are listed as follows:

1. Injection rate does not affect the breakthrough time and the total amount of gas produced for a miscible displacement process. A small increase in recovery is observed for miscible displacement process at lower injection rates.

2. Injection rate does affect the breakthrough time, recovery and total amount of gas produced for an immiscible displacement process. At lower injection rate the increase in recovery is higher in this process compared with that in the miscible displacement process. In an immiscible displacement process, the effects of injection rate at high mobility ratios between the oil and solvent are more pronounced on breakthrough time and total gas produced than at lower mobility ratios.

3. A small increase of intermediate components in the solvent can increase the recovery value drastically and can

change the displacement mechanism from immiscible to miscible one.

4. The presence of increased amounts of a heavy hydrocarbon component in the oil causes lower recovery of oil compared with that of the oil which contains less heavy hydrocarbon. But the heavy hydrocarbon components in the oil do not have significant effect on breakthrough time.

6.2 Conclusions of Numerical Simulations

6.2.1 Two-Phase Flash Calculations

A coupled method was developed for two-phase flash calculations. The conclusions obtained from the testing of the developed method are listed as follows:

1. An acceleration scheme based on the DEM was coupled with Newton's method for two-phase flash calculations where the logarithm of K-factors are used as iteration variables. The coupled method takes advantage of both the accelerated linear convergence speed of the SS method and the super-linear convergence speed of Newton's method.

2. Two-effective switching criteria are proposed to change the iteration process from the accelerated successive substitution method to Newton's method.

3. The proposed coupled method is reliable and computationally fast when it is applied to calculations in which the specifications are near the critical-state values of the fluids.

4. It is shown that the dominant eigenvalue method is an equally effective acceleration method as the general dominant eigenvalue method when applied for flash calculations.

6.2.2 Saturation Pressure Calculations

An acceleration method for saturation pressure calculations was developed in this study. The conclusions obtained from the testing of this accelerated method are the following;

1. A multivariate Newton's method may be accelerated using a semi-empirical approach which is based on the history of iterates.

2. The acceleration method developed is simple to use and requires an insignificant amount of computing effort.

3. In general, a saving of 20 percent computation time can be expected for the saturation pressure calculations in the vicinity of the critical point.

4. The proposed accelerated method is reliable in comparison

with the other accelerated methods (Richardson extrapolation and Overrelaxation methods).

6.2.3 Simulation with Phase Behaviour Models

An one-dimensional compositional reservoir simulator was developed for describing the oil displacement process using gas injection. Two phase behaviour models were used to account for the compositional effects of fluids. The conclusions obtained from the simulation results are listed in the following;

1. A non-equilibrium phase behaviour model along with a mixing parameter model can be used to describe the incomplete mixing between the oil and the gas in a displacement process. It is shown that a mixing parameter model can be incorporated into reliable compositional simulation without introducing more than one adjustable parameter and without the need for creating an artificial phase envelope (Crump, 1988).

2. The simulation results show that the use of the assumption of incomplete mixing for the fluids in a grid block under presumed miscible process conditions is also valid. The prediction capability of the non-equilibrium model is found to be similar to that of the fingering model proposed by Nghiem et al. (1989).

3. The non-equilibrium phase behaviour model used in the compositional simulator is based on the concept of the Murphree efficiency factor used in multicomponent, multistage separation calculations. In this study, this new approach has been successfully applied to the simulation of immiscible displacement processes.

4. Simulation based on the non-equilibrium model does not require much extra computational load than that required in the simulation based on equilibrium model .

5. It is anticipated that this approach of non-equilibrium phase calculations can also be applied to other chemical process calculations if non-equilibrium calculations are required.

CHAPTER 7

RECOMMENDATIONS

1. The coupled algorithm developed in this study for two-phase flash calculations may be applied for saturation pressure calculations and saturation temperature calculations. The proposed switching criteria to change the iteration process from successive substitution method to Newton's method may be applied for other numerical calculations which involve iteration process.

2. The semi-empirical approach developed for the acceleration of saturation pressure calculations using Newton's method, may be applied for other numerical applications which involve Newton's method as an iteration process. The proposed acceleration method may be generalized by the development of a correlation which will generate the values of the relaxation parameter within the iteration scheme. In the particular application of saturation pressure calculations, a fixed value of the relaxation parameter seems to work well.

3. The optimal functional dependency of the empirical parameter, α, used in the non-equilibrium phase behaviour model may be determined. Extensive testing of the results

from the non-equilibrium model simulation with the experimental data involving a wide range of hydrocarbon components is needed.

4. The simulation results from the non-equilibrium model may be compared with the experimental data obtained from the laboratory scale reservoirs of rectangular cross-sections with different length to width ratios. In this study, validations of the simulation results from the non-equilibrium model were made based on the experimental data obtained from a laboratory scale reservoir of circular cross-section.

CHAPTER 8

REFERENCES

Appleyard, J.R., Cheshire, I.M. and Pollard, R.K.: " Special Techniques for Fully-Implicit Simulators," Proceedings of the third European Symposium on Enhanced Oil Recovery, held in Bournemouth, U.K., September 21-23, 1981, 395-408.

Asselineau, L., Bogdanic, G. and Vidal, J.: "A Versatile Algorithm for Calculating Vapour-Liquid Equilibria," Fluid Phase Equlibria, vol. 3(1979), 273-290.

Aziz, K. and Settari, A.: " Petroleum Reservoir Simulation," Applied Science Publishers Ltd., 1979.

Bahralolom, I.M. and Orr, F.M. Jr.: " Solubility and Extraction in Miscible Displacements: Comparison of N_2 and CO_2 Flow Visualization Experiments," Soc. Pet. Eng. Res. Eng. (1988), 213-219.

Baker, L.E. and Luks, K.D.: " Critical Point and Saturation Pressure Calculations for Multicomponent Systems," Soc. Pet. Eng. J. (1980), 15-24.

Banks, D. and Ponting, D.K.: " Interphase Mass Transfer Effects in Implicit Black Oil Simulators," Proceedings of the third European Symposium on Enhanced Oil Recovery, held in Bournemouth, U.K., September 21-23, 1981, 441-450.

Benham, A.L., Dowden, W.E. and Kunzman, W.J. : " Miscible Fluid Displacement - Prediction of Miscibility," Pet. Trans., AIME, vol. 219 (1960), 229-237.

Benham, A.L. and Olson, R.W.: " A Model Study of Viscous Fingering," Soc. Pet. Eng. J. (1963), 138-144.

Bentsen, R.G.: " A New Approach to Instability Theory in Porous Media," Soc. Pet. Eng. J. (1985), 765-779.

Blackwell, R.J., Rayne, J.R. and Terry, W.M.: " Factors Influencing the Efficiency of Miscible Displacement," Pet. Trans., AIME, vol. 216 (1959), 1-8.

Blackwell, R.J.: " Miscible Displacement: Its Status and Potential for Enhanced Oil Recovery," Proceedings of the third European Symposium on Enhanced Oil Recovery, held in Bournemouth, U.K., September 21-23, 1981, 237-245.

Blair, P.M. and Weinaug, C.F.: " Solution of Two-Phase Flow Problems Using Implicit Difference Equations," Pet. Trans.,

AIME, vol. 246 (1969), 62-70.

Blanton, J.R., McCaskill, N. and Herbeck,E.F.: " Performance of a Propane Slug Pilot Watered-Out-Sand-South Ward Field," J. Pet. Tech. (1970), 1209-1214.

Boston, J.F. and Britt, H.I.:" A Radically Different Formulation and Solution of the Single-Stage Flash Problem," Comput. Chem. Eng., vol. 2 (1978), 109-122.

Brannan, G. and Whitington, H.M. Jr.: " Enriched-Gas Miscible Flooding: A Case History of the Levelland Unit Secondary Miscible Project," J. Pet. Tech. (1977), 919-924.

Buckley, S.E. and Leverett, M.C.: " Mechanisms of Fluid Displacement in Sands," Trans. AIME, vol. 143 (1942), 107-116.

Chase, C.A., Jr. and Todd, M.R.: " Numerical Simulation of CO_2 Flood Performance," Soc. Pet. Eng. J. (1984), 597-605.

Christian, L.D., Shirer, J.A., Kimbel, E.L. and Blackwell, R.J.: " Planning a Tertiary Oil Recovery Project for Jay/LEC Fields Unit," J. Pet. Tech. (1981), 1535-1544.

Christiansen, R.L. and Haines, H.K.: " Rapid Measurement of Minimum Miscibility Pressure with the Rising-Bubble Apparatus," Soc. Pet. Eng. Res. Eng. (1987), 523-527.

Coats, K.H., Nielsen, R.L. and Weber, A.G.: " Simulation of Three-Dimensional Two-Phase Flow in Oil and Gas Reservoirs," Soc. Pet. Eng. J. (1967), 377-388.

Coats, K.H.: " An Equation-of-State Compositional Model," Soc. Pet. Eng. J. (1980), 363-376.

Coats, K.H.: " Reservoir Simulation: State of the Art," J. Pet. Tech. (1982), 1633-1642.

Collins, D.A., Nghiem, L.X. and Li, Y.-K.: " An Efficient Approach to Adaptive Implicit Compositional Simulation with an Equation of State," Soc. pet. Eng. Res. Eng. (1992), 259-264.

Connally, C.A. Jr.: " Tertiary Miscible Flood in Phelgy Unit, Washington County, Colorado," paper SPE 3775 presented at the 1972 SPE Improved Oil Recovery Symposium, Tulsa, April 16-19.

Cook, R.E., Jacobi, R.H. and Ramesh, A.B.: " A Beta-Type Reservoir Simulator for Approximating Compositional Effects During Gas Injection," Soc. Pet. Eng. J. (1974), 471-481.

Crowe, C.M. and Nishio, M.: "Convergence Promotion In the Simulation of Chemical processes- The General Dominant

Eigenvalue Method", AIChEJ, vol. 21 (1975), 528-533.

Crump, J.G.: " Detailed Simulations of the Effects of Process Parameters on Adverse Mobility Ratio Displacements," presented at the SPE/DOE Enhanced Oil Recovery Symposium held in Tulsa, Oklahoma, April 17-20, 1988.

Culham, W.E., Ali, Farouq S.M. and Stahl, C.D.: " Experimental and Numerical Simulation of Two-Phase Flow with Interphase Mass Transfer in One and Two Dimensions," Soc. Pet. Eng. J. (1969), 323-337.

DesBrisay, C.L., El Ghussein, B.F., Holst, P.H. and Misellati, A.: " Review of Miscible Flood Performance, Intisar "D" Field, Socialist People's Libyan Arab Jamahiriya," J. Pet. Tech. (1982), 1651-1660.

Dolan, J.P., Ellington, R.T. and Lee, A.L.: " Viscosity of Methane-n-Butane Mixtures," J. Chem. Eng. Data, vol. 9 (1964), 485-487.

Dougherty, E.L.: " Mathematical Model of an Unstable Miscible Displacement," Soc. Pet. Eng. J. (1963), 155-163.

Everett, J.P., Gooch, F.W., Jr.: " Liquid-Liquid Displacement in Porous Media as Affected by the Liquid-Liquid Viscosity Ratio and Liquid-Liquid Miscibility," Pet. Trans., AIME, vol. 189 (1950), 215-224.

Fayers, F.J.: " An Approximate Model with Physically Interpretable Parameters for Representing Viscous Fingering," Soc. Pet. Eng. Res. Eng. (1988a), 551-558.

Fayers, F.J. and Newley, T.M.J.: " Detailed Validation of an Empirical Model for Viscous Fingering with Gravity Effects," Soc. Pet. Eng. Res. Eng. (1988b), 542-550.

Fayers, F.J., Blunt, M.J. and Christie, M.A.: " Comparisons of Empirical Viscous-Fingering Models and Their Calibration for Heterogeneous Problems," Soc. Pet. Eng. Res. Eng. (1992), 195-203.

Fung, L.S.-K., Collins, D.A. and Nghiem, L.X.: " An Adaptive Switching Criterion Based on Numerical Stability Analysis," Soc. Pet. Eng. Res. Eng. (1989), 45-51.

Fussell, D.D. and Yanosik, J.L.: " An Iterative Sequence for Phase Equilibrium Calculations Incorporating the Redlich-Kwong Equation of State," Soc. Pet. Eng. J. (1978), 173-182.

Fussell, L.T.: " A Technique for Calculating Multiphase Equilibria," Soc. Pet. Eng. J. (1979), 203-208.

Fussell, L.T. and Fussell, D.D.: " An Iterative Technique for Compositional Reservoir Models," Soc. Pet. Eng. (1979), 211-220.

Gardner, J.W., Orr, F.M. Jr. and Patel, P.D.: " The Effect of Phase Behaviour on CO_2 Flood Displacement Efficiency," J. Pet. Tech. (1981), 2067-2081.

Gardner, J.W. and Ypma, J.G.J.: " An Investigation of Phase-Behaviour/Macroscopic-Bypssing Interaction in CO_2 Flooding," Soc. Pet. Eng. J. (1984), 508-520.

Gottfried, B.S., Guilinger, W.H. and Snyder, R.W.: " Numerical Solutions of the Equations for One-Dimensional Multi-Phase Flow in Porous Media," Soc. Pet. Eng. J. (1966), 62-72.

Griewank, A.: " On Solving Nonlinear Equations with Simple Singularities or Near Singular Solutions," SIAM Review, vol. 27 (1985), 537-563.

Griffith, J.D. and Cyca, L.G.: " Performance of South Swan Hills Miscible Flood," J. Pet. Tech. (1981), 1319-1326.

Gupta, A.K., Bishnoi, P.R. and Kalogerakis, N.," An Accelerated Successive Substitution Method for Single Stage Flash Calculations," Can. J. Chem. Eng., vol. 66 (1988), 291-296.

Habermann, B.: " The Efficiency of Miscible Displacement as a Fuction of Mobility Ratio," Pet. Trans., AIME, vol. 219 (1960), 264-272.

Hall, H.N. and Geffen, T.M.: " A laboratory Study of Solvent Flooding," Pet. Trans., AIME, vol. 210 (1957), 48-57.

Handy, L.L.: " An Evaluation of Diffusion Effects in Miscible Displacement," Pet. Trans., AIME, vol. 216 (1959), 61-63.

Hardy, J.H. and Robertson, H.: " Miscible Displacement at High-Pressure Gas at Block 31," Pet. Eng. (1975), 24-28.

Harmon, R.A. and Grigg, R.B.: " Vapor-Density Measurement for Estimating Minimum Miscibility Pressure," Soc. Pet. Eng. Res. Eng. (1988), 1215-1220.

Henderson, J.H., Gove, N.B., Ledbetter, H.J. and Griffith, J.D.: " A Laboratory Investigation of Oil Displacement from Porous Media by a Liquefied Petroleum Gas," Pet. Trans., AIME, vol. 198 (1953), 33-40.

Henry, R.L. and Metcalfe, R.S.: " Multiple-Phase Generation During Carbon-Dioxide Flooding," Soc. Pet. Eng. J. (1983), 595-601.

Hirose, Y. , Kawase, Y. and Kudoh, M.: " General Flash Calculation by the Newton-Raphson Method," J. Chem. Eng. Japan (1978), 150-152.

Holm, L.W. and Josendal, V.A.: "Mechanisms of Oil Displacement by Carbon-Dioxide," J. Pet. Tech. (1974), 1427-1436.

Holm, L.W. and Josendal, V.A.: " Effect of Oil Composition on Miscible-Type Displacement by Carbon-Dioxide," Soc. Pet. Eng. J. (1982), 87-98.

Huang, E.T.S.: " A Sensitivity Study of Reservoir Performance Using a Compositional Reservoir Simulator," Soc. Pet. Eng. J. (1972), 3-12.

Huang, S.S. and Dyer, S.B.: " Miscible Displacement in the Weyburn Reervoir-A Laboratory Study," Petroleum Society of CIM and CANMET Paper No. 20, presented at the Fourth Petroleum Conference of the South Saskatchewan Section, Regina, October 7-9, 1991.

Hutchinson, C.A. Jr. and Braun, P.H.: " Phase Relations of Miscible Displacement in Oil Recovery," AIChE J., vol. 7 (1961), 64-72.

Kazemi, H., Vestal, C.R. and Shank, G.D.: " An Efficient Multicomponent Numerical Simulator," Soc. Pet. Eng. J. (1978), 355-368.

Kelly, C.T. and Suresh, R.: " A New Acceleration Method at Singular Points," SIAM J. Num. Anal., vol. 20 (1983), 1001-1009.

Kinoshita, M. and Takamatsu, T.: " A Powerful Solution Algorithm for Single Stage Flash Problems," Comput. Chem. Eng., vol. 10 (1986), 353-360.

Koch, H.A. Jr. and Hutchinson, C.A: " Miscible Displacements of Reservoir Oil Using Flue Gas," Pet. Trans., AIME, vol. 213 (1958), 7-19.

Koval, E.J.: " A Method for Predicting the Performance of Unstable Miscible Displacement in Heterogeneous Media," Soc. Pet. Eng. J. (1963), 145-154.

Kyle, C.R. and Perrine, R.L.: " Experimental Studies of Miscible Displacement Instability," Soc. Pet. Eng. J. (1965), 189-195.

Lacey, J.W., Faris, J.E. and Brinkman, F.H.: "Effect of Bank Size on Oil Recovery in the High-Pressure Gas Driven LPG-Bank Process," J. Pet. Tech. (1961), 806-816.

Latil, M.,: " Enhanced Oil Recovery," Gulf Publishing Company, 1980.

Lantz, R.B.: " Rigorous Calculation of Miscible Displacement Using Immiscible Reservoir Simulators," Soc. Pet. Eng. J. (1970), 192-202.

Leach, M.P. and Yellig, W.F.: " Compositional Model Studies-CO_2 Oil-Displacement Mechanism," Soc. Pet. Eng. J. (1981), 89-97.

Lee, A.L., Gonzalez, M.H. and Eakin, B.E.: " Viscosity of Methane-n-Decane Mixtures," J. Chem. Eng. Data, vol. 11 (1966), 281-287.

Leverett, M.C.: " Capillary Behaviour in Porous Solids," Trans. AIME, vol. 142 (1941), 152-169.

Lohrentz, J., Bray, B.G. and Clark, C.R.: " Calculating Viscosities of Reservoir Fluids from Their Compositions," J. Pet. Tech. (1964), 1171-1176.

Martin, W.E.: "The Wizard Lake D-3A Miscible Flood", paper SPE 10026 presented at the 1982 SPE Intl. Pet. Exhibition and Technical Sympoium Beijing, China, March 19-22.

Mehra, R.K., Heidemann, R.A. and Aziz, K.:" An Accelerated Successsive Substitution Algorithm," Can. J. Chem. Eng., vol. 61 (1983),590-596.

Metcalfe, R.S., Fussell, D.D. and Shelton, J.L.: " A Multicell Equilibrium Separation Model for the Study of Multiple Contact Miscibility in Rich Gas Drives," Soc. Pet. Eng. J. (1973), 147-155.

Michelsen, M.L. , "Calculation of Phase Envelopes and Critical Points for Multicomponent Mixtures", Fluid Phase Equilibria, vol. 4 (1980), 1-10.

Michelsen, M.L.: " The Isothermal Flash Problem. Part II. Phase Split Calculation," Fluid Phase Equilibria, vol. 9 (1982), 21-40.

Mungan,N.: " Carbon-Dioxide Flooding-Fundamentals," J. Can. Pet. Tech. (1981), 87-92.

Murphree, E.V.: " Rectifying Column Calculations with Particular Reference to N Component Mixtures," Ind. Eng. Chem., vol. 17 (1925), 747-750.

Nghiem, L.X., Fong, D.K. and Aziz, K.: " Compositional Modelling with an Equation of State," Soc. Pet. Eng. J.

(1981), 687-698.

Nghiem, L.X. and Heidemann, R.A.:" General Acceleration Procedure for Multiphase Flash Calculation with Application to Oil-Gas-Water Systems," Presented at the 2nd European Symposium on Enhanced Oil Recovery, Paris, France, Nov. 8-10, 1982.

Nghiem, L.X., Aziz, K. and Li, Y.-K.: " A Robust Iterative Method for Flash Calculations Using Soave-Redlich-Kwong or the Peng-Robinson Equation of State," Soc. Pet. Eng. J. (1983), 521-530.

Nghiem, L.X. and Li, Y.-K.: " Computation of Multiphase Equilibrium Phenomena with an Equation of State," Fluid Phase Equilibria, vol. 17 (1984), 77-94.

Nghiem, L.X. and Li, Y.-K.: " Application of the Tangent Plane Criterion to Saturation Pressure and Temperature Computations," Fluid Phase Equilibria, vol. 21 (1985), 39-60.

Nghiem, L.X. and Li, Y.-K.: " Effect of Phase Behaviour on CO_2 Displacement Efficiency at Low Temperatures: Model Studies with an Equation of State," Soc. Pet. Eng. Res. Eng. (1986), 414-422.

Nghiem, L.X., Li, Y.-K. and Agarwal, R.K.: " A Method for Modelling Incomplete Mixing in Compoitional Simulation of Unstable Diplacements," presented at the Reservoir Simulation Symposium held in Houston, Texas, February 6-8, 1989.

Nolen, J.S.: " Numerical Simulation of Compositional Phenomena in Petroleum Reservoirs," presented at the third SPE Symposium on Numerical Simulation of Reservoir Performance, held in Houston, Texas, January 11-12, 1973.

Nouar, A. and Flock, D.L.: " Parametric Analysis on The Determination of The Minimum Miscibility Pressure in Slim Tube Displacements," Proceedings of the 34th Annual Technical Meeting of the Petroleum Society of CIM, May 10-13, (1983).

Novosad, Z. and Costain, T.G.: " New Interpretation of Recovery Mechanisms in Enriched Gas Drives," J. Can. Pet. Tech. (1988), 54-60.

Novosad, Z. and Costain, T.G.: " Mechanisms of Miscibility Development in Hydrocarbon Gasdrives: New Interpretation," Soc. Pet. Eng. Res. Eng. (1989), 341-347.

Orbach, O. and Crowe, C.M. ," Convergence Promotion in the Simulation of Chemical Processes with Recycle- The Dominant Eigenvalue Method", Can. J. Chem. Eng., vol. 49 (1971), 509-

513.

Orr, F.M. Jr., Silva, M.K., Lien, C.L. and Pelletier, M.T.: " Laboratory Experiments To Evaluate Field Prospects for CO_2 Flooding," J. Pet. Tech. (1982), 888-898.

Orr, F.M. Jr. and Pande, K.K.: " Effect of Multicomponent, Multiphase Equilibria in Gas Injection Processes," Fluid Phase Equilibria, vol. 52 (1989), 247-261.

Ortega, J. and Rhienboldt, W.: " Iterative Solution of Nonlinear Equations in Several Variables," Academic Press, 1970.

Peng, D.-Y. and Robinson, D.B.: " A New Two-Constant Equation of State," Ind. Eng. Chem. Fund., vol. 15 (1976), 59-64.

Peng, D.-Y. and Robinson, D.B.: " Two- and Three-Phase Calculations for Systems Containing Water," Can. J. Chem. Eng., vol. 5 (1976), 595-599.

Peng, D.-Y. and Robinson, D.B.: " A Rigorous Method for Predicting the Critical Properties of Multicomponent Systems from an Equation of State," AIChE J., vol. 23 (1977), 137-144.

Peng, D.-Y.: " Accelerated Successive Substitution Schemes for Bubble-Point and Dew-Point Calculations," Can. J. Chem. Eng., vol. 69 (1991), 978-985.

Perkins, T.K. and Johnston, D.C.: " A Review of Diffusion and Dispersion in Porous Media," Soc. Pet. Eng. J. (1963), 70-84.

Perkins, T.K., Johnston, O.C. and Hoffman, R.N.: " Mechanics of Viscous Fingering in Miscible Systems," Soc. Pet. Eng. J. (1965), 301-317.

Perrine, R.L.: " Stability Theory and Its Use to Optimize Solvent Recovery of Oil," Soc. Pet. Eng. J. (1961), 9-16.

Perrine, R.L.: " A Unified Theory for Stable and Unstable Miscible Displacement," Soc. Pet. Eng. J. (1963), 205-213.

Peters, E.J. and Flock, D.L.: " The Onset of Instability Diring Two-Phase Immiscible Displacement in Porous Media," Soc. Pet. Eng. J. (1981), 249-258.

Poel, C. V. D.: " Effect of Lateral Diffusivity on Miscible Displacement in Horizontal Reservoirs," Soc. Pet. Eng. J. (1962), 317

Powell, M.J.D.: " A Hybrid Method for Nonlinear Equations," Numerical Methods for Nonlinear Algebraic Equations, P.

Rabiniwitz (ed.), Gordon and Breach, London, 1970.

Price, H.S. and Donohue, D.A.T.: " Isothermal Displacement Processes with Interphase Mass Transfer," Soc. Pet. Eng. J. (1967), 205-220.

Redlich, O. and Kwong, J.N.S.: " On the Thermodynamics of Solutions. V. An Equation of State. Fugacities of Gaseous Solutions," Chem. Rev. (1949), 233.

Reitzel, G.A. and Callow, G.O.: " Pool Description and Performance Analysis Leads to Understanding Golden Spike's Miscible Flood," J. Can. Pet. Tech. (1977), 39-48.

Renner, T.A., Metcalfe, R.S., Yellig, W.F., Jr., and Spencer, M.F.: " Displacement of a Rich Gas Condensate by Nitrogen: Laboratory Corefloods and Numerical Simulations," Soc. Pet. Eng. Res. Eng. (1989), 52-58.

Rhuma, A.N.: " Minimum Miscibility Pressures of CO_2/ Hydrocarbon Systems; Evaluation of Existing Prediction Methods and Development of a New Correlation," M.Sc Dissertation, 1992, University of Saskatchewan.

Risnes, R.: " Phase Equlibrium Calculations in the Near Critical Region", Proceedings of the 3rd European Symposium on Enhanced Oil Recovery, held in Bournemouth, U.K., September 21-23, 1981, 329-350.

Roebuck, I.F., Jr., Henderson, G.E. and Ford, W.T.: " The Compositional Reservoir Simulator: Case I-The Linear Model," Soc. Pet. Eng. (1969), 115-130.

Rose, W. and Bruce, W.A.: "Evaluation of Capillary Character in Petroleum Reservoir Rock," Pet. Trans., AIME (1949), 127-142.

Rosenberg, D.U.V: " Mechanics of Steady-State Single-Phase Fluid Displacement from Porous Media," AIChE J., vol. 2 (1956), 55-58.

Sage, B.H. and Lacey, W.N.: " Thermodynamic Properties of the Lighter Paraffin Hydrocarbons and Nitrogen," API Research Report (1951), 203-212.

Sayegh, S.G. and McCaffery, F.G.: " Laboratory Testing Procedures for Miscible Floods," Proceedings of the third European Symposium on Enhanced Oil Recovery, held in Bournemouth, U.K., September 21-23, 1981, 285-298.

Sayegh, S.G., Krause, F.F. and Fosti, J.E.: " Miscible Displacements of Crude Oil by CO_2/SO_2 Mixtures,", Soc. Pet.

Eng. Res. Eng. (1987), 199-208.

Sheldon, J.W., Zondek, B. and Cardwell, W.T.: " One-Dimensional Incompressible Non-Capillary, Two-Phase Fluid Flow in a Porous Medium," Pet. Trans., AIME, vol. 216 (1959) 290-296.

Sigmund, P.M., Aziz, K., Lee, J.I., Nghiem, L.X. and Mehra, R.: " Laboratory CO_2 Floods and Their Computer Simulation," presented at the World Petroleum Congress, Bucharest, Romania (September, 1979).

Slobod, R.L. and Koch, H.A. Jr.: " High-Pressure Gas Injection-Mechanism of Recovery Increase," Oil and Gas J. (1953) 84

Staggs, H.M. and Herbeck, E.F.: " Reservoir Simulation Models-An Engineering Overview," J. Pet. Tech. (1971), 1428-1436.

Stalkup,F.I. Jr.: " Miscible Dissplacement," SPE Monograph Volume 8, (1984).

Stone, H.L. and Crump, J.S.: "The Effect of Gas Composition upon Oil Recovery by Gas Drive," Pet. Trans., AIME, vol. 105 (1956), 105-110.

Stone, H.L.: " Iterative Solution of Implicit Approximations of Multi-Dimensional Partial Differential Equations," SIAM J. Numer. Anal., vol. 5 (1968), 530-558.

Thele, K.J., Lake, L.W. and Sepehrnoori, K.: " A Comparison of Three Equation-of-State Compositional Simulators," pesented at the Reservoir Simulation Symposium held in San Francisco, November 15-18, 1983.

Thomas, G.W. and Thurnau, D.H.: " Reservoir Simulation Uing an Adaptive Implicit Method," Soc. Pet. Eng. J. (1983), 759-768.

Todd, M.R. and Longstaff, W.J.: " The Development, Testing and Application of a Numerical Simulator for Predicting Miscible Flood Performance," J. Pet. Tech. (1972), 874-882.

Trimble, R.H. and McDonald, A.E.: " A Strongly Coupled, Fully Implicit, Three-Dimensional, Three Phase Well Coning Model," Soc. Pet. Eng. J. (1981), 454-458.

Van Quy, N., Simandoux, P. and Corteville, J.: " A Numerical Study of Diphasic Multicomponent Flow," Soc. Pet. Eng. J. (1972), 171-184.

Watkins, R.W.: " A Technique for the Laboratory Measurement of Carbon-Dioxide Unit Displacement Efficiency in Reservoir

Rock," presented at the 53rd Annual fall Technical Conference and Exhibition of SPE of AIME, Houston, Texas, October 1-3, 1978.

Weise, H.C., Reamer, H.H. and Sage, B.H.: " Phase Equilibria in Hydrocarbon Systems: Phase Behaviour in the Methane-Propane -n-Decane System," J. Chem. Eng. Data, vol. 15 (1970), 75-82.

Weise, H.C., Jacobs, J. and Sage, B.H.: " Phase Equilibria in the Hydrocarbon Systems. Phase Behaviour in the Methane-Propane -n-Deacne System," J. Chem. Eng. Data, vol. 15 (1970), 82-91.

Welge, H.J.: "Displacement of Oil from Porous Media by Water or Gas," Presented at Tulsa Meeting, Petroleum Division, AIME, (October, 1947).

Whorton, L.P. and Kieschnick, W.F. Jr.: " A Preliminaary Report on Oil Recovery by High-Pressure Gas Injection," Oil and Gas J. (1950), 78.

Willams, J.K. and Dawe, R.A.: " Near-Critical Condensate Fluid Behaviour in Porous Media- A Modelling Approach," Soc. Pet. Eng. Res. Eng. (1989), 221-227.

Wilson, G.: " A Modified Redlich-Kwong Equation of State, Applications to General Physical Data Calculations," presented at the AIChE National Meeting, held in Cleveland, Ohio, May 4-7, 1969.

Wu, R.S., Batycky, J.P., Harker, B. and Rancier, D.: " Enriched Gas Displacement: Design of Solvent Compositions," J. Can. Pet. Tech. (1986), 55-59.

Yarborough, L.: " Vapor-Liquid Equilibrium Data for Multicomponent Mixtures Containing Hydrocarbon and nonhydrocarbon Mixtures," J. Chem. Eng. Data, vol. 17 (1972), 129-133.

Yellig, W.F. and Metcalfe, R.S.: " Determination and Prediction of CO_2 Minimum Miscibility Pressures," J. Pet. Tech. (1980), 160-168.

Young, L.C. and Stephenson, R.E.: " A Generalized Compositional Approach for Reservoir Simulation," Soc. Pet. Eng. (1983), 727-742.

APPENDIX A

Measurement of Physical Properties of Slim-Tube and Experimental Data Analysis

A-1 Pore Volume Measurement of Slim-Tube

Pore volume of the slim-tube was measured by the following method:

a. Nitrogen at 120°F was injected into the slim-tube for 36 hours at the rate of 15 ml/hr. The pressure drop across the slim-tube was maintained at 300 psi. At this point, the slim-tube was considered to be dry and filled with nitrogen.

b. To evacuate nitrogen from the slim-tube, vacuum was drawn at the downstream end of the slim-tube for 24 hrs. Slim-tube was considered to be dry and clean.

c. The pressure of toluene at a floating piston cylinder was raised to 1000 psia by the Ruska positive displacement pump and the initial reading of the pump was noted. Then this cylinder was brought in contact with the evacuated slim-tube until the pressure drop became less than 10 psi. The toluene cylinder was disconnected from the slim-tube and the pressure of toluene was raised to 1000 psi. Then the toluene in the cylinder was again brought in contact with the slim-tube. This process was repeated until the toluene pressure remained constant at 1000 psi while the cylinder was in contact with

the slim-tube. Then the final reading of the pump was noted. By subtracting the initial reading of the pump from the final pump reading, the volume of toluene injected into the slim-tube was obtained and this volume of toluene represented the pore volume of the slim tube.

Steps a, b and c were repeated three times to check the repeatability of the experiments. The measured pore volume of the slim-tube in the three experiments were 156.9 ml, 156.9 ml, 155.7 ml respectively. The pore volume of the slim-tube was chosen to be 156.9 ml.

A-2 Permeability Measurement of the Slim-Tube

The slim-tube was cleaned by toluene injection. Two pore volumes of toluene was injected at the rate of 15 ml/hr and a further four pore volumes of toluene was injected at the rate of 10 ml/hr at 120^{o} F. When steady state, which was determined by measuring the output rate of toluene and pressure drop across the slim-tube, was obtained, the pressure drop across the slim-tube was noted. This procedure was repeated twice. The pressure drop across the slim tube in the experiments were 25 psi (0.17 Mpa) and 27.5 psi (0.19 Mpa), respectively.

Now, permeability of the slim-tube was measured by using Darcy's equation;

$$q = K A \Phi \Delta P / \mu \Delta x \qquad (A.1)$$

where q = rate of output = 10 ml/hr

A = cross sectional area of slim tube = 0.1693 cm^2

Φ = porosity of the slim tube = 0.3798

ΔP= pressure drop in dynes/cm^2

μ = viscosity of toluene = 0.36 cp at 120^oF

ΔX= length of slim tube= 2440 cm

Putting the values of pressure drop in equation (A-1), permeability values were obtained. In the two experiments permeability values obtained were 22.0 E-8 cm^2 and 20.0 E-8 cm^2, respectively.

A-3 Experimental Data Analysis

The raw data for all the fifteen experiments are provided in the Appendix E.

To calculate the recovery of oil , gas-oil ratio and the pore volume of gas injected, the following calculations were made. The amount of gas injected in terms of pore volume (PV) was obtained by the following method;

PV of Gas Injected= (VW/PVS).CF (A.2)

where VW= volume of water injected from the pump to the floating piston cylinder which contained the gas.

PVS= Pore volume of the slim-tube.

CF= Correction factor for water volume

The correction factor was calculated by taking the ratio of the specific volume of water at the experimental condition and at the atmospheric condition.

The percent cumulative recovery of oil was calculated from the following equation:

% Cumulative Recovery= (SV/PVS).VF.100 (A-3)

where SV= separator liquid volume

VF= volume factor

The volume factor was calculated by taking the ratio of the specific volume of oil at atmospheric condition and at the experimental condition. The specific volume of the oil was calculated theoretically by using the Peng-Robinson equation of state.

The cumulative gas-oil ratio was calculated from the following equation:

Cumulative GOR= VG/VL (A-4)

where VG= total gas produced.

VL= total liquid collected since the gas production started.

APPENDIX B

Formulations of the Equations for Numerical Simulations

B-1 Finite Difference Forms of Equations

Expansion of the differential term of the left hand side of equation (4.8) into the finite difference form is the following:

$$\Delta_x(T_o y_{mo} \Delta P + T_g y_{mg} \Delta P) = [T_{o,i+1/2} y_{mo,i+1/2}(P_{i-1}-P_i) - T_{o,i-1/2} y_{mo,i-1/2}(P_i - P_{i+1})] + [T_{g,i+1/2} y_{mg,i+1/2}(P_{i-1}-P_i) - T_{g,i-1/2} y_{mg,i-1/2}(P_i - P_{i+1})] \quad \text{(B.1)}$$

where i=index of grid block and m=index of component

$T_{o,i+1/2}$ and $T_{o,i-1/2}$ are the transmissibilities of the oil phase at the intersections of the i and the i+1 grid blocks and the i and the i-1 grid blocks, respectively. Similarly, $T_{g,i+1/2}$, $T_{g,i-1/2}$, $y_{mj,i+1/2}$, and $y_{mj,i-1/2}$ are defined.

Transmissibilities of the phases at the intersections of the grid blocks are calculated by single point upstream differencing method;

$$T_{j,i+1/2} = T_{j,i} \quad \text{(B.2)}$$

$$T_{j,i-1/2} = T_{j,i-1} \quad \text{(B.3)}$$

where j=o,g

Phase compositions at the intersection of the grid blocks are calculated by two-point upstream differencing method;

$$Y_{mj,i+1/2} = Y_{mj,i} + 0.5(Y_{mj,i}-Y_{mj,i-1}) \quad \text{(B.4)}$$

$$Y_{mj,i-1/2} = Y_{mj,i-1} + 0.5(Y_{mj,i-1}-Y_{mj,i-2}) \quad \text{(B.5)}$$

To control the overshooting or undershooting problem in the numerical calculations the following limiting criteria are set for the $Y_{mj,i+1/2}$;

$$\text{If } Y_{mj,i+1/2} \geq \max(Y_{mj,i} \, , \, Y_{mj,i+1}) \quad \text{(B.6)}$$

$$\text{then } Y_{mj,i+1/2} = \max(Y_{mj,i} \, , \, Y_{mj,i+1}) \quad \text{(B.7)}$$

and

$$\text{If } Y_{mj,i+1/2} \leq \min(Y_{mj,i} \, , \, Y_{mj,i+1}) \quad \text{(B.8)}$$

$$\text{then } Y_{mj,i+1/2} = \min(Y_{mj,i} \, , \, Y_{mj,i+1}) \quad \text{(B.9)}$$

Similarly for $Y_{mj,i-1/2}$, the limiting criteria are the following;

$$\text{If } Y_{mj,i-1/2} \geq \max(Y_{mj,i-1} \, , \, Y_{mj,i}) \quad \text{(B.10)}$$

$$\text{then } Y_{mj,i-1/2} = \max(Y_{mj,i-1} \, , \, Y_{mj,i}) \quad \text{(B.11)}$$

and

$$\text{If } Y_{mj,i-1/2} \leq \min(Y_{mj,i-1} \, , \, Y_{mj,i}) \quad \text{(B.12)}$$

$$\text{then } Y_{mj,i-1/2} = \min(Y_{mj,i-1} \, , \, Y_{mj,i}) \quad \text{(B.13)}$$

B-2 Derivative of the Compressibility Factor with Respect to Pressure

The derivative term $\partial z_j / \partial P$ used in the equation

(4.21) are derived from the following equation which is the cubic equation for the compressibility factor obtained from Peng-Robinson equation of state (described in Appendix C);

$$z_j^3 - (1-B)z_j^2 + (A-3B^2-2B)z_j - (AB-B^2-B^3) = 0 \qquad \text{(B.14)}$$

The final form of the derivative will be,

$$\frac{\partial z_j}{\partial P} = \frac{1}{P}\left[\frac{2AB-2B^2-3B^3-z_j(A-6B^2-2B)-z_j^2B}{3z_j^2-2z_j(1-B)+(A-3B^2-2B)}\right] \qquad \text{(B.15)}$$

APPENDIX C

Peng-Robinson Equation of State

The two-parameter Peng-Robinson equation of state is,

$$P=\frac{RT}{v-b}-\frac{a}{v(v+b)+b(v-b)} \qquad (C.1)$$

where $b= 0.0778\ RT_c/P_c$ (C.2)

$a= 0.45724\ R^2T_c^2\alpha/P_c$ (C.3)

$\alpha^{0.5}=1+m(1-T_r^{0.5})$ (C.4)

where $T_r = T/T_c$

and $m= 0.37464+1.54226\omega-0.2699\omega^2$ (C.5)

The cubic equation for the compressibility factor $z=Pv/RT$ is;

$z^3-(1-B)z^2+(A-3B^2-2B)z-(AB-B^2-B^3)=0$ (C.6)

where $A = aP/R^2T^2$ (C.7)

and $B = bP/RT$ (C.8)

The mixing rules used for the Peng-Robinson equation are;

$b = \sum_i x_i b_i$ (C.9)

$a = \sum_i\sum_j x_i x_j a_{ij}$ (C.10)

$a_{ij}= (1-\delta_{ij})a_i^{0.5} a_j^{0.5}$ (C.11)

where i,j are the components,

and δ_{ij} are the binary interaction coefficients.

With the mixing rules defined above, the fugacity coefficient of component k is given by;

$$\ln\phi_k = \frac{b_k}{b}(z-1) - \ln(z-B) - \frac{A}{2\sqrt{2}B}$$

$$\left(\frac{2\sum_i x_i a_{ik}}{a} - \frac{b_k}{b}\right) \ln\frac{z+2.414B}{z-0.414B} \qquad \text{(C.12)}$$

APPENDIX D

Acceleration Schemes for Newton's Method

The results of the acceleration scheme developed in this study for Newton's method, to be applied for saturation pressure calculations are compared with those of other two acceleration schemes for Newton's method. Two other acceleration schemes are Richardson extrapolation and Overrelaxation (Kelly et al.,1983).

Richardson extrapolation: This scheme is applied to accelerate the Newton's method at the near singularities of the Jacobian matrices. Each accelerated step by the Richardson extrapolation scheme is taken after every three Newton steps. This procedure is recommended by Griewank (1985) for multivariate Newton's method.

The accelerated step by the Richardson extrapolation scheme will be

$$u^{l+1} = (k+1)\, g(u^l) - k\, u^l \qquad \text{(D.1)}$$

where u is the vector of iteration variables, k is the order of singularity , l is the iteration index and

$$g(u^l) = u^l - J(u^l)^{-1}\, f(u^l) \qquad \text{(D.2)}$$

where J is the Jacobian matrix and f is the vector of objective function.

Since in the near singularity of Jacobian matrix Newton steps take roughly half of the distance to the actual solution, the proposed value of k =1 (Griewank, 1985) for extrapolation of the iterates is used. Thus, the final form of the accelerated step will be

$$u^{l+1} = u^{l} - 2\, J(u^{l})^{-1}\, f(u^{l}) \qquad \text{(D.3)}$$

Overrelaxation: The Convergence speed of Newton's method can be improved by incorporating a certain degree of overrelaxation in the Newton's step. The overrelaxation scheme proposed by Kelly et al. (1983) is implemented. The accelerated step according to this scheme will be

$$u^{l+1} = u^{l} - \alpha_2\, J(u^{l})^{-1}\, f(u^{l}) \qquad \text{(D.4)}$$

where α_2 is the relaxation parameter.

Comparing the equation (D.3) with the equation (D.4), it can be seen that the overrelaxation method is similar to the Richardson extrapolation except that the parameter α_2 is used as the relaxation parameter in the overrelaxation method whereas a fixed value, 2, is used in the Richardson extrapolation. In the overrelaxation method, the value of α_2 is calculated at each accelerated step and each accelerated step is taken after three Newton steps. α_2 is calculated by the following equation;

$$\alpha_2 = k+1 - c\| g(u^{l})-u^{l}\| p \qquad \text{(D.5)}$$

where k is the order of singularity, p is the order of convergence and c is a parameter.

As in Richardson extrapolation, the value of k is selected here to be 1. The value of p which is the order of convergence is set equal to 1/2 as proposed by Griewank (1985). The parameter c is set equal to 1. Different values of the parameter c are tried, but c=1 seems to be the best value.